Adaptive Optics & Wavefront Control in Microscopy & Ophthalmology

5-7 October 2015, Paris, France

Topics

Adaptive optics methods
Wavefront control in scattering tissue
Novel techniques in microscopy
Applications in biology
Retinal imaging

Invited speakers

E. Beaurepaire, Ecole Polytechnique, Palaiseau
M. Cui, Purdue University, West Lafayette
C. Dainty, University College London, London
D. Débarre, Université Joseph Fourier, Grenoble
W. Drexler, Medical University, Vienna
V. Emiliani, Université Paris V, Paris
M. Fink, Institut Langevin, Paris
N. Ji, Janelia Farm, Ashburn
J. Mertz, Boston University, Boston
M. Paques, Institut de la Vision, Paris
A. Sentenac, Institut Fresnel, Marseille
M. Tanter, Institut Langevin, Paris

http://aomicro.sciencesconf.org

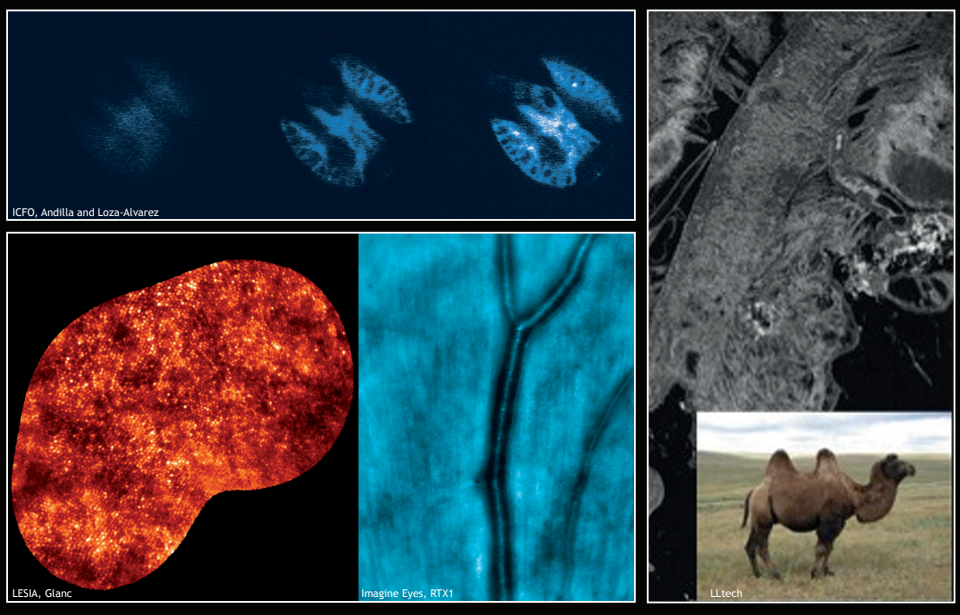

Maquette S. CNUDDE @ SFO CAL

Adaptive Optics & Wavefront Control in Microscopy & Ophthalmology

5-7 October 2015, Paris, France

Monday, October 5, 2015

08:30 - 09:15 Registration

09:15 - 09:30 **Conference opening**

chair: G. Rousset, LESIA, Observatoire de Paris

09:30 - 10:10 Inaugural lecture by C. Dainty, *University College London*: "Adaptive optics, from big science to the lab and clinic" page 7

10:10 - 12:30 **Adaptive optics methods I**

10:10 - 10:50 D. Débarre (invited speaker), *LIPhy, Université J. Fourier*: "Spatial variations of optical aberrations within complex tissues" page 9

10:50 - 11:10 Coffee Break

chair: D. Débarre, LIPhy, Université J. Fourier

11:10 - 11:30 C. Butler, *Interdisciplinary Institute for Neurosciences & Imagine Optic*: "3D single molecule super-resolution microscopy beyond the coverslip using adaptive optics" page 11

11:30 - 11:50 I. Doudet, *Phasics*: "Tissue tomographic phase image contrast improvement with adaptive optics" page 13

11:50 - 12:10 A. Masson, *Institut des Technologies Avancées en sciences du Vivant*: "High-resolution in-depth imaging of optically cleared deep samples by using an adaptive SPIM" page 16

12:10 - 12:30 M. Zurauskas, *University of Oxford*: "Method for deformable mirror characterization inside of a full field optical microscope" page 18

12:30 - 14:00 *Lunch Break*

14:00 - 15:40 **Adaptive optics methods II**

chair: V. Emiliani, Neurophotonics Laboratory, Paris Descartes University

14:00 - 14:40 N. Ji (invited speaker), *Janelia Farm Research Campus*: "Adaptive optical microscopy and wavefront shaping for in vivo brain imaging" page 21

14:40 - 15:00 J. Gallagher, *LIPhy, Université J. Fourier & ALPAO*: "Comparison of metrics and strategies in sensorless AO microscopy for imaging and fluorescence fluctuation measurements in tissue" page 23

15:00 - 15:20 W. Akemann, *IBENS, Ecole Normale Supérieure*: "Holographic wavefront control by acousto-optic diffraction for fast 3D-microscopy" page 26

15:20 - 15:40 P. Kirkby, *University College London - NPP*: "Rapid and precise wavefront control with an acousto-optic lens of bulk biological tissue at cellular resolution" page 29

15:40 - 16:10 *Coffee Break*

16:10 - 18:10 **Applications in biology**

chair: N. Ji, Janelia Farm Research Campus

16:10 - 16:50 E. Beaurepaire (invited speaker), ***Laboratoire d'Optique et Biosciences, Ecole Polytechnique***: "Multicolor and light-sheet excitation approaches for high-content multiphoton imaging of tissues" **page 31**

16:50 - 17:30 V. Emiliani (invited speaker), ***Neurophotonics Laboratory, Paris Descartes University***: "Wavefront shaping and optogenetics" **page 33**

17:30 - 17:50 M. Pedrazzani, ***Laboratoire Aimé Cotton, Université Paris-Sud***: "Micromirror structured illumination microscopy with adaptive optics for in vivo drosophila brain imaging" **page 36**

17:50 - 18:10 A. Malvache, ***Institut Fresnel & INMED***: " Enhanced imaging of hippocampal activity using adaptive optics in living mice" **page 39**

18:10 - 21:00 **Poster session and buffet dinner** **page 105**

Tuesday, October 6, 2015

09:00 - 12:20 **Retinal imaging**

chair: W. Drexler, Medical University Vienna

09:00 - 09:40 M. Paques (invited speaker), ***Institut de la Vision***: "Adaptive optics as a tool for the in vivo exploration of photoreceptor substructures" page 42

09:40 - 10:00 S. Meimon, ***ONERA***: "Towards adaptive optics assisted laser retinal microsurgery" page 45

10:00 - 10:20 C. Kulcsar, ***Laboratoire Charles Fabry de l'Institut d'Optique***: "Simple control of an adaptive optics retinal imaging system using pupil tracker measurements without pupil stabilization" page 48

10:20 - 10:40 *Coffee Break*

chair: C. Dainty, University College London

10:40 - 11:20 W. Drexler (invited speaker), ***Medical University Vienna***: "Compact AO-OCT" page 51

11:20 - 11:40 K. Grieve, ***Institut de la Vision***: "Full field optical coherence microscopy of ocular tissues" page 54

11:40 - 12:00 P. Xiao, ***Institut Langevin***: "Pre-study of retinal imaging by adaptive optics full-field OCT with transmissive liquid crystal spatial light modulator" page 56

12:00 - 12:20 M. Glanc, ***LESIA, Observatoire de Paris***: "Adaptive optics corrected full-field OCT for 3D retinal imaging" page 59

12:20 - 14:00 *Lunch Break*

14:00 - 18:10 **Wavefront control in scattering tissues**

chair: J. Mertz, Boston University

14:00 - 14:40 M. Cui (invited speaker), ***ECE, Purdue University***: "Wavefront control for in vivo fluorescence microscopy" page 62

14:40 - 15:00 T. Chaigne, ***Institut Langevin & Laboratoire Kastler Brossel***: "Light control in scattering medium via photoacoustic-guided wavefront shaping" page 65

15:00 - 15:20 A. Badon, ***Institut Langevin***: "A random matrix approach of optical imaging and detection through turbid media" page 68

15:20 - 15:40 M. Mounaix, ***Laboratoire Kastler Brossel***: "Spatio-temporal focusing of an ultrashort pulse through a scattering medium using the multi spectral transmission matrix" page 71

15:40 - 16:00 H. B. de Aguiar, ***Institut Fresnel***: "Wavefront shaping in the realm of nonlinear microscopy: prospects for label-free deep imaging in scattering media" page 74

16:00 - 16:30 *Coffee Break*

chair: M. Cui, ECE, Purdue University

16:30 - 17:10 M. Fink (invited speaker), ***Institut Langevin***: "Exploiting the time reversal operator and the Van-Cittert Zernike theorem for adaptive ultrasonic imaging" **page 77**

17:10 - 17:30 N. Stasio, ***LO, Ecole Polytechnique Fédérale de Lausanne***: "Multimodal imaging through a capillary waveguide using digital phase conjugation" **page 79**

17:30 - 17:50 S. Sivankutty, ***Institut Fresnel***: "Two-photon lensless endoscopy by controlling the wave front in a multi-core optical fiber" **page 82**

17:50 - 18:10 E. Morales, ***LAPD, Ecole Polytechnique Fédérale de Lausanne***: "Towards a multimode fiber two-photon endoscope" **page 85**

21:00 **Conference dinner at the Eiffel Tower**

Wednesday, October 7, 2015

09:00 - 12:40 **Novel techniques in microscopy**

chair: S. Gigan, Laboratoire Kastler Brossel

09:00 - 09:40 J. Mertz (invited speaker), ***Boston University***: "Wide-field adaptive optics without guide stars" **page 87**

09:40 - 10:00 J. Glückstad, ***DTU Fotonik***: "Wavefront control by GPC" **page 89**

10:00 - 10:20 O. Hernandez, ***Neurophotonics Laboratory, Paris Descartes University***: "Remote axial positioning of temporally focused holographic patterns" **page 92**

10:20 - 10:40 *Coffee Break*

10:40 - 11:20 A. Sentenac (invited speaker), ***Institut Fresnel***: "Super-resolution in marker-free optical far-field microscopy: The interest of digital reconstruction" **page 94**

11:20 - 11:40 O. Haeberlé, ***Laboratoire Modélisation Intelligence Processus Systèmes***: "Tomographic diffractive microscopy combining sample and illumination rotation delivers 3-D isotropic resolution in the 100 nm range" **page 97**

11:40 - 12:00 J. Andilla, ***ICFO - Institut de Ciències Fotòniques***: "Depth of field extension for fast volumetric imaging using light-sheet microscopy" **page 100**

12:00 - 12:40 M. Tanter (invited speaker), ***Institut Langevin***: "New perspectives for ultrasound in the brain : fUltrasound imaging and ultrasound localization microscopy" **page 102**

End of the conference

Adaptive Optics : from big science to the lab and clinic

Chris Dainty

UCL Institute of Ophthalmology, 11-43 Bath Street, London EC1V 9EL, UK

c.dainty@ucl.ac.uk

Keywords: Adaptive optics

SUMMARY

Adaptive optics (AO) was first proposed by Babcock[1] as a means of compensating for the deleterious effects of atmospheric turbulence in ground-based astronomy. The technology to implement his idea was not available at the time, and was developed by principally by Itek Corporation in the 1970s, first for the Real Time Atmospheric Compensation (RTAC) system[2] (using a 21 actuator deformable mirror) and then for the Compensated Imaging System (CIS), which used a 168 actuator DM and a separate tip-tilt mirror. The first astronomical adaptive system was the joint ESO-France COME-ON system[3], commission in 1990, which used a 19-actuator DM. Since that time, all large telescopes have been equipped with AO, with each latest system outperforming previous installations in terms of technical specification.

The first generation of astronomical AO systems employed a single wavefront sensor and single deformable mirror (DM). Nowadays, many other options are being investigated, or deployed, including : ground layer adaptive optics (GLAO), laser guide star adaptive optics (LGSAO), multi-object adaptive optics (MOAO), laser tomography adaptive optics (LTAO), multi-conjugate adaptive optics (MCAO) and extreme adaptive optics (XAO). As a rule, these employ multiple DMs, multiple wavefront sensors and non-trivial control systems. Astronomical AO systems are built by large teams of engineers, and the process involves numerous design reviews and technology gating steps, with costs of many millions of Euros. Adaptive optics is an integral part the 39m European Extremely Large Telescope, a >€1B Euro project due for first light in 2024.

In the mid-1990s, it became clear that the single DM AO systems being deployed for astronomy could be adapted for laboratory-based projects at low cost in a university setting, without the need for teams of engineers. Our group was one of several groups who demonstrated that AO – at least at the single DM level – was not rocket science[4], and that any competent research student could design and build an AO system. This was considered with great scepticism in the big science community, where the culture was ‘‘bigger is better’’.

Since that time, AO has been applied extensively in retinal imaging, vision simulation, and in numerous modalities of microscopy, as well as in lasers, both intra-cavity and for beam shaping. In this talk I will trace the advances in AO, from the technology-leading implementations in astronomy to the elegant experiments in scattering media.

REFERENCES

[1] H. Babcock, “The possibility of compensating atmospheric seeing”, Pub. Astr. Soc. Pac., **65** 229-236, 1953.

[2] J. Hardy et al, “Real time phase correction of optical imaging systems”, OSA Topical Meeting on Optical Propagation Through Turbulence, Boulder, CO, July 1974.

[3] G. Rousset et al, “First diffraction-limited astronomical images with adaptive optics”, Astron. Astrophys. **230** L29-L32, 1990.

[4] C Paterson, I Munro and J C Dainty, “A low cost adaptive optics system using a membrane mirror”, Optics Express, **6** 175-186, 2000.

Spatial variations of optical aberrations within complex tissues

Delphine Débarre[1,2], Jun Zeng[2], Pierre Mahou[2], Marie-Claire Schanne-Klein[2], Emmanuel Beaurepaire[2]

[1] *Lab. for Interdisciplinary Physics, 140, rue de la Physique, 38402 St Martin d'Hères, France*
[2] *Lab. for Optics and Biosciences, Ecole Polytechnique, 91128 Palaiseau, France*

delphine.debarre@ujf-grenoble.fr

Keywords: Aberration mapping, isoplanetism, multiconjugate adaptive optics.

Over the past decade, adaptive optics has received increasing attention as a means to restore the quality of microscopy images inside thick, aberrating samples. Such approach has proven particularly useful in the case of nonlinear imaging which will be discussed in this presentation.

Here I will first present and illustrate the main methods used for aberration correction in nonlinear microscopy and discuss their advantages and limitations. One of the key parameters for efficient correction on real samples is the number of photons required for correction, and I will propose a comparison of the photon budget for various existing methods.

I will then focus on the problem of correcting for the spatially varying aberrations encountered in real samples [1]. Using experimentally measured aberration maps and simulations, I will discuss the number of aberration modes required for accurate correction and the typical size of isoplanetism regions as a function of the structure of the sample. Finally, I will derive guidelines for efficient aberration correction in various samples.

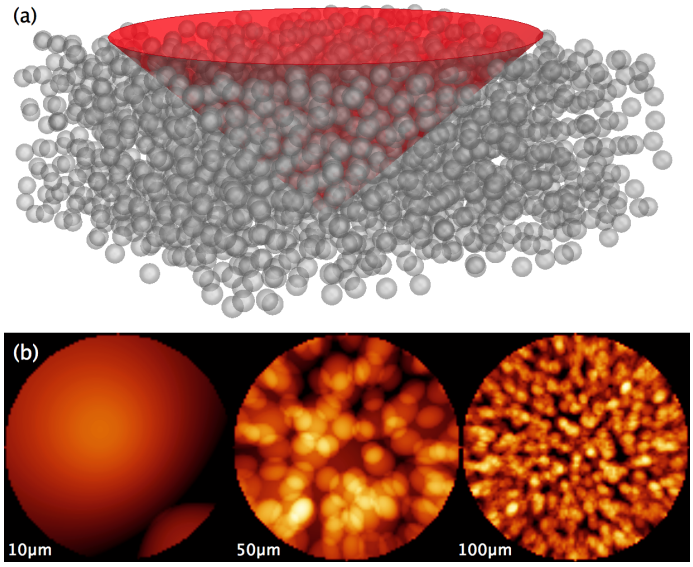

Figure 1: (a), Simulation of an aberrating sample with given size heterogeneities, and (b) corresponding aberrated phases calculated at different depths.

REFERENCES

[1] J. Zeng, P. Mahou, M.C. Schanne-Klein, E. Beaurepaire, and D. Débarre, "3D resolved mapping of optical aberrations in thick tissues", *Biomedical Optics Express, vol.* 3, pp. 1898-1913 (2012)

3D Single Molecule Super-Resolution Microscopy beyond the coverslip using Adaptive Optics

Corey Butler[1,2,3], Remi Galland[1,2], Jean-Baptiste Sibarita[1,2]

[1]*University of Bordeaux, Interdisciplinary Institute for Neuroscience, UMR 5297, F-33000 Bordeaux, France*
[2]*CNRS, UMR 5297, F-33000 Bordeaux, France*
[3]*Imagine Optic, 18 rue Charles de Gaulle, 91400 Orsay, France*

Corresponding author: jean-baptiste.sibarita@u-bordeaux2.fr

Keywords: Super-resolution, dSTORM, 3D, adaptive optics, aberration correction.

Single-molecule localization (SML) microscopy such as PALM and STORM circumvent the diffraction limit by precisely localizing individual sequentially activated fluorescent molecules, resulting in a resolution up to an order of magnitude higher than traditional epifluorescence microscopes. This resolution is primarily restricted by the efficiency with which each individual fluorophore can be localized and is mainly limited by the number of collected photons above the background signal. Therefore, SML microscopes use high numerical aperture (NA) oil immersion objectives to collect the maximum number of photons and reduce the background. Imaging away from the coverslip using such high NA objectives introduces depth-dependent spherical aberrations stemming from the index mismatch between the coverslip and the typically aqueous imaging medium, reducing the photon count in the focal plane and thus degrading the image resolution. Additionally, 3D SML imaging requires PSF engineering to axially discriminate molecules in the focal volume. Typically, a cylindrical lens is employed to introduce a fixed astigmatism to the detection path. However, when combined with depth-dependent spherical aberrations, the PSF elongation from a fixed astigmatic element is reduced, deteriorating the axial resolution and limiting 3D SML imaging to within a few microns from the coverslip.

We describe how we can overcome these limits using an adaptive optics system designed specifically for SML applications (MicAO-3DSR, Imagine Optic). First, we correct inherent system aberrations. Second, we quantify spherical aberration as a function of imaging depth, and apply this calibration curve to correct for the depth-dependent spherical aberrations. Third, we add a controlled astigmatism for 3D localization. Finally, we show that with these corrections, single molecules more than 10 microns above the coverslip can be precisely localized, and we demonstrate 3D STORM imaging of various biological structures at these depths. Additionally, we discuss how SML can be extended to more physiological biological systems by combining adaptive optics with novel illumination techniques, opening the method to a wide range of biological applications.

Tissue Tomographic Phase Image Contrast Improvement with Adaptive Optics

I. Doudet[1], S. Aknoun[1], P. Bon[2], B. Wattellier[1], S. Monneret[3]

[1] *Phasics S.A, Espace technologique de Saint Aubin, Route de l'Orme des Merisiers, 91190 Saint Aubin, France*

[2] *CNRS, Institut d'Optique (LP2N), UMR 5298, Bordeaux Univ. Talence, France*

[3] *Aix-Marseille Université, CNRS UMR 7249, Institut Fresnel, Campus de Saint-Jérôme, 13013 Marseille, France*

bw@phasics.fr

Keywords: optical tomography, adaptive optics, quantitative phase imaging, spherical aberration.

We describe here the use of adaptive optics (AO) to correct optical aberrations and enhance the contrast of tomographic phase images above several hundreds of µm imaging depth.

It is known that for high numerical aperture high magnification microscopy, images are degraded by optical aberrations for depths of more than tens of micrometers. Microscope objectives are optimized to image samples close to the coverslip. When the object plane is set far from the coverslip, the index mismatches between the medium, coverslip, immersion oil and objective glass generate spherical aberration at the image center and off-axis aberrations at the edges. These aberrations are predictable since they mostly depend on the imaging depth and the sample mean index. However the optical rays emitted or diffracted by the sample are refracted also by the sample inhomogeneities. This distorts the image wave front and degrades the image quality. Both effects are now one of the limiting factors for deep imaging, scattering being another one.

We developed a tomographic phase imaging system based on quadriwave lateral shearing interferometry [1,2]. Its specificity is the use of spatially incoherent illumination which improves the axial and transverse resolution. In particular, axial sectioning is created and label-free quantitative thick tissue imaging is now possible. However when applied to 100-µm thick mouse brain slices (see Figure 1), we observed that intracellular components such as nucleoli or vesicles get dimmer and dimmer as the observation depth increases. We attributed this contrast decrease to optical aberrations and decided to couple our tomographic system to adaptive optics in order to keep the image contrast even for deep imaging planes.

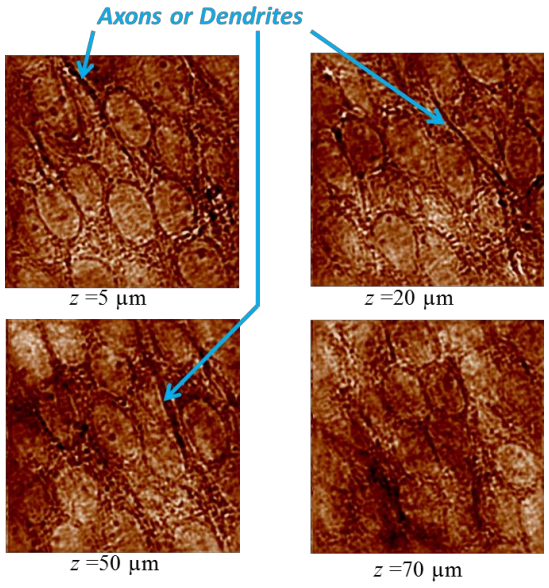

Figure 1: Tomographic images of mouse brain biopsy at different depths (z). The contrast of intracellular components degrades as the depth increases.

The 3D volume is imaged by axially scanning the sample with a quadri-wave lateral shearing interferometer (SID4bio from Phasics) while using spatially incoherent white-light illumination. We use a non-modified inverted microscope equipped with a z-axis piezo-controlled microscope objective (PIFOC). A z-stack is recorded by objective translation along the optical axis in order to reconstruct the 3D object structure. The native halogen source of the microscope is used with a 700 ± 30 nm band-pass filter to neglect the sample dispersion.

The correction loop is composed of a deformable mirror (DM97-15 from Alpao) and a SID4 standard wave front sensor. The adaptive optics is inserted after the microscope exit port and imaged with the microscope objective exit pupil. The deformable mirror is calibrated to compensate for spherical aberration and maintain a constant resolution along the sample depth. For the correction, a calibration for different planes is previously done on the sample using for example a metric such as the image sharpness or contrast. We choose to optimize the correction for a set of six plans between 20 and 100 µm depth. Then, knowing that the spherical aberration varies linearly with depth, we could interpolate the requested correction for intermediate planes and apply it in real time while scanning the different depths.

Using this method, we were able to improve the intracellular contrast as seen in Figure 2. We will present tomographic reconstruction of fixed tissue of 100 µm thick and its adaptive optics correction for spherical aberration.

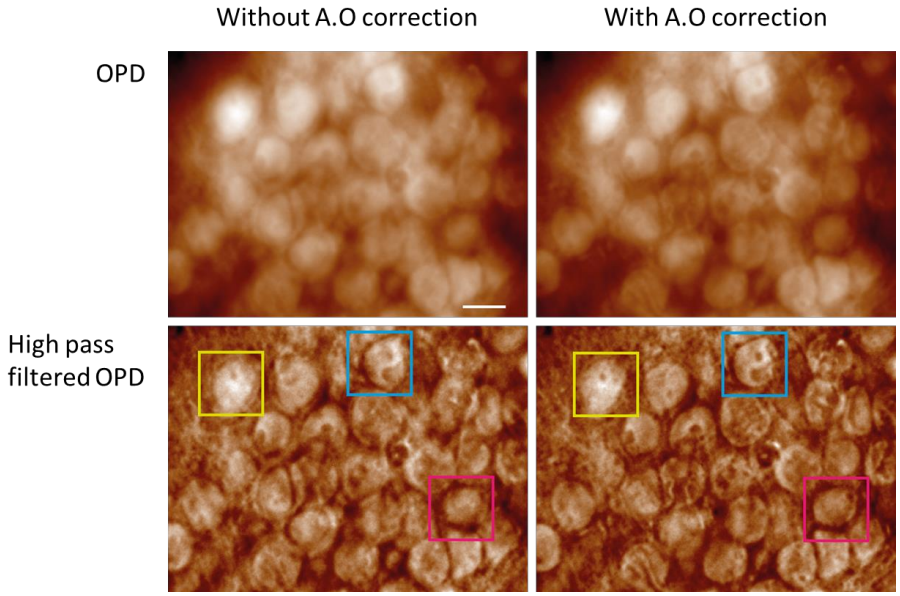

Figure 1: Example of mouse brain tissue tomographic phase imaging at a depth of 53.4µm. (left) without correction (right) with correction. In the colored square, we can see that intracellular componSents are more contrasted when the correction is applied..

REFERENCES

[1] P. Bon, G. Maucort, B. Wattellier, and S. Monneret, "Quadriwave lateral shearing interferometry for quantitative phase microscopy of living cells," Opt. Express, vol. 17, pp. 13080–13094, Jul 2009.

[2] P. Bon, S. Aknoun, S. Monneret, and B. Wattellier, "Enhanced 3d spatial resolution in quantitative phase microscopy using spatially incoherent illumination," Opt.Express, vol. 22, pp. 8654–8671, Apr 2014.

High-resolution in-depth imaging of optically cleared deep samples by using an adaptive SPIM

Aurore MASSON [1,2], Paul ESCANDES[1,2], Céline FRONGIA[1,2], Grégory CLOUVEL[4], Bernard DUCOMMUN[1,2,3] and Corinne LORENZO[1,2].

[1]*Université de Toulouse, ITAV-USR3505, F-31106 Toulouse, France*
[2]*CNRS, ITAV-USR3505, F-31106 Toulouse, France*
[3]*CHU de Toulouse, F-31059 Toulouse, France*
[4]*Imagine Optic, Orsay F-91400, France*

corinne.lorenzo@itav.fr

Keywords: Light Sheet Microscopy, SPIM, Adaptive Optics, clearing methods

Today, Light Sheet Fluorescence Microscopy (LSFM) makes it possible to image fluorescent samples with high lateral and axial resolution through depths of several hundreds of microns[1, 2]. However, as with all optical microscopes, LSFM also suffers from scattering, absorption and optical aberrations. Spatial variations in the refractive index of samples cause major changes to the light path resulting in loss of signal and contrast in the deepest regions, thus impairing in-depth imaging capability. These effects are particularly marked when inhomogeneous, deep, complex biological samples are investigated[3]. Recently, chemical treatments have been developed to render a sample transparent[4] by homogenizing its refractive index (RI), consequently enabling (1) a reduction of scattering phenomena and (2) a simplification of optical aberration patterns. One drawback of these methods is that the resulting RI of cleared samples does no match with the working RI medium of LSFM detection lenses generally used. This RI mismatch leads to the presence of low-order aberrations and therefore to a degradation of image quality. In this work, we introduce an original optical-chemical combined method based on an adaptive SPIM and a water-based clearing protocol enabling (1) the compensation of aberrations arising from the RI mismatches induced by optical clearing methods and (2) the acquisition of high resolution in-depth images of optically cleared complex thick samples such as Multi-Cellular Tumor Spheroids.

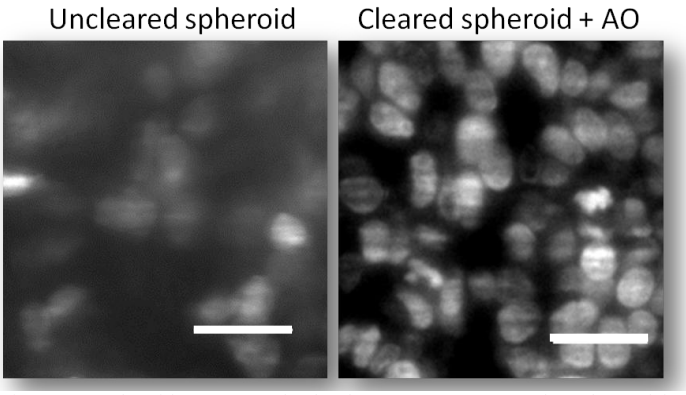

Figure 1 : Adaptive SPIM images of HCT116 spheroids at 200µm depth. Fluorescence corresponds to the nuclei of the proliferative cells. On the left, an uncleared spheroid was imaged without optical correction. On the right, the image was taken at the same depth in a spheroid cleared by the CUBIC protocol and aberrations were compensated by the adaptive optics correction method. Scale bar 25µm.

REFERENCES

1. Huisken, J., et al., *Optical sectioning deep inside live embryos by selective plane illumination microscopy.* Science, 2004. **305**(5686): p. 1007-9.
2. Lorenzo, C., et al., *Live cell division dynamics monitoring in 3D large spheroid tumor models using light sheet microscopy.* Cell division, 2011. **6**: p. 22.
3. Jorand, R., et al., *Deep and clear optical imaging of thick inhomogeneous samples.* PLoS One. **7**(4): p. e35795.

4. Erturk, A., et al., *Three-dimensional imaging of solvent-cleared organs using 3DISCO.* Nature protocols, 2012. **7**(11): p. 1983-95.

Method for deformable mirror characterization inside of a full field optical microscope

Mantas Zurauskas[1], Martin J. Booth[1,2]

[1] *Centre for Neural Circuits and Behaviour, University of Oxford, Mansfield Road, Oxford OX1 3SR, UK*
[2] *Department of Engineering Science, University of Oxford, Parks Road, Oxford, OX1 3PJ, UK*

mantas.zurauskas@cncb.ox.ac.uk

Keywords: Wavefront sensing, deformable mirror, microscopy.

We propose a direct wavefront sensing method for deformable mirror (DM) characterization in (widefield ?) microscopy systems. The transport of intensity equation (TIE) based phase retrieval method is particularly useful as a diagnostic tool for characterizing typical DM based systems where users have access to the image and pupil planes. The method requires only a light emitting diode (LED) light source and inexpensive camera for pupil plane measurements, therefore it offers a low cost and compact alternative to high footprint interferometry based wavefront sensing methods or Shack Hartman wavefront sensing [1]. Alternatively it can register higher aberration amplitudes than phase retrieval methods that rely on point spread function measurement [2].

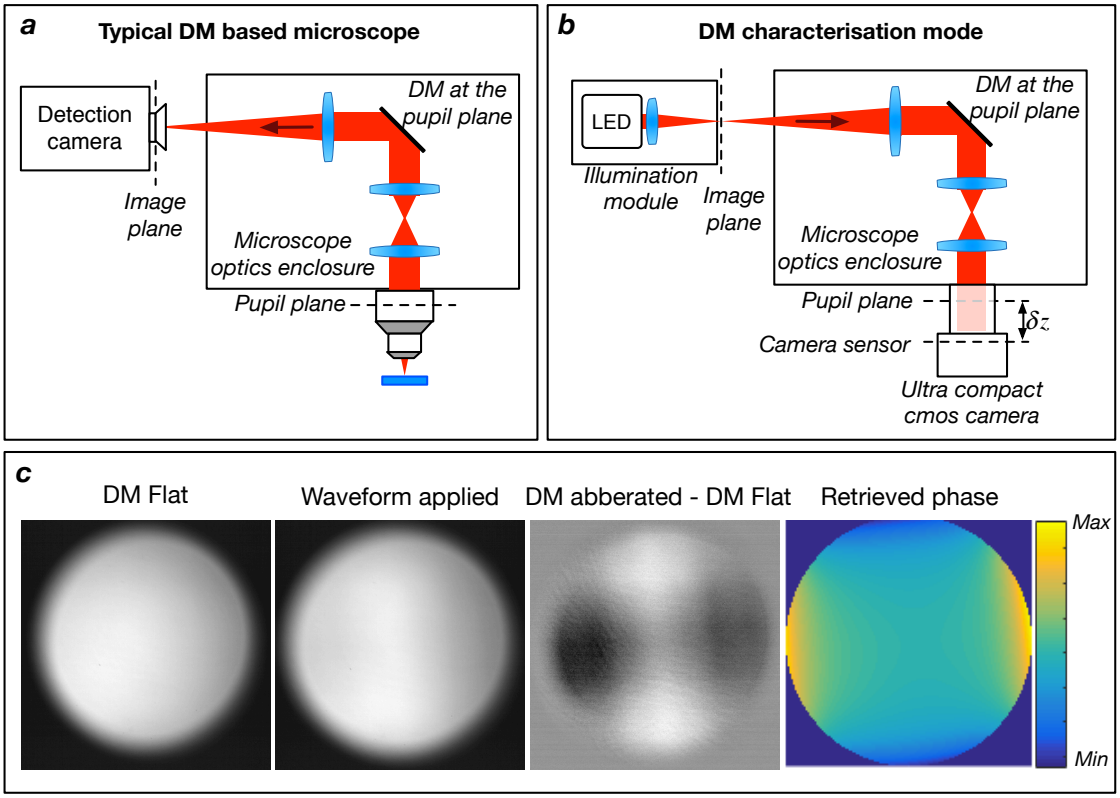

Figure 1: Method for characterizing a deformable mirror inside a microscope. (a) In a typical DM based microscope the user has easy access to the camera and objective lens. (b) To characterize the mirror the camera is replaced with an illumination module and the objective lens is replaced with an ultra compact camera. (c) Typical images obtained by the pupil camera and the retrieved wavefront.

For mirror characterization, the optical train is illuminated by replacing the imaging camera with LED based light source while the pupil plane is be imaged by replacing the microscope objective lens with an ultra compact CMOS camera, positioned at a distance δz away from the pupil plane, as depicted in Fig. 1a and b. The TIE based wavefront sensing method takes advantage of the mathematical model presented in [3].

However, instead of measuring the intensity distributions at two different defocus positions, it relies on the intensity distributions measured with different modes applied to the deformable mirror to provide an intensity variation $\delta I(x,y)$ that can be used to solve the TIE:

$$\frac{\delta I(x,y)}{\delta z} = I_{ab} - I_{flat}\,, \tag{1}$$

where I_{ab} and I_{flat} are the intensity maps registered with aberrated and flat DM respectively (Fig. 1c). The method to solve the TIE is based on the following equation

$$\varphi_{(N)} = N_F M_{(N)}^{-1} \delta_z I_{(N)}\,, \tag{2}$$

where $\delta_z I_{(N)}$ is a vector from the decomposition of the intensity variation in a series of Zernike modes, N_F is the constant magnification factor and the δz is the distance at which the camera is positioned away from the pupil plane

$$N_F = \frac{2\pi R^2}{\lambda \delta z}\,. \tag{3}$$

$M_{(N)}^{-1}$ is an inverse matrix with elements M_{ij} calculated for the series of Zernike modes applied to the mirror.

$$M_{ij} = \int_0^{2\pi}\int_0^{R} I(r,\theta)\nabla Z_i(r/R,\theta)\cdot\nabla Z_j(r/R,\theta) r dr d\theta\,. \tag{4}$$

The DM is then characterized and calibrated to produce orthogonal modes by analysing wavefronts created at the pupil plane with series of basis deformation modes applied to the mirror.

In conclusion, this approach permits the easy, in-situ calibration of deformable mirrors with simple and compact hardware. This tool will be use in the implementation and calibration of adaptive optics inside existing microscope systems. Applications of this method will be shown in adaptive optical microscopes for biological imaging.

REFERENCES

[1] S.A.Rahman, M. Booth, "Direct wavefront sensing in adaptive optical microscopy using backscattered light", *Applied optics*, vol. 52, no. 22, pp. 5523-5532, (2013).

[2] D. Débarre, T. Vieille, E. Beaurepaire, "Simple characterisation of a deformable mirror inside a high numerical aperture microscope using phase diversity", *Journal of microscopy*, vol. 244, no. 2, pp. 136-143, 2011.

[3] T. E. Gureyev, K. A. Nugent, "Phase retrieval with the transport-of-intensity equation. II. Orthogonal series solution for nonuniform illumination", *JOSA A*, vol. 13, no. 8, pp. 1670-1682, 1996,

Adaptive optical microscopy and wavefront shaping for in vivo brain imaging

Na Ji[1]

[1] *Janelia Research Campus, Howard Hughes Medical Institute, 19700 Helix Dr., Ashburn, VA 20147*

jin@janelia.hhmi.org

Keywords: adaptive optics, brain, multi-photon fluorescence microscopy, microendoscopy.

Imaging neurons deep within the brain of a living mouse shares many similarities with gazing at distant stars with a telescope. In both cases, imaging quality is limited by optical aberration and scattering [1]. Wavefront shaping using adaptive optics (AO) has revolutionized astronomy by allowing us to obtain sharp images of celestial objects through the turbulent atmosphere. Similar technology can be applied to microscopy for optically transparent samples but not mammalian brains, which are highly scattering. In this talk, I will describe our work to extend AO microscopy to these more optically challenging systems [2–6], which has allowed us to image both the input and output of mouse cerebral cortex with diffraction-limited resolution. I will also describe how, by combining AO with microendoscope, diffraction-limited imaging can be achieved anywhere inside the scattering mouse brain *in vivo* [7-8].

REFERENCES

[1] N. Ji, "The practical and fundamental limits of optical imaging in mammalian brains", Neuron, vol. 83, pp. 1242-1245, 2014.

[2] N. Ji, D. E. Milkie, E. Betzig, "Adaptive optics for high resolution imaging in biological tissues", Nature Methods, vol. 7, pp. 141-147, 2010.

[3] D. E. Milkie, E. Betzig, N. Ji, "Pupil-segmentation-based adaptive optical microscopy with full-pupil illumination", Optics Letters, vol. 36, pp. 4206-4208, 2011.

[4] R. Liu, D. E. Milkie, A. Kerlin, B. Maclennan, N. Ji, "Direct phase measurement method in zonal wavefront reconstruction using multidither coherent optical adaptive technique", Optics Express, vol. 22, pp. 1619-1628, 2014.

[5] C. Wang, D. E. Milkie, W. Sun, Z. Tan, T.-W. Chen, D. S. Kim, N. Ji, "Multiplexed aberration measurement for deep tissue imaging *in vivo*", Nature Methods, vol. 11, pp. 1037-1040, 2014.

[6] K. Wang, W. Sun, C. T. Richie, B. K. Harvey, E. Betzig, N. Ji, "Direct wavefront sensing for high-resolution *in vivo* imaging in scattering tissue", Nature Communications, vol. 6, article no. 7276, 2015.

[7] C. Wang, N. Ji, "Pupil-segmentation-based adaptive optical correction of a high-NA GRIN lens for two-photon uorescence endoscopy", Optics Letters, vol. 37, pp. 2001-2003, 2012.

[8] C. Wang, N. Ji, "Characterization and improvement of three-dimensional imaging performance of GRIN-lens-based two-photon florescence endomicroscopes with adaptive optics", Optics Express, vol. 21, pp. 27142-27154, 2013.

Comparison of metrics and strategies in sensorless AO microscopy for imaging and fluorescence fluctuation measurements in tissue.

Joseph Gallagher[1,2], Antoine Delon[1], Charles-Edouard Leroux[3], Giovanni Cappello[1], Irène Wang[1]

[1] *LIPhy, Univ. Grenoble Alpes, 38000 Grenoble, France.*
[2] *ALPAO, 345 Rue Lavoisier, 38300 Montbonnot, France.*
[3] *Institut Langevin, ESPCI ParisTech, CNRS, 1 rue Jussieu, 75238 Paris Cedex 05, France*

irene.wang@ujf-grenoble.fr

Keywords: Confocal Microscopy, Sensorless Adaptive Optics, Fluorescence Correlation Spectroscopy.

Adaptive optics in microscopy is developing in two major directions: improving imaging quality, especially in terms of resolution and 3D field of view; and improving associated quantitative measurements, such as of molecular concentration and dynamics. For obtaining the latter information, a very successful and well-established technique is Fluorescence Correlation Spectroscopy (FCS). In this study we compare metrics used for sensorless adaptive optics systems in microscopy and assess their relevance to imaging and FCS measurements. It has already been shown that FCS metrics are extremely sensitive to aberrations and thus can be used to measure the amplitude of aberration present [1]. Is this an efficient strategy to correct aberrations in imaging? Equally, can image metrics be used to apply AO correction efficiently for FCS measurements, for example in tissues, where aberrations vary quickly and significantly in a sample?

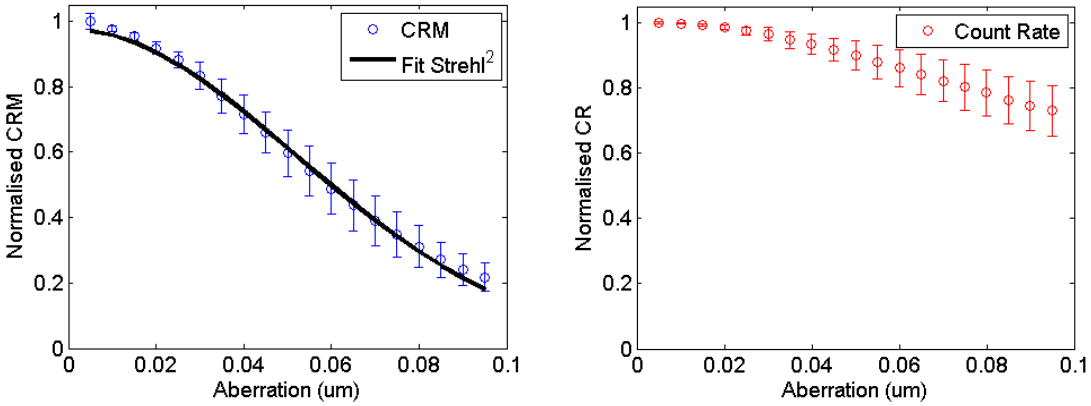

Figure 1 : A comparison of the dependence of the count rate per molecule (CRM, left), which is an FCS metric, and the fluorescence signal (CR, right) on the quantity of induced aberration by the DM, for 7 Zernike modes (Z = 3,5,7,8,9,10,12). The data points represent the average values for the 7 modes for a given aberration value shown with their respective standard deviations. The dependence of the CRM is shown to be in good agreement with Strehl ratio squared for all modes tested.

It is of interest to understand the dependence of each of these metrics on the amplitude of aberration mode present and examine if this dependence varies with the contrast of the sample. We have already shown that the metric of FCS has a dependence on Zernike aberration modes which is approximately equal to the Strehl ratio squared for low order Zernike modes [1]. We examine if this dependence holds for higher order modes (up to the 8th radial Zernike order). We compare measurements of FCS measurements with measurements of the fluorescence signal, a metric which is commonly used in sensorless AO systems [2]. Furthermore, using samples with varying levels of contrast, we examine if this has an effect on the image based metrics.

The metric of fluorescence intensity alone is far less sensitive to aberrations than the FCS metrics for point wise measurements in solution, as shown in Figure **1**. However, the estimation precision of the count rate itself is much higher. We compare theoretically and experimentally the efficiency of each metric, the efficiency being the quantity of photons required to achieve a certain precision of aberration correction.

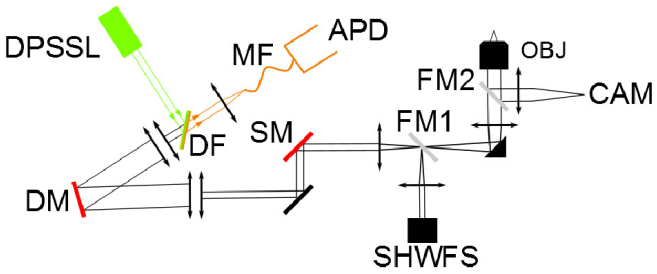

Figure 2 : The optical layout. DPSSL: 561 nm diode-pumped solid state laser (Cobolt); DM: 97 actuator deformable mirro (ALPAO); OBJ: 63x /1.2 water immersed microscope objective (Zeiss); SM: 3 mm X/Y galvanometric mirrors (Cambridge Technology); APD: single photon counting avalanche photodiode (Perkin Elmer); MF: 50 µm multimode fiber; DF: 600 nm long-pass dichroic filter (Chroma); SHWFS: 32 x32 Shack-Hartmann wavefront sensor for DM calibration (ALPAO); CAM: wide field camera; FM1: flip mirror for DM calibration with SHWFS; FM2: flip mirror for transmission microscopy.

For these experiments we use a custom built confocal microscope (Figure **2**) equipped with a deformable mirror (ALPAO HSDM 97-15) and a high NA objective (Zeiss 1.2W) to take images and FCS measurements in samples with aberrating phantoms. With this setup we are capable of accurately generating aberrations up to the 8th radial Zernike order.

Adaptive optics is an indispensible technique for optical quantification methods in tissues [3]. Even with modest amplitudes of aberrations present, which would not pose significant problems for imaging, quantification measurements such as FCS become unusable. Through this study we wish to determine efficient strategies to correct optical aberrations to enable the application of quantification microscopy methods in deep tissues.

REFERENCES

[1] C.-E. Leroux, I. Wang, J. Derouard, and A. Delon, "Adaptive optics for fluorescence correlation spectroscopy," Opt. *Express* **19**, 26839-26849 (2011)

[2] D. Débarre, E. J. Botcherby, T. Watanabe, S. Srinivas, M. J. Booth, and T. Wilson, "Image-based adaptive optics for two-photon microscopy," *Opt. Lett.* **34**, 2495-2497 (2009)

[3] C.-E Leroux, S. Monnier, I. Wang, G. Cappello, and A. Delon, "Fluorescent correlation spectroscopy measurements with adaptive optics in the intercellular space of spheroids," Biomed. Opt. Express **5**, 3730-3738 (2014)

Holographic Wave Front Control by Acousto-Optic Diffraction for Fast 3D-Microscopy of Bulk Biological Tissue at Cellular Resolution

Walther Akemann[1], Jean-François Léger[1], Cathie Ventalon[1], Benjamin Mathieu[1],
Stéphane Dieudonné[1], Laurent Bourdieu[1]

[1]*Institute of Biology (IBENS), CNRS UMR 8197, École Normale Supérieure (ENS)*
46 rue d'Ulm, 75005 Paris, France
akemann@biologie.ens.fr

Keywords:
Two-photon microscopy, Holography, Acousto-Optics, Diffraction lens,
Random-address, Laser pulse amplification

BACKGROUND: Decoding of information from large physiological neuronal networks, such as the mammalian cerebral cortex, is difficult because of complex recurrent connectivity, large neuron number in dense package and extensive neuronal heterogeneity. Even a single cortical column in mouse sensory cortex, composed of neurons sharing the same receptive field, contains more than 5000 neurons. The most exhaustive spike sampling from in-vivo cortical networks, of up to 500-1000 single units, is attained today by time-resolved two-photon imaging of molecular Ca^{2+}-sensitive probes in resolved neuron cell bodies [1]. However, laser scanning by pivoting mirrors limits fast sampling to a single image plane whereas sampling from neurons in 3D networks, like the cortical column, requires fast control of the excitation focus in 3D space. Holography, in principle, would allow shaping the laser beam to almost any desirable 3D template [2]. However, common liquid crystal-based spatial light modulators (SLMs) are too slow to match neuronal activity timescales. In the present work we explore acousto-optic phase gratings for holographic wave front control of excitation light at high refresh rates compatible with fast random-address, two-photon imaging for extended sampling of 3D cortical networks. A dedicated microscope implementing these principles is currently being set up.

EXPERIMENT: Acousto-optic deflectors (AODs) permit generation of one-dimensional phase gratings at a refresh rate limited ultimately by the time the sound wave takes to fill the AOD optical aperture, 40 kHz in our case, up to 3 orders of magnitude faster than by current generation SLMs. We set up a system consisting of two AODs for beam diffraction in perpendicular directions, together with a third AO crystal for compensation of spatial and temporal dispersion [3-4]. To avoid non-stationarity of diffraction induced by the propagation of the acoustic wave-form we synchronized the laser source to the write cycle of the acoustic wave. Since in this way only 0.2 % of laser pulses emitted from a standard 80 MHz mode-locked laser oscillator are used, we compensate for the loss in mean excitation power by amplifying the used pulses by regenerative and parametric amplification, yielding 5 µJ pulses of 200 fs at 40 kHz, tuneable from 800 to 1300 nm. Acoustic wave-forms are obtained from a digital wave synthesizer running on a 14 MHz write clock.

RESULTS: To verify the principle of AOD wave front control we tested for the ability to reproduce Zernike polynomial wave fronts up to 13^{th} order. As can be seen in Fig. 1, tilts (j=1, 2), focus (j=4), and 0° astigmatism (j=5, 13) are completely reproduced, while trefoil (j=6, 9), coma (j=7, 8) and spherical aberration (j=12) are reproduced partially. Not reproduced, and therefore omitted from the figure, are 45° astigmatism (j=3, 11) and quadrafoil (j=10).

In the case of first order spherical aberration the template match is 46 %, as expected from the contribution of a non-orthogonal polynomial term, not producible with two orthogonal phase gratings.

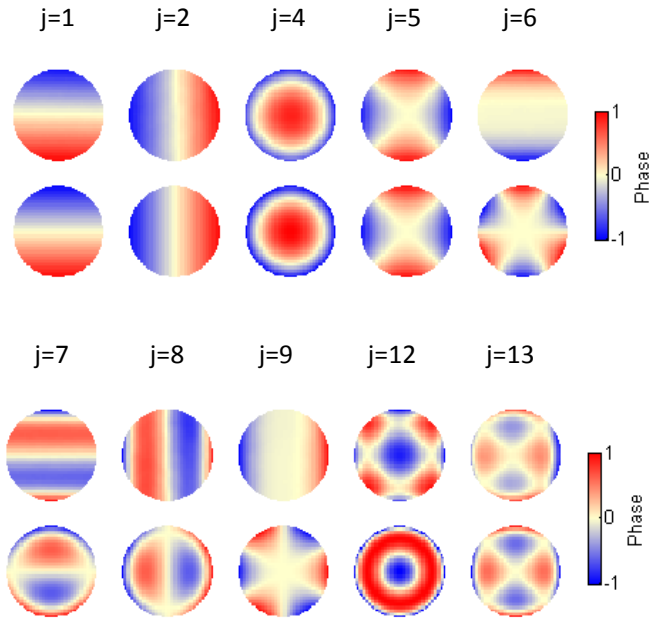

Fig.1 Normalized phase patterns of a laser beam (840 nm) shaped by two orthogonal, AOD-generated phase gratings approximating Zernike polynomial functions of Noll order j, shown together with their respective Zernike templates (below). Experimental phases acquired with a 32x40 Shack-Hartmann sensor.

Our results suggest that AODs could in principle be employed for adaptive correction of optical aberrations in cases where aberrations of low order dominate. For optimal compensation of spherical aberration, a third AOD oriented at 45° could be added as a generator for the non-orthogonal term. Fast 3D focus control only requires tilt and focus, both of which are fully consistent with the two-AOD-configuration.

Another benefit of holographic control of the excitation light is the possibility to generate several foci within the area of single cell bodies with the aim to improve signal-to-noise ratio, which in turn will permit shorter dwell times and hence help to sample more neurons at given temporal resolution. For this, we tested AOD-compatible phase functions producing 3x3 and 4x4 grid foci. We will show results obtained from phase functions calculated with an iterative Fourier transform algorithm as compared to multiple-tilt pupil segmentation.

REFERENCES

[1] S.P. Peron, J. Freeman, V. Iyer, C. Guo and K. Svoboda, "A cellular resolution map of barrel cortex activity during tactile behavior", Neuron, vol. 86, no. 3, pp. 783-799, 2015.

[2] A. Vaziri and V. Emiliani, "Reshaping the optical dimension in optogenetics", Curr Opin Neurobiol., vol. 22, no. 1, pp 128-137, 2012.

[3] R. Salomé, Y. Kremer, S. Dieudonné, J.F. Léger, O. Krichevsky, C. Wyart, D. Chatenay and L. Bourdieu, "Ultrafast random-access scanning in two-photon microscopy using acousto-optic deflectors", J. Neurosci. Methods, vol. 154, no. 1-2, pp. 161-174, 2006.

[4] Y. Kremer, J.F. Léger, R. Lapole, N. Honnorat, Y. Candela, S. Dieudonné and L. Bourdieu, "A spatio-temporally compensated acousto-optic scanner for two-photon microscopy providing large field of view", Opt. Express, vol. 16, no. 14, pp. 10066-10070, 2008.

Rapid and precise wavefront control with an Acousto-Optic Lens

Paul A. Kirkby[1] and George Konstantinou[1], K. M. Naga Srinivas Nadella[1], Victoria Griffiths[1], John E. Mitchell[2], Geoffrey Evans[1] and R. Angus Silver[1]

[1] *Neuroscience, Physiology and Pharmacology Department, University College London, Gower Street London WC1E6BT UK*
[2] *Electronic and Electrical Engineering Department, University College London, Gower Street London WC1E6BT UK*

a.silver@ucl.ac.uk

Keywords: wavefront control, acousto-optics

ABSTRACT

Shaping optical wavefronts with deformable mirrors and Liquid crystal on Silicon (LCOS) spatial light modulators has a wide range of applications in astronomy, biology, physics and chemistry. However, choosing between them involves a trade-off between response speed, spatial frequency and precision. Moreover, these devices are too slow for use with acousto-optic lens (AOL)-based 3D imaging microscopes, which perform random access laser pointing at rates of 30-50 kHz. To address this we have explored the possibility of performing wavefront shaping with an AOL. Optical phase patterns were generated by driving the AOL with nonlinear frequency vs time waveforms using a custom-designed FPGA control system.

We first demonstrate that, with 2 AODs forming a cylindrical AOL, introduction of third order phase aberrations enabled continuous linear scanning of the focal point spread function in the X-Z plane, while introduction of 4th order phase aberrations corrected for the spherical-type (fourth order cylindrical phase) aberration introduced by a fixed optical element. Our results establish that aberration correction can be performed with a wavefront shift of up to more than 25λ of continuous correction at a pulsed rate of 30 kHz with a precision of better than $\lambda/35$.

Preliminary results with a recently developed 3D AOL microscope with non-linear RF drive capability on all four AODs forming the AOL, suggests that high speed line scans with X,Y and Z components can be achieved with adding 3rd order non-linear phase terms. Moreover, curved scans can be formed by adding 4th order phase terms. These results suggest that AOL based waveform shaping could be useful for high speed imaging of arbitrarily tilted planes or curved surfaces respectively.

ACKNOWLEDGEMENTS

Funded by the Wellcome Trust and ERC.

Multicolor and light-sheet excitation approaches for high-content multiphoton imaging of tissues

Emmanuel Beaurepaire[1], Pierre Mahou[1], Nelly Vuillemin[1], Katie Matho[1,2], Lamiae Abdeladim[1], Delphine Débarre[1,3], Karine Loulier[2], Xavier Morin[4], Sébastien Wolf[5], Raphael Candelier[5], Georges Debrégeas[5], Jean Livet[2], Willy Supatto[1]

[1] *Lab. for optics and biosciences, Ecole polytechnique, CNRS, INSERM, Univ Paris-Saclay, 91128 Palaiseau, France*
[2] *Institut de la Vision, Université Pierre et Marie Curie, INSERM, 75012 Paris, France*
[3] *Lab. for interdisciplinary physics, Université Joseph Fourier, CNRS, 38402 St Martin d'Hères, France*
[4] *Institut de biologie de l'Ecole Normale Supérieure, ENS, CNRS, INSERM, 75005 Paris, France*
[5] *Laboratoire Jean Perrin, Université Pierre et Marie Curie, CNRS, 75005 Paris, France*

emmanuel.beaurepaire@polytechnique.edu

Keywords: multiphoton microscopy, wavelength mixing, light-sheet.

Current issues in developmental biology and neuroscience require tissue-scale measurements of multiple cell parameters. Multiphoton fluorescence microscopy has proven invaluable for tissue studies with its ability to provide cellular resolution in thick/live samples. However established methods are still limited in terms of their speed, depth, absence of toxicity, and ability to simultaneously probe multiple parameters.

We will discuss some recent advances towards high-content and/or large volume multiphoton tissue imaging. First, the approach of wavelength mixing [1] enables the simultaneous acquisition of several multiphoton signals, enabling efficient combination of fluorescence with coherent contrasts (SHG, THG), or multicolor fluorescence imaging of brainbow[2]-labelled tissues. Second, two-photon light-sheet excitation enables rapid two-photon imaging with reduced photobleaching, and delivers an interesting combination of imaging speed and depth [3], while being compatible with multicolor excitation [4].

We will present the application of these methods to some practical cases, and related experimental issues.

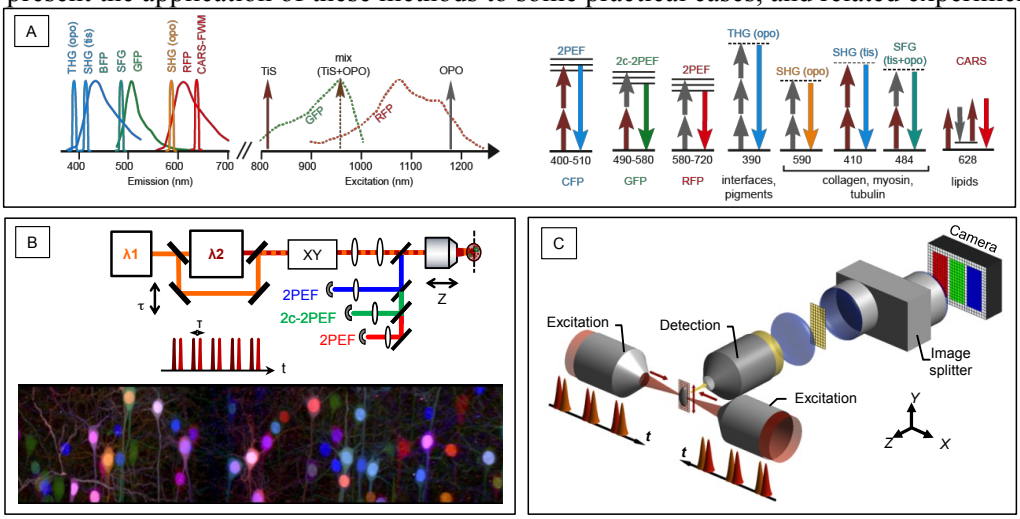

Figure 1: (A), multiphoton signals produced during a two-color wavelength mixing experiment. (B), implementation in a point-scanning microscope and application to Brainbow tissue imaging (adapted from [1]). (C), implementation in a light-sheet geometry (adapted from [4]).

REFERENCES

[1] P. Mahou et al, "Multicolor two-photon tissue imaging by wavelength mixing", *Nat. Methods, vol.* 9, pp. 815-818 (2012).

[2] J. Livet et al, "Transgenic strategies for combinatorial expression of fluorescent proteins in the nervous system", *Nature, vol.* 450, pp. 56-62 (2012).

[3] S. Wolf et al, "Whole-brain functional imaging with two-photon light-sheet microscopy", *Nat. Methods, vol.* 12, pp. 379–380 (2015).

[4] P. Mahou et al, "Multicolor two-photon light-sheet microscopy", *Nat. Methods, vol.* 11 pp. 600-601 (2014)

Wave front shaping and optogenetics

Valentina Emiliani

Wavefront Engineering microscopy group (CNRS UMR8250), Neurophotonics Laboratory,

University Paris Descartes, Sorbonne Paris Cité, 45 rue des Saints Pères, 75006 Paris, France

valentina.emiliani@parisdescartes.fr

Keywords: optogenetics, two photon microscopy, temporal focusing, computer generated holography.

The ability to perturb and manipulate the flow of excitation and inhibition, enabled by a rapidly developing repertoire of optogenetic actuators, is essential for elucidating causal relationships between neural circuit activity and function. Optogenetic tools have spurred a parallel revolution in optical technology to realize their full potential for brain circuit interrogation, specifically through the development of methods for light patterning. An ideal light delivery method should be: efficient, robust to scattering, span multiple spatial scales, and feature high spatial (micron) and temporal (millisecond) resolution.

To accomplish these goals, our laboratory utilizes computer generated holography (CGH) [3] generalized phase contrast (GPC) [4], and temporal focusing (TF) [5] to generate shaped single- and two-photon (2P) excitation volumes into neural tissue. Specifically, we have shown that wave front shaping, accomplished with a liquid crystal matrix, enables dynamic control of the light at the sample plane matching the geometry of structures or circuits of interest with micrometer lateral and axial resolution. With these approaches efficient 2P stimulation of single and multiple cells expressing ChR2, in culture and brain slices can be achieved [1, 6]. Furthermore, temporally focused shapes propagate deep into scattering brain tissue with high spatial fidelity at depths up to 500μ [7]. This robustness to scattering further underscores the potential of this technology for *in vivo*, multi-layer circuit manipulation, with spatial and temporal sophistication approaching that of observed intrinsic neuronal activity.

The fascinating prospect of optically orchestrating neuronal circuitry *in vivo* motivate the development of wavefront-shaping-based illumination schemes compatible with applications on awake and freely behaving mice. In this case an all-optical approach combining patterned photo stimulation and Ca^{2+} imaging is of particular interest. We have recently demonstrated patterned photostimulation and functional imaging with optical sectioning in freely behaving animals by using a new fiberscope composed by a fiber bundle and a micro-objective. 1P excitation patterns for targeted photoactivation are created by CGH and focused onto the input surface of a flexible fiber-bundle. The bundle and associated micro-objective transmit and image the excitation patterns into the mouse brain. Functional imaging is obtained by combining the system with a versatile imaging system that permits, through the use of a digital micromirror devices, fluorescence imaging with different modalities comprising widefield epifluorescence, structured illumination and multipoint confocal imaging. The capabilities of the fiberscope are demonstrated in mice co-expressing ChR2-tdTomato and GCaMP5-G in cerebellar interneurons. Single and multiple cell photostimulation with near cell resolution and Ca^{2+} imaging with optical sectioning are demonstrated in anesthetized and freely behaving mice [8]. The holographic fiberscope permits the control and monitoring of circuit dynamics in freely behaving mice with unprecedented spatial precision, and will permit elucidating the link between neural circuit dynamics and animal behaviour.

REFERENCES

1. Papagiakoumou, E., et al., *Scanless two-photon excitation of channelrhodopsin-2.* Nature Methods, 2010. **7**(10): p. 848-54.
2. Lutz, C., et al., *Holographic photolysis of caged neurotransmitters.* Nat Methods, 2008. **5**(9): p. 821-7.
3. Curtis, J.E., B.A. Koss, and D.G. Grier, *Dynamic holographic optical tweezers.* Opt. Communi., 2002. **207**: p. 169.
4. Glückstad, J., *Phase contrast image synthesis.* Opt.Commun, 1996. **130**: p. 225.
5. Oron, D., Tal, E., Silberberg, Y., *Scanningless depth-resolved microscopy.* Opt. Express, 2005. **13**(5): p. 1468-1476.
6. Begue, A., et al., *Two-photon excitation in scattering media by spatiotemporally shaped beams and their application in optogenetic stimulation.* Biomed Opt Express, 2013. **4**(12): p. 2869-79.
7. Papagiakoumou, E., et al., *Functional patterned multiphoton excitation deep inside scattering tissue.* Nature Photonics, 2013. **7**(4): p. 274-278.
8. Szabo, V., et al., *Spatially Selective Holographic Photoactivation and Functional Fluorescence Imaging in Freely Behaving Mice with a Fiberscope.* Neuron, 2014. **84**(6): 1157-1169.

Micromirror structured illumination microscopy with adaptive optics for *in vivo* drosophila brain imaging

Mélanie Pedrazzani[1], Daniele Nutarelli[1], Thomas Préat[3], Paul Tchenio[1,3], Alexandra Fragola[2], Vincent Loriette[2]

[1] *Laboratoire Aimé Cotton, CNRS, Université Paris-Sud 11, ENS Cachan, Campus d'Orsay, Orsay, France*
[2] *LPEM UMR8213, ESPCI CNRS UPMC, 10 rue Vauquelin, 75005 Paris, France*
[3] *GDSM, Laboratoire de Neurobiologie, UMR7637, ESPCI, 10 rue Vauquelin, 75005 Paris, France*

melanie.pedrazzani@gmail.com

Keywords: in vivo imaging, structured illumination microscopy, drosophila melanogaster, adaptive optics.

Cellular and neural network dynamics during memory formation remain poorly known. *Drosophila melanogaster* is a unique model to better understand them. Its main advantages are the small size of its brain which gives an optical access to the whole brain after microsurgery, the tractability of global analysis of the whole network and the availability of powerful genetic methods while *Drosophila melanogaster* demonstrate remarkable learning abilities [1]. Genetically encoded fluorescent reporters have given a special place to optical microscopy in drosophila neurobiology research because they allow *in vivo* analyses of biochemical processes, with good temporal resolution in targeted well-defined cells owing to the binary UAS-GAL4 system. In this field, current optical implementations rely on commercial optical set-up, usually confocal microscope. Integrated analysis of most brain functions, like memory for instance, would benefit from a global 3D monitoring of activity of the neurons involved in the function which is out of reach of current confocal approaches. To take advantage of the potential temporal resolution of the reporter, we developed a wide-field microscope based on structured illumination [2] by a micromirror matrix technology. This microscope exhibits both high speed imaging and optical sectioning ability compatible with *in vivo* imaging [3]. However, wavefront distortion strongly limits its ability to image structures burried tens of microns inside tissues due to degradation of the structuration of the illumination (Figure 1). In order to overcome this limitation and preserve the high temporal resolution, we have implemented an adaptive optics loop in both illumination and emission pathways of our wide-field fluorescence microscope. This original implementation of adaptive optics for aberration correction in HiLo microscopy significantly improves *in vivo* fluorescence imaging contrast and resolution (Figures 2 and 3).

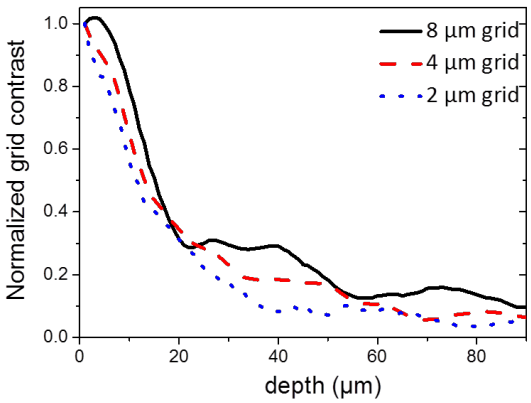

Figure 1: Evolution of the contrast of patterns used for structured illumination microscopy with depth imaging in drosophila brain. The periods of the structuration are given in the sample plane.

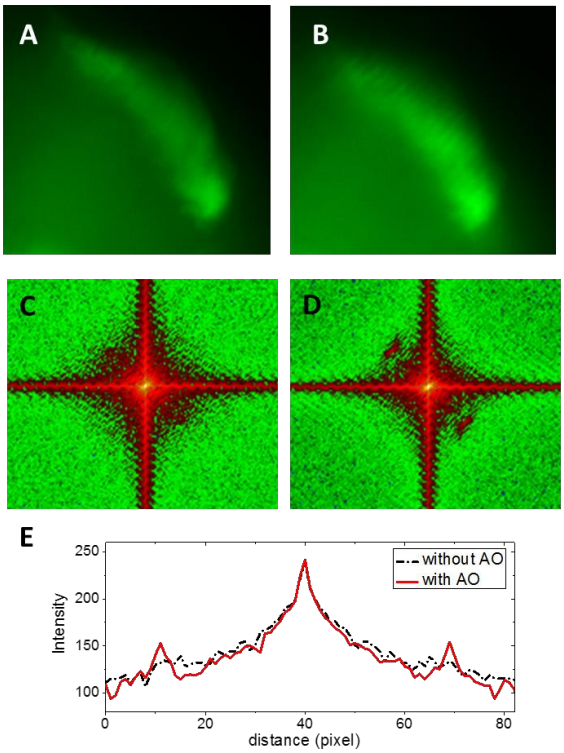

Figure 2: (A) Grid projection into drosophila brain at 40 µm depth without adaptive optics. (B) Grid projection into drosophila brain at 40 µm depth without adaptive optics. Image size: 80 x 80 µm. (C) Fourier diagram corresponding to image shown in A. (D) Fourier diagram corresponding to image shown in B. (E) Fourier line plots without (black line) and with implementation of adaptive optics (red line).

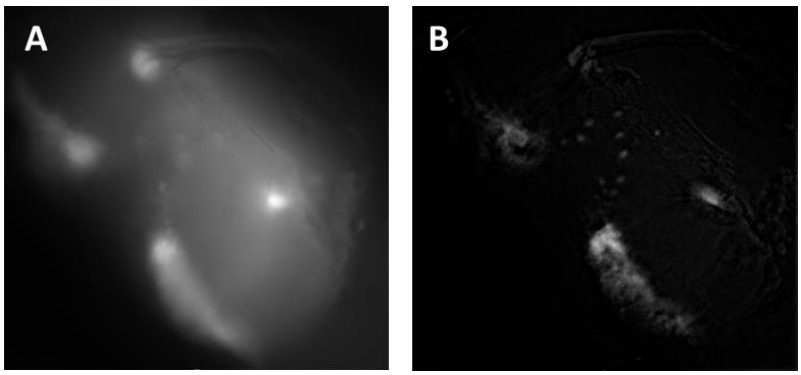

Figure 3: (A) Wide-field image into drosophila brain at 40 µm depth. (B) HiLo reconstruction image into drosophila brain at 40 µm depth with adaptive optics. Image size: 180 x 180 µm.

REFERENCES

[1] A. Pascual and T. Preat, "Localization of Long-Term Memory Within the Drosophila Mushroom Body," *Science*, 294, 5544, pp. 1115–1117, 2001.

[2] J. Mertz and J. Kim, "Scanning light-sheet microscopy in the whole mouse brain with HiLo background rejection," *J. Biomed.Opt.*, 15, 1, 2010.

[3] A. Masson; M. Pedrazzani; S. Benrezzak; P. Tchenio; T. Preat and D. Nutarelli, "Micromirror structured illumination microscope for high-speed in vivo drosophila brain imaging," *Optics express*, 22, 2, pp. 1243-1256, 2014.

Enhanced imaging of hippocampal activity using adaptive optics in living mice

Dorian Champelovier[1,2], Joel Teixeira[3], Thomas Tressard[1], Jean-Marc Conan[3], Laurent Mugnier[3], Serge Monneret[2], Serge Meimon[3], Rosa Cossart[1], Hervé Rigneault[2], Arnaud Malvache[1,2]

[1] *Institut de Neurobiologie de la Méditerranée, INSERM U901, BP13 13273 Marseille Cedex 09, France*
[2] *Aix-Marseille Université, CNRS, Centrale Marseille, Institut Fresnel UMR 7249, 13013 Marseille, France*
[3] *Onera - the French Aerospace Lab, F-92322 Châtillon, France*

arnaud.malvache@inserm.fr

Keywords: Hippocampus, adaptive optics, two-photon microscopy.

1. IN VIVO IMAGING OF THE HIPPOCAMPUS

The hippocampus is a region of the brain involved during navigation and in certain type of epilepsy. Imaging its neural activity using calcium probes allows recording simultaneously hundreds of neurons. This technique, recently applied to *in vivo* experiments in the mouse hippocampus using two-photon fluorescence led to pioneer results [1-3]. However, chronical imaging is rendered difficult due to the evolution of the field of view quality across days and the accessible depth is intrinsically limited. Indeed, wavefront aberrations drastically reduce the contrast inside the brain tissue and thus the maximal depth of imaging highly depends on the sample optical quality (linked to the surgeon performance).

The hippocampus is divided in sub-regions containing well-defined layers (Fig.1). Everyday experiments are currently done at 200μm deep in the CA1 region where neuron cell bodies are densely packed. With the animal head-fixed on a treadmill, we studied the spatial information held by the network [2] and the pathological activity in epileptic mice [3]. To obtain more reliable samples and to be able to image deeper, optical aberration correction is required.

In the *in vivo* preparation, optical aberrations induced to the exciting laser beam come from two distinct processes: "surface aberrations" that are due to the interface between the glass window and the tissue surface and "volume aberrations" that originate from the succession of different layers. The "surface aberrations" evolves across animal (surgery) and from one day to the next (tissue inflammation). In this study we characterize these aberrations and define the optimal method to compensate them in order to enhance the imaging quality of the neural activity.

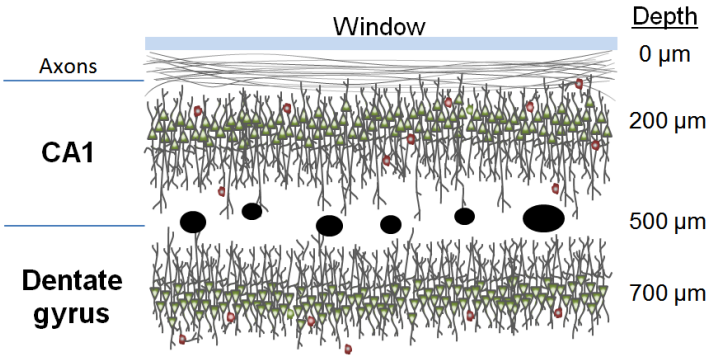

Figure 1: Layered structure of the hippocampus, axons and dendrites (black lines), cell bodies (green triangles and red circles) and blood vessels (black ellipses).

2. OPTIMAL WAVEFRONT CORRECTION METHOD

In order to find the optimal wavefront correction scheme, we compare theoretically and experimentally the two families of indirect aberration measurement that have been proposed so far, the modal-based method [4] and the pupil segmentation method [5].

We use realistic numerical simulations to define the different aberration regimes for which each method is suitable. The analysis is based on the evaluation of the return flux derived from a precise modeling of the interaction between the fluorescent neurons and the illuminating laser beam in the presence of aberrations, and for various values of the numerical aperture (NA). We found that there are conditions where the two methods complement each other; this confirms previous qualitative observations [6].

For experimentally testing the methods, we built a wavefront-controlled two-photon microscope that includes a deformable mirror (IRISAO 37 actuators). We use the modal-based method to measure the spatial aberration map. This method relies on a metric that quantifies the image quality. We studied the outcome of different metrics and found out that a metric including pattern recognition can be much better than standard metrics. In order to separately characterize "surface aberrations" and "volume aberrations" we applied the modal-based method with this new metric in different samples: fixed brain slices for volume aberration and *in vivo* mice for surface aberrations (Figure 2). We especially use this data to define the conditions where sub-region correction [7] is required. We finally quantify the increased quality of imaging of neural activity at different depths in the hippocampus.

Further experiment will use a combination of pupil segmentation and modal-based methods in order to reach the Dentate gyrus (700μm deep) of the hippocampus.

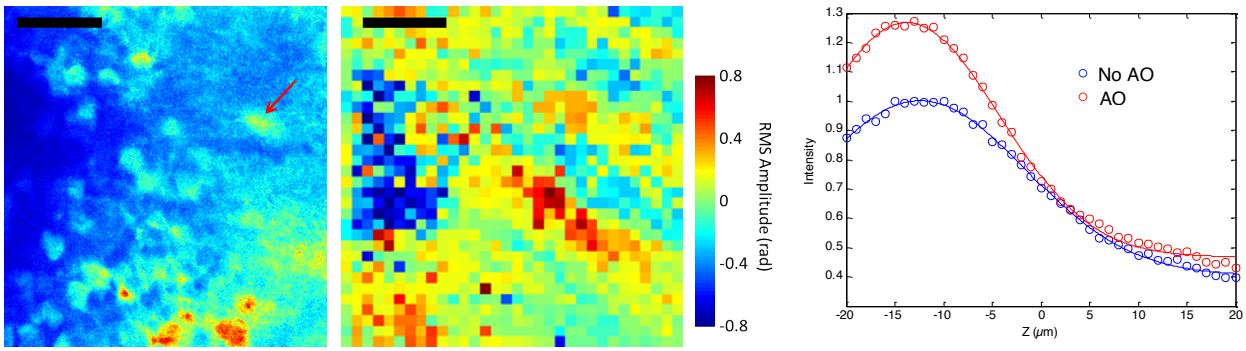

Figure 2. Left: *In vivo* image of neurons of the pyramidal cell layer (scale bar 50µm); Middle: Spatial map of the aberration amplitude of astigmatism (scale bar 50µm); Right: Axial profile of the intensity of a chosen neuron (red arrow on left panel) with and without wavefront correction; the absolute signal is increased by 27% and the resolution (axial width) is increased by 13%.

Acknowledgments: This research is partly funded by Fondation pour la Recherche Médicale

REFERENCES

[1] M. Lovett-Barron, P. Kaifosh, MA Kheirbek, N. Danielson, JD Zaremba, TR Reardon, GF Turi, R Hen, BV Zemelman, A Losonczy, "Dendritic inhibition in the hippocampus supports fear learning." Science 343 (6173), (2014)

[2] V. Villette, A. Malvache, T. Tressard, N. Dupuy, R. Cossart, "Internally recurring hippocampaal sequences as a population template of spatio-temporal information", Neuron in review.

[3] S. Feldt, V. Villette, T. Tressard, A. Malvache, S. Reichinnek, F. Bartolomei, R. Cossart, "GABAergic inhibition shapes interictal dynamics in awake epileptic mice", Brain in revision.

[4] D. Débarre, E. J. Botcherby, T. Watanabe, S. Srinivas, M. J. Booth, and T. Wilson, "Image-based adaptive optics for two-photon microscopy", Opt. Lett., 34, 2495-2497 (2009).

[5] N. Ji, D. E. Milkie, and E. Betzig, "Adaptive optics via pupil segmentation for high resolution imaging in biological tissues", Nature Methods, 7(2), 141-147 (2009).

[6] S. Meimon, J-M. Conan, L. M. Mugnier, V. Michau, R. Cossart, and A. Malvache, "Adaptive optics for in vivo two-photon calcium imaging of neuronal networks", Proc. SPIE, 8978, (2014).

[7] J. Zeng, P. Mahou, M-C Schanne-Klein, E. Beaurepaire and D. Débarre, "3D resolved mapping of optical aberrations in thick tissues", Biom. Opt. Expr. 3(8), 1898-1913 (2012).

Adaptive optics as a tool for the in vivo exploration of photoreceptor substructures

Michel Paques[1], Chahira Miloudi[1], Jonathan Benesty[1], Edouard Koch[1], Laurent Mugnier[2], Celine Chaumette[1], Florence Rossant[3], Guy Le Besnerais[2], Caroline Kulcsar[4], Isabelle Bloch[5], Serge Meimon[2]

[1] *Clinical Investigation Center 1423, Quinze-Vingts Hospital, 28 rue de Charenton 75012 Paris, France*
[2] *Office National d'Etudes et de Recherches Aéronautiques, 92320 Châtillon, France*
[3] *Institut Supérieur d'Electronique de Paris, LISITE, Issy-les-Moulineaux, France*
[4] *Institut d'Optique Graduate School, Palaiseau,France*
[5] *TelecomParis Tech,Paris, France*

michel.paques@gmail.com

Keywords: adaptive optics, retina, photoreceptors.

Adaptive optics (AO) is an optoelectronic technique that compensates for optical aberrations by the mean of a deformable mirror. AO imaging was first developed in astronomy and later applied to fundus images. AO-based fundus cameras allow in vivo visualization of microstructures of the human retina, making the retina the only human tissue in which subcellular structures may be routinely observed. The diameter of the largest cone photoreceptors reaches ~3µm, making them visible under the aspect of a mosaic of hyperreflective dots (Figure 1). The rods photoreceptors are smaller (~1µm) hence are not as easy to visualize. There are basically two techniques for en face imaging on which AO systems are implemented: Scanning laser ophthalmoscopy (SLO) based systems and flood illumination. Here we will refer solely to flood-illumination systems.

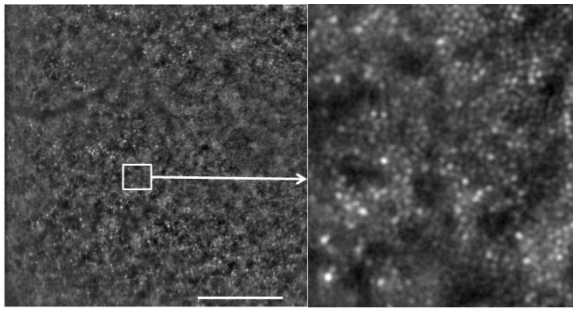

Figure 1. Imaging of the normal cone mosaic by AO flood illumination imaging (bar, 300µm).

Image processing has brought major improvements to flood-illumination AO imaging. As flood-illumination systems usually produce noisy images making microscopic structures hardly visible, a commonly used solution is to register these images and average them to increase the signal-to-noise ratio. Sub-pixellic registration [1] had a significant impact on the resulting image quality, through the suppression of peripheral rotational artifacts and hence enlarging the field over which photoreceptors can be counted. One of the most reliable and accurate approach is based on a recursive construction of thresholded components, when the seeds of the recursions are the regional maxima of the input image [2,3]. These automatic analysis algorithms benefits from advanced preprocessing methods.

Medical interpretation of high resolution images of the retina is still largely empirical. Even in normal eyes, there are a number of factors that modulate the reflectance of individual cells, to such an extent that photoreceptor show a large temporal and spatial variability. Among these factors are the spatial orientation of photoreceptors, the length of specific substructures such as the outer segment, blood circulation, the

degree of dark-adapted state… The Stiles-Crawford effect (SCE) [4] is the variation of absorbance and reflectance related to the orientation of photoreceptors, specifically cones. This may be observed by the variations of the cone mosaic under different illumination incidence. We have recently shown that this may even lead to an extinction of cone reflectance with preservation of rod reflectance (Miloudi et al, in press). Myopic deconvolution of AO images has contributed to the compensation of temporal variability of photoreceptor reflectance [5] since it enables to extract cone mosaics from raw (i.e. non-averaged) images hence avoiding artifacts related to photoreceptor scintillation and/or subsequent image processing. We subsequently developed fusion image in order to compensate for temporal and spatial variability of photoreceptor reflectance. Cone counting algorithms have thus now reached a high degree of reliability.

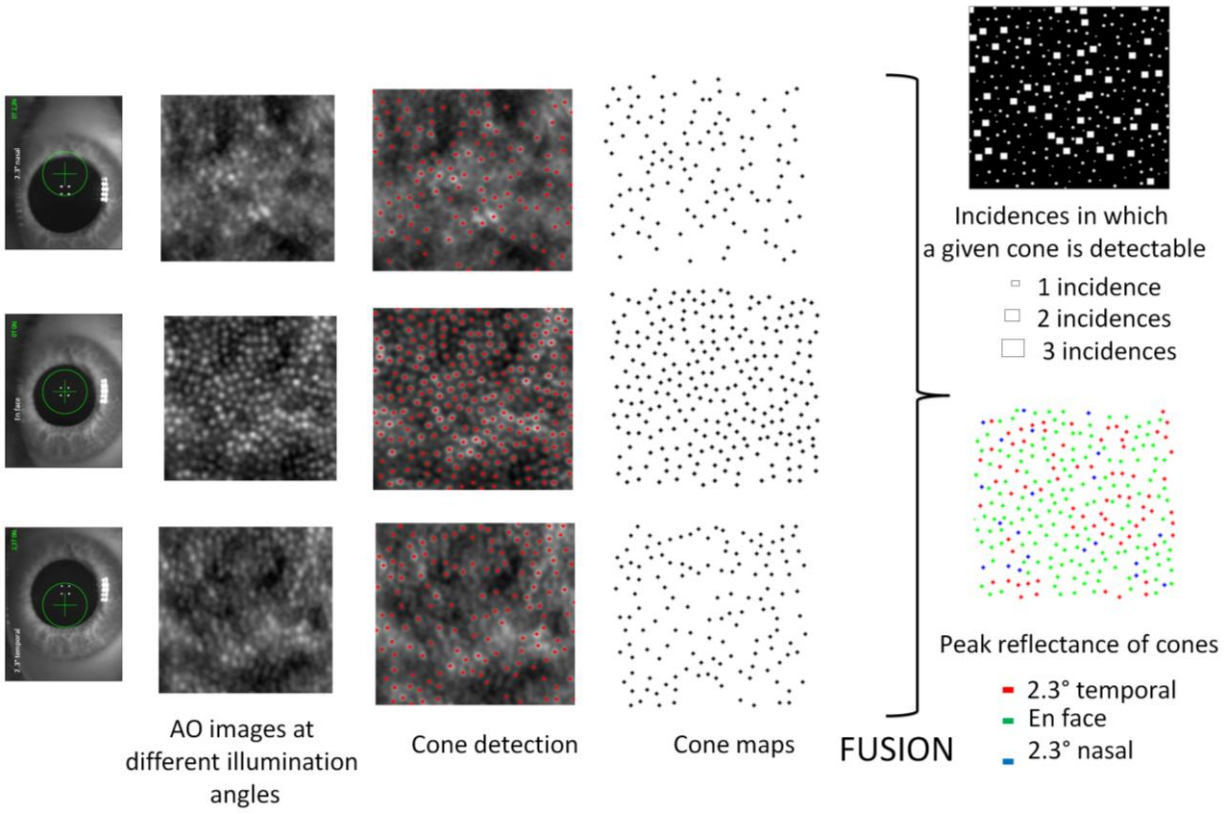

Figure 2. Processing of multiange AO images. The fusion of photoreceptor maps taken at different point of entry in the pupil increased the number of detected cones.

REFERENCES

[1] C. Kulcsár, G. Le Besnerais, E. Ödlund, X. Levecq, « Robust processing of images sequences produced by an adaptive optics retinal camera", *Optical Society of America, Adaptive Optics: Methods, Analysis and Applications*, page OW3A.3, 2013.

[2] K. Loquin, I. Bloch, K. Nakashima, F. Rossant, M. Paques, "Photoreceptor detection in in-vivo adpative optics images of the retina: towards a simple interactive tool for the physician", *IEEE International Symposium of Biomedical Imaging (ISBI'11)*, Chicago, USA, 2011.

[3] K. Loquin, I. Bloch, K. Nakashima, F. Rossant, P.-Y. Boelle and M. Paques, "Automatic Photoreceptor Detection in In-Vivo Adaptive Optics Retinal Images: Statistical Validation", *International Conference on Image Analysis and Recognition* (ICIAR 2012), Portugal, 2012

[4] G. Westheimer, "Directional sensitivity of the retina: 75 years of Stiles-Crawford effect," *Proc. Biol. Sci.* 275(1653):2777-2786 (2008).

[5] L. Blanco, L.M. Mugnier, « Marginal blind deconvolution of adaptive optics retinal images", *Opt Express*, pp-23227-(2011)

Towards Adaptive Optics assisted laser retinal microsurgery

Serge Meimon[1], Jessica Jarosz[1,2] , Cyril Petit[1], Michel Paques[3], Christian Chabrier[2], Patrice Gayot[2], Joseph Montri[1], Francis Mendez[1], Bruno Fleury[1], Jean-Marc Conan[1], Nicolas Vedrenne[1]

[1] *ONERA – the French Aerospace Lab, Châtillon, France*
[2] *Quantel Medical, Cournon d'Auvergne, France*
[3] *Clinical Investigation Center – CIC 1423 INSERM, Quinze-Vingts National Eye Hospital, Paris, France*

Serge.meimon@onera.fr

Keywords: Adaptive optics, retina, surgery, laser.

1. GOALS

Laser photocoagulation is commonly used in ophtalmology to treat a frequent cause of visual acuity degradation, the macular edema. Macular edemas may result from various pathologies, the first of which is diabetic retinopathy, affecting one to two million people in France alone. The standard treatment for macular edema is a photocoagulation at the center of the retina. However, the way this treatment is administered remains highly empirical. Increasing its precision should help one improve its efficiency while reducing undesirable side effects.

The therapeutic target of the laser can be twofold: retinal pigment epithelium (RPE) or retinal vessels. Whatever the aimed target is, it is virtually impossible, with current lasers, to prevent some degree of damage to healthy neighbouring tissues, which can entail a permanent degradation of visual acuity. This is due to a lack of control of the localisation of the laser impact, which can be explained by two reasons: firstly, current systems do not allow a real-time visualization of the volume of tissues being photocoagulated, and secondly the laser focusing quality is degraded by unintentional eye movements and by optical defects of the eye.

Retinal imaging, both in 2D and in 3D (with OCT), has been revolutionized in the past ten years by the use of adaptive optics (AO) [1,2], which allows for a real-time correction of the eye's aberrations and movements. AO is currently applied to laser beam focusing in metallurgy, to optical telecommunications, and to high-power lasers used in Physics experiments. AO thus brings a sound and proven solution both for visualizing the retina and for focusing laser beams.

Our goal is to build an ophthalmological laser system that integrates a real-time 3D visualization and an AO system in order to better control the laser delivery. Such a system will allow the surgeon to choose on the OCT image the impact point of the laser; the latter will be locked in real-time so that the laser impact is better defined in space, in the three dimensions. This revolution of the surgical procedure will bring considerable gains both in efficiency and time.

2. PRELIMINARY RESULTS

To reach this goal, current photocoagulation lasers numerical aperture has to be increased, leading to a typical 5mm entrance pupil in the eye, for which adaptive optics has to be used. We have therefore conducted a wide aberrometry campaign on more than 75 eyes, in order to precisely characterize aberration dynamics and derive AO specifications for laser photocoagulation, with an unprecedented precision and completeness [3-7]. The SCRAT bench (see fig. 1) was integrated and used at 15-20 Hospital.

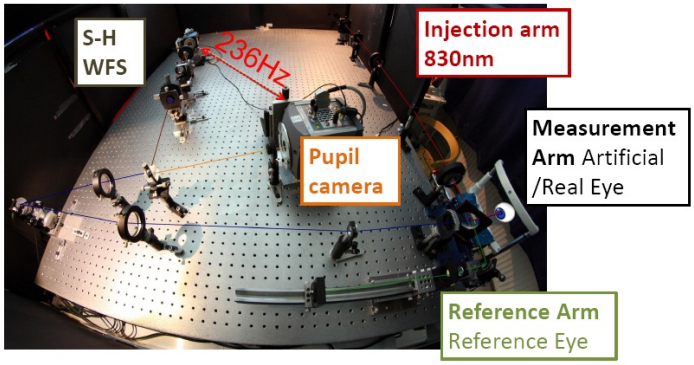

Figure 1 : SCRAT bench for fast and high resolution aberrometry with pupil tracking

From the data recorded, we picked 50 eyes for which the pupil size was bigger than 5mm, and simulated the performance of an adaptive optics closed loop system with a 5mm entrance pupil, assuming a 2 frame delay, and an integrator control law with 0.5 gain. The Strehl Ratio at 550nm as a function of the adaptive optics loop frame rate is shown in figure 2:

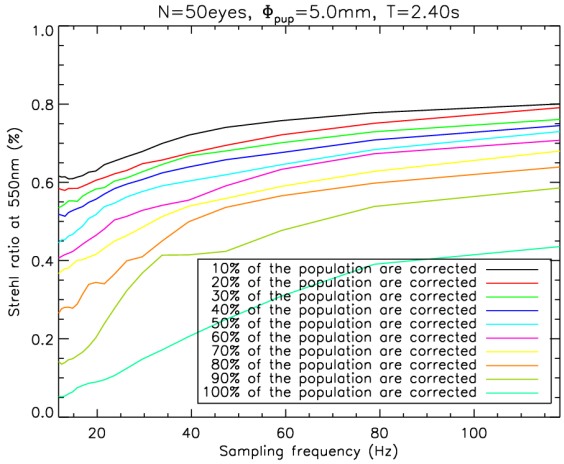

Figure 2 : Strehl Ratio as a function of the adaptive optics loop frame rate

Further results on the photocoagulation laser adaptive optics design will be presented, as well as preliminary performance of a recently built pathfinder fast rate AO imager.

REFERENCES

[1] J. F. Bille, "The development of wavefront technology and its application to ophthalmology," in Aberration-free refractive surgery (Springer-Verlag Berlin Heidelberg, 2003), pp. 1–23.

[2] J. Liang, D. R. Williams, and D. T. Miller, "Supernormal vision and high-resolution retinal imaging through adaptive optics," J. Opt. Soc. Am. A 14, 2884–2892 (1997).

[3] Diaz-Santana L, Torti C, Munro I, Gasson P, Dainty C. Benefit of higher closed–loop bandwidths in ocular adaptive optics. Optics Express. 2003; 11: 2597–2605.

[4] Nirmaier T, Pudasaini G, Bille J. Very fast wave-front measurements at the human eye with a custom CMOS-based Hartmann–Shack sensor. Optics Express. 2003; 11(21): 2704–2716.

[5] Mira-Agudelo A, Lundström L, Artal P. Temporal dynamics of ocular aberrations: Monocular vs binocular vision. Ophthal. Physiol. Opt. 2009; 29: 256-263.

[6] Leahy C, Dainty C. A non-stationary model for simulating the dynamics of ocular aberrations. Optics Express. 2010; 18: 21386–21396.

[7] Hampson K, Mallen E. Multifractal nature of ocular aberration dynamics of the human eye. Biomedical Optics Express. 2011; 2(3): 464–470.

Simple control of an adaptive optics retinal imaging system using pupil tracker measurements without pupil stabilization

Caroline Kulcsár, Vladyslav Potapchuk, Henri-François Raynaud

Laboratoire Charles Fabry – Institut d'Optique Graduate School – CNRS UMR8501, 2 av. Augustin Fresnel, Palaiseau, France

Caroline.kulcsar@institutoptique.fr

Keywords: Adaptive optics, retinal imaging, integral controller, pupil tracker.

1. CONTEXT

We propose to study the possible improvement brought by the use of pupil tracker measurements for the adaptive optics (AO) control of a retinal imaging system. This simulation study is based on the rtx1® camera built by the company Imagine Eyes® (Orsay, France). This camera features an AO system, where a Shack-Hartmann wave-front sensor (WFS, a HASO® with 32x32 sub-apertures) delivers measurements used to compute the voltages to be sent to the DM52® deformable mirror (52 voice-call actuators) in order to correct for optical aberrations. The AO system is currently controlled at 10 Hz by an integral controller, no pupil tracking is used, and there is no optical pupil stabilization. This however allows obtaining 4°x4° images with a resolution of 250 lppm (line pairs per millimeter). In this presentation, we consider the use of pupil tracker measurements together with a simple control law based on WFS measurements averaged over time.

2. SIMULATION OF THE AO SYSTEM

The system, which chronogram is illustrated in Figure 1, is simulated using 860 aberration phase screens obtained from healthy subjects, displaced using 43 different sequences of pupil displacements obtained by filtering and resampling at 1 kHz of pupil tracking measurements recorded at 80 Hz. An example of PT measurements in x (blue) and y (green) axis is given in Figure 2, together with the true positions in red. For this sequence, the standard deviation of the measurement noise is 2 µm for the x-axis and 3 µm for the y-axis, leading to a ±3σ average error in the range of [−6 µm, +6 µm] and [−9 µm, +9 µm] respectively. The maximum range on the whole data set is [−18 µm, +18 µm], depending on the displacement variance itself.

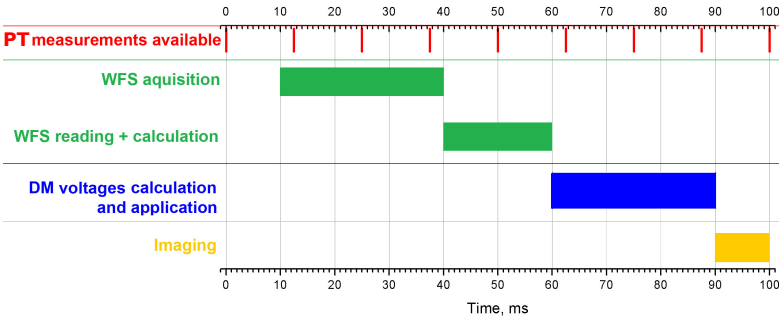

Figure 1: Chronogram used for the simulator. The unit simulation step is 1 ms.

The baseline chronogram does not use the pupil tracker. The control law is an integral controller, so voltages u_k to be applied are computed according to

$$u_k = u_{k-1} + gM_{\text{com}}y_k \tag{1}$$

where g is the gain set to 1 in this set-up, and M_{com} is the control matrix, obtained by inversion and filtering of the interaction matrix that links voltages u to slopes y. The AO loop simulator is based on an IDL code initially developed by S. Meimon (Onera) for the ANR iPhot project.

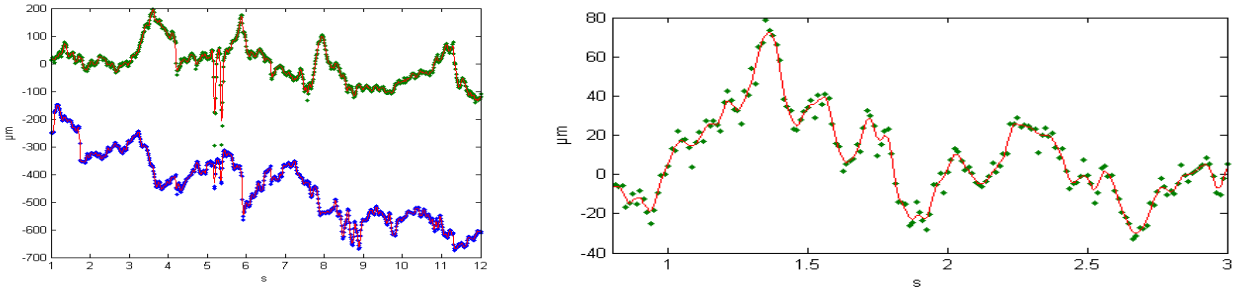

Figure 2: real PT measurements in x (blue) and y (green) axis, together with the simulated true positions in red. On the right, a zoom of the real y-axis measurements (dots) and simulated true positions (red).

3. USING A PUPIL TRACKER FOR CONTROL

We study the possible improvement brought by accounting for PT measurements for a simple control strategy based on the hypothesis that the eye aberrations are frozen aberrations displaced solely by the eye movements, in the line of what has been presented in [1]. This hypothesis has been globally validated in [2], where a test of adaptive optics correction has been conducted using only a formerly measured phase aberration displaced according to the pupil tracking measurements, instead of using WFS measurements.

The simple strategy that has been simulated here is to average WFS measurements after having shifted them to a fixed reference position. This shift is computed by averaging the 3 PT measurements recorded during WFS acquisition. Then, the averaged WFS measurements are shifted to the last PT measurement before imaging, *i.e.* the position measured just before 90ms in Figure 2.

Results are summarized in Figure 3. The histogram of residual phase variances normalized by the incoming phase variances is plotted for the two control strategies, integrator in blue and averaged measurements in green, with a median value of 6.6 10^{-4} and 2.3 10^{-4} respectively. These results show that it is interesting to develop this further by using for example better defined pupil displacements.

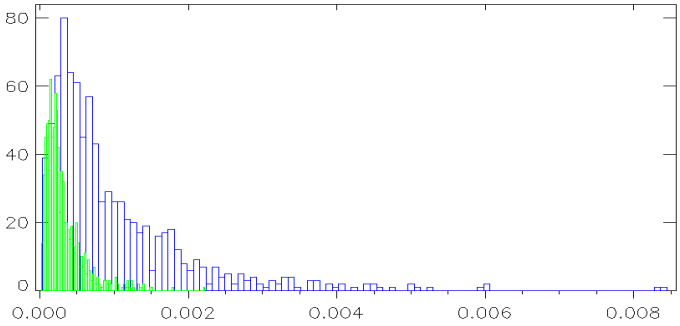

Figure 3: Histogram of normalized residual phase variances for integrator (blue) and averaged measurements (green). The y-axis corresponds to the number of simulations.

ACKNOWLEDGEMENTS

This work is supported by the French National Research Agency (ANR ReVeal) under contract ANR-12-TECS-0015. We thank very much X. Levecq (Imagine Eyes) for providing the data, and J.-M. Conan and S. Meimon (Onera) for the use of the baseline simulator and associated interesting discussions.

REFERENCES

[1] Meimon, S., Kulcsár, C., El Mrabet, Y., Sahin, B., Raynaud, H.-F. and Conan, J.-M., "Commande d'OA pour INOVEO : impact du mouvement pupillaire." JRIOA, Nantes, France, 2008.

[2] Sahin, B., Lamory, B., Levecq, X., Harms, F. and Dainty, C., "Adaptive optics with pupil tracking for high resolution retinal imaging," *Biomed. Opt. Express* 3, 225-239, 2012.

Compact adaptive optics fundus camera/Optical coherence tomography system for high resolution retinal imaging

Matthias Salas[1], Wolfgang Drexler[1], Xavier Levecq[2], Barbara Lamory[2], Anna Ledolter[3], Markus Ritter[3], Ursula Schmidt-Erfurth[3], Michael Pircher[1]

[1] *Center for Medical Physics and Biomedical Engineering, Medical University of Vienna, Währinger Gürtel 18-20 - E.4L, Vienna, Austria*
[2] *Imagine Eyes, 18 rue Charles de Gaulle, Orsay, France*
[3] *Department of Ophthalmology and Optometry, Medical University of Vienna, Währinger Gürtel 18-20, Vienna, Austria*

matthias.salas@meduniwien.ac.at

Keywords: Adaptive Optics, Optical coherence tomography, Fundus camera, Ophthalmology.

1. SUMMARY

Optical coherence tomography (OCT) has shown to be a powerful tool in detecting retinal diseases [1]. The combination of this imaging modality with adaptive optics (AO) yields high isotropic image resolution of the retina [2-5]. However, the complexity and size of such devices has been an obstacle for translating this technology to a clinical environment where space constraints are a critical issue. In order to provide additional, sometimes complimentary information, multimodal AO imaging has been proposed which combines scanning laser ophthalmoscopy with OCT [6, 7]. Here we present results of a new compact prototype imager which uses a different combination of imaging modalities: Adaptive optics fundus camera and AO-OCT (cf. Fig. 1).

The AO-fundus camera is based on a commercial product (RTX1, France) and records images with a field of view of 4°x4° at 10 frames per second. The AO-OCT is operated at 840nm with an A-scan rate of 200kHz, which is translated into a volume acquisition rate of 1.25 volumes per second (2ºx2º field of view consisting of 400x365pixels). With the AO-OCT instrument a sensitivity of 86dB was achieved. Both imaging modalities share the same AO correction path. The relay optics of the AO system is entirely based on lenses, which allows a very compact design (cf. Fig. 1C). AO is based on wavefront measurements using a Hartmann Shack wavefront sensor in combination with a laser beacon and wavefront correction is done using a 52 element deformable mirror (Mirao 52).

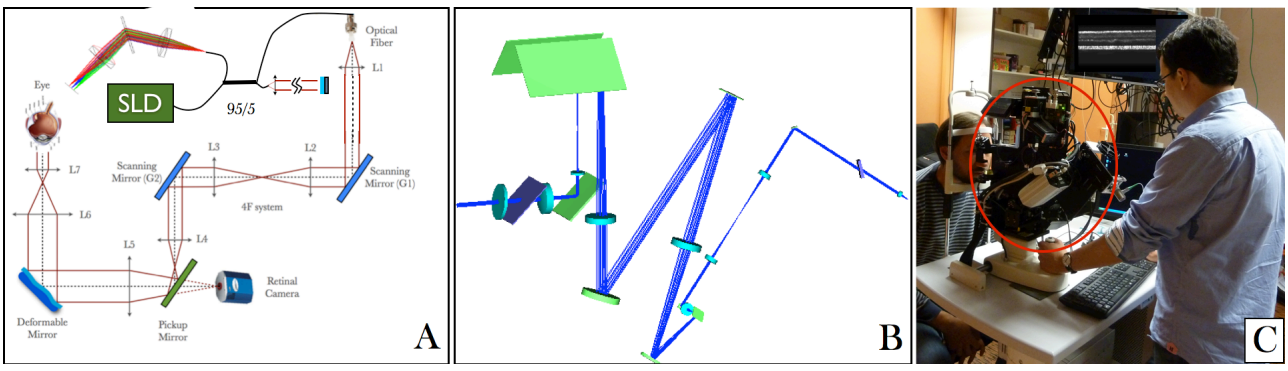

Figure 1: A) Schematic of the AO-fundus camera/ AO-OCT instrument, B) Zemax simulation of the beam propagation through the instrument, C) Picture of the compact AO-fundus camera/AO-OCT instrument during operation at the laboratory (The AO scanhead is entirely confined within the red ellipse and can be moved in three dimensions).

2. RESULTS

The prototype instrument has been used to image several healthy volunteers and patients with retinal diseases. Figure 2 presents representative images obtained in a healthy volunteer. The relatively large field of view of the AO-fundus image (red square in Fig. 2A) allows the precise determination of the imaged location. The AO-OCT volume (indicated by the orange square in Fig. 2A) is recorded at the central part of the AO fundus image. The focus of these images was set at the photoreceptor layer. Thus individual photoreceptors can be resolved in both AO imaging modalities.

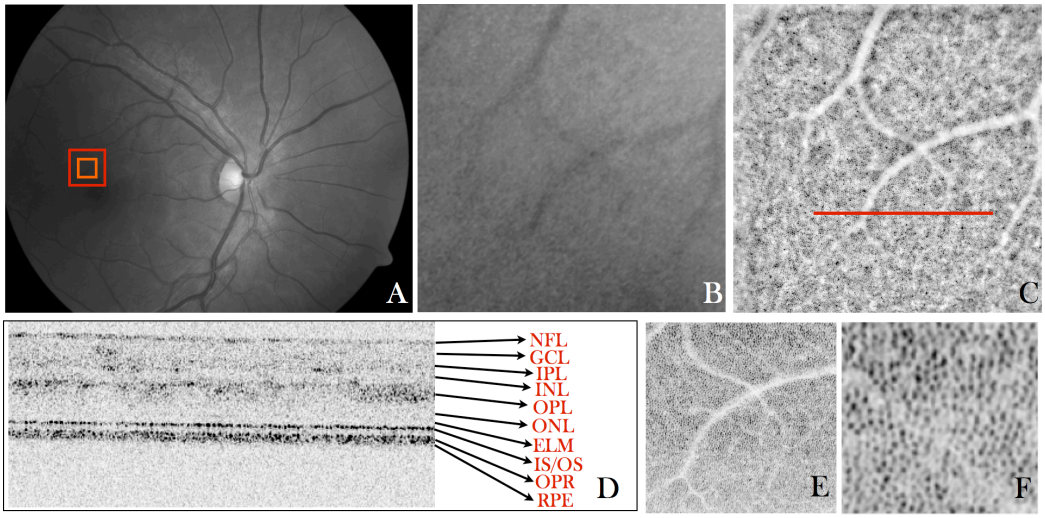

Figure 2: A) Wide field (50ºx50º) fundus image of the retina of a healthy volunteer, B) Enlarged region of interest from the wide field image indicated with the red square in A), C) AO-fundus image (4ºx4º) acquired with the new instrument at the same location as in B). The small black spots correspond to individual cone photoreceptors, D) Single B-scan acquired at the location indicated with a red line in C) and extracted from a volume scan acquired with the AO-OCT instrument at a location indicated with the orange square in A). A regular spacing corresponding to individual cone photoreceptor can be observed at the junction between inner and outer segments (IS/OS) and the outer photoreceptor layer (OPR). E) Extracted en-face image from the AO-OCT volume scan by depth integrating over the photoreceptor bands, F) Enlarged region from E) showing individual photoreceptors.

REFERENCES

[1] W. Drexler, and J.G Fujimoto, "State-of-the-art retinal optical coherence tomography," *Progress in Retinal and Eyes Research*, vol. 27, no. 1, pp. 45–88, 2008.

[2] O.P. Kocaoglu, T.L. Turner, Z. Liu, and D.T. Miller, "Adaptive optics optical coherence tomography at 1MHz," *Biomedical Express*, vol. 5, no. 12, pp. 4186–4200, 2014.

[3] S.H. Lee, J.S. Werner, and R.J. Zawadzki, "Improved visualization of outer retinal morphology with aberration cancelling reflective optical design for adaptive optics – optical coherence tomography," *Biomedical Optics Express*, vol. 4, no. 11, pp. 2508–2517, 2013.

[4] C.E. Bigelow, N.V. Iftimia, R.D. Ferguson, T.E. Ustun, B. Bloom, and D.X. Hammer, "Compact multimodal adaptive-optics spectral-domain optical coherence tomography instrument for retinal imaging," *Journal of the Optical Society of America A - Optics Image Science and Vision*, vol. 24, no. 5, pp. 1327–1336, 2007.

[5] E.J. Fernandez, B. Hermann, B. Povazay, A. Unterhuber, H Sattmann, B. Hofer, P.K. Ahnelt, and W. Drexler, "Ultrahigh resolution optical coherence tomography and pancorrection for cellular imaging of the living human retina," *Optics Express*, vol. 16, no. 15, pp. 11083–11094, 2008.

[6] D.X. Hammer, R.D. Ferguson, M. Mujat, A. Patel, E. Plumb, N. Iftimia, T.Y.P. Chui, J.D. Akula, and A.B. Fulton, "Multimodal adaptive optics retinal imager: design and performance," *Journal of the Optical Society of America A - Optics Image Science and Vision*, vol. 29, no. 12, pp. 2598–2607, 2012.

[7] F. Felberer, J.S. Kroisamer, B. Baumann, S. Zotter, U. Schmidt-Erfurth, C.K. Hitzenberger, and M. Pircher, "Adaptive optics SLO/OCT for 3D imaging of human photoreceptors in vivo," *Biomedical Optics Express*, vol. 5, no. 2, pp. 439-456, 2014.

Full field optical coherence microscopy of ocular tissues

Kate Grieve[1,2], Michel Paques[1,2] , Vincent Borderie[1,2]

[1] *CHNO des XV-XX, Paris France*
[2] *Institut de la Vision, Paris, France*

kategrieve@gmail.com

Keywords: optical coherence tomography, microscopy, ophthalmology, cornea, retina

Full field optical coherence microscopy (FFOCM) enables non invasive micron-resolution imaging in ex vivo tissues in three dimensions without staining or slicing. Analysis of transplant corneas in eye banks with this technology provides precise information about the health of the cornea, therefore optimizing tissue usage and positively influencing the outcome of the graft. Cell culture growth can be monitored non invasively at different time points with FFOCM, aiding the development of artificial cornea. In the retina, individual axons and cells are revealed without staining. Understanding of retinal, scleral and limbal anatomy in pathology such as glaucoma is assisted by FFOCM imaging of fresh surgical specimens. Future development of FFOCM for in vivo ophthalmic imaging requires increased acquisition speeds, and for retinal imaging, correction of aberrations from the anterior segment by adaptive optics.

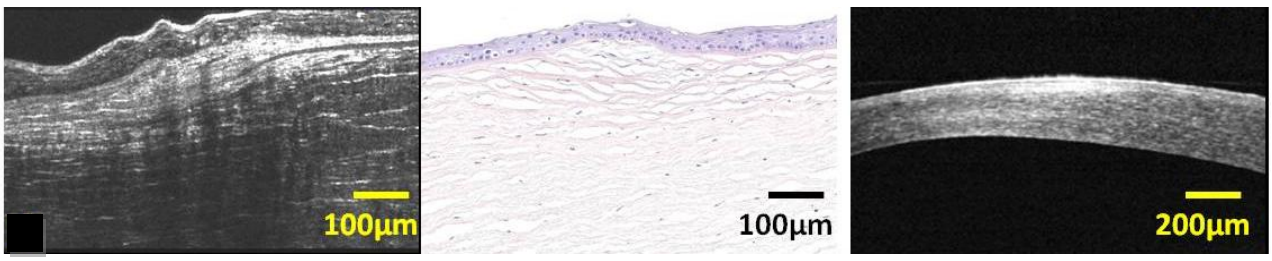

Figure 1: Keratoconus in human cornea viewed with FFOCM (left), histology (center) and SD-OCT (right).

REFERENCES

[1] Ghouali W, Grieve K, Bellefqih S et al. Full-field optical coherence tomography of human donor and pathological corneas. Cur Eye Res 2014;1-9.

[2] Grieve K, Paques M, Dubois A et al. Ocular tissue imaging using ultrahigh-resolution, full-field optical coherence tomography. Invest Ophthalmol Vis Sci 2004;45:4126-4131.

Pre-study of Retinal Imaging by Adaptive Optics Full-Field OCT with Transmissive Liquid Crystal Spatial Light Modulator

Peng Xiao, Mathias Fink and A. Claude Boccara

Institut Langevin, ESPCI ParisTech, PSL Research University, 1 rue Jussieu, 75005 Paris, France

claude.boccara@espci.fr

Keywords: Adaptive optics, Optical coherence tomography.

1. INTRODUCTION

Biological tissues are heterogeneous systems that strongly scatter light. In order to get images of in-depth structures that are hidden by scattering part, one must select ballistic photons. This is achieved by a number of optical approaches: confocal microscopy, multiphoton microscopy or optical coherence tomography (OCT). Our laboratory has developed a specific "en face" approach of OCT, Full-Field OCT or FFOCT, that uses incoherent broadband light sources coupled to imaging interferometers (e.g. Linnik) to select slices perpendicular to the optical axis. These systems do not require the usual large depth of field of standard OCT approaches and thus allow getting micron scale resolution in 3D by the use of microscope objectives [1].

If small-scale heterogeneities induce scattering, there are also multi-scale aberrating structures that reduce the spatial coherence of the imaging beams and strongly reduce the FFOCT signal. For this reason building a wavefront adaptive system is strongly needed when going in depth while keeping the high resolution of FFOCT.

Indeed the correction in many adaptive optics systems implies a conjugation of the image focal plane of the microscope objective with the wavefront senor or correction devices. These telescopes increase the optical path length that has to be balanced within less than one micrometer due to the axial sectioning of FFOCT. This strict pupil conjugation appears to be mandatory when very high order aberrations are involved because one cannot rely on a simple geometrical optics propagation of the wavefront but one has to account for the diffraction. The problem appears differently for the eye where mostly low order aberrations dominate. Several studies on eye aberrations [2] have shown that the majority of the Zernike polynomials that are involved in a large number of eyes aberrations tests are mostly of low order ones, meaning that at different steps of the propagation, the wavefront looks like a homothetic image of itself.

In order to overcome complex setups realizations and to be able to apply FFOCT to the retinal examination we have built a setup that intends to stimulate the eye examination using transmissive liquid crystal spatial light modulators (LCSLMs) [3] that could be roughly positioned close to the eyes just as the lenses that are used to correct e.g. myopia and astigmatism. By electronically varying the orientation of the molecules inside the pixels of the LCSLM, the refractive indexes of the pixels are changed; result in variable retardance abilities to the polarized light passed through. Let us underline that LCSLMs have already been used for adaptive optics to alter the refractive state [4] and also to correct the aberrations of the eye [5]. Nevertheless in both cases pupil conjugation-using telescope have been used. As mentioned before we intend to get rid of these telescopes in order to simplify the setup. Last but not least we would like to avoid the use of the pupil to observe the aberrations and their reduction. We prefer to rely on the improvement of image quality that is well adapted to the FFOCT detection [6, 7].

2. EXPERIMENT SETUP AND ABERRATION CORRECTION ALGORITHM

The apparatus schematic diagram is shown in Fig.1. The main part is the typical FFOCT system based on a Linnik interferometer. A LED (Thorlabs 660nm) is used as the low coherence light source and the two Nikon 4X/0.2NA Plan APO objectives are used to simulate the human eye. For conducting the wavefront correction, a transmissive LCSLM is installed in the sample arm right after the back aperture of the objective lens, while another identical LCSLM is set in the reference arm for dispersion correction. A polarizer is added in the illumination path since the LCSLM works only with polarized light. The setup is well aligned to ensure the focusing of the two arms and their optical paths are matched.

In our experiment, we demonstrated the wavefront sensorless correction of aberrations based on the FFOCT image quality [7]. The method consists the sequential adjustment of the coefficients of low order orthogonal Zernike Polynomial functions applied to the LCSLM. Optimization is based on the FFOCT image intensity by using the average intensity of the maximum 300 pixels as the metric function.

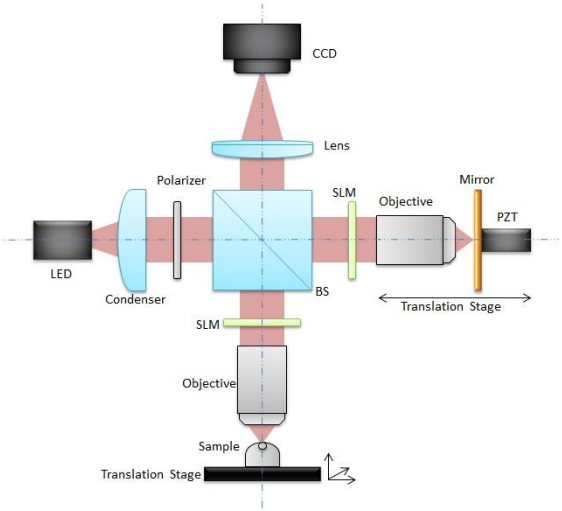

Fig.1 Schematic of adaptive optics FFOCT system coupled with LCSLMs

3. EXPERIMENT RESULTS

To test the performance and the algorithm of our AO-FFOCT system, we imaged an USAF resolution target. Here, we used the SLM in the sample arm as both aberration generator and corrector. USAF was set at the best focus position and a random aberration mask was added to the SLM. Then, defocus, astigmatism, coma and spherical aberration are corrected sequentially. Figure 2 shows that the improvement in intensity after optimization is so apparent. The increase in metric function after the correction of each Zernike mode is also presented in Fig.2.

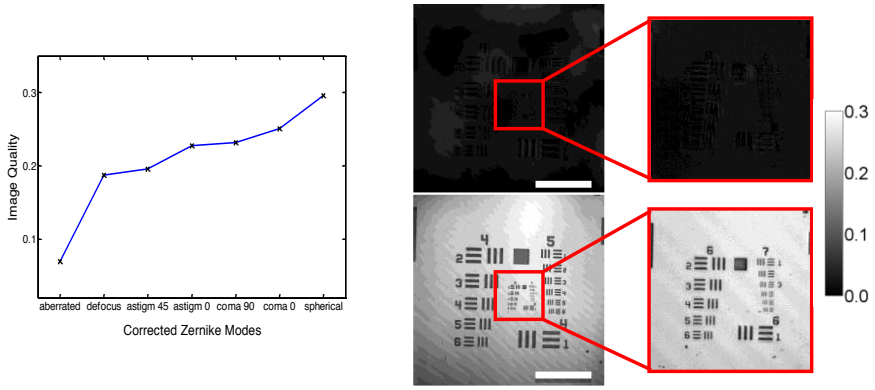

Fig.2 Left: Metric function increase after correction of each Zernike mode. Right: Comparison of the FFOCT images of USAF before (top) and after (bottom) correction of the induced random aberration. Scale bar is 500 um. Zoom in area is 425*425 um.

In order to demonstrate our system to self-induced aberration correction, a Ficus leaf was used as a scattering sample. FFOCT imaging was done at a depth of 75um under the leaf surface. And the self-induced aberration of the in depth imaging was corrected step by step as formal described. As showed in Fig.3, the optimized image shows an intensity increase and from the zoom-in images, more structure information is resolved. The graph of the metric function of FFOCT images for different coefficients of aberrations is also displayed. The highest position corresponds to the coefficient we used for the correction of each mode. The increase in metric function is also presented.

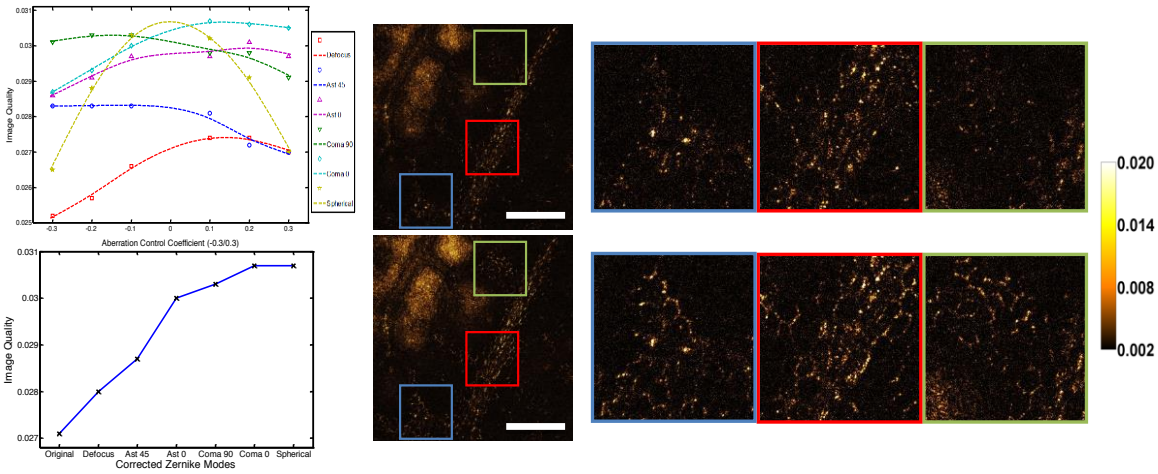

Fig.3 Left: The graph of the metric function of FFOCT images for different coefficients of aberrations (top) and the increase in metric function (bottom). Right: Comparison of the FFOCT images of the leaf before (top) and after (bottom) optimization. Scale bar is 500 um. Zoom in area is 425*425 um.

4. CONCLUSION

This preliminary approach that simulates eyes aberrations correction opens the path to a simple implementation of FFOCT adaptive optics for retinal examinations. We will soon use the new fast CMOS cameras working in the kHz range that will solve the problem of eye movements. This work was supported by the HELMOLTZ Synergy ERC project.

REFERENCES

[1] Vabre L, Dubois A and Boccara AC, Opt. Lett. **27**, 530-533 (2002).
[2] Jason Porter and David R. Williams, http://cfao.ucolick.org/pubs/presentations/eyedesign/06_Aberrations_JP.pdf (2003)
[3] D3128 Spatial Light Modulator Meadowlark Optics.
[4] L. N. Thibos and Arthur Bradley, Optometry and vision science **74**, 581-587 (1997)
[5] Fernando Vargas-Martin, Pedro M. Prieto and Pablo Artal, J. Opt. Soc. Am. A. **15**, 1998.
[6] Labiau S, David G, Gigan, S and Boccara AC, Optics Letters **34**(10), 1576-1578 (2009)
[7] Bonora S and Zawadzki RJ, Optics Letters **38**(22), 4801-4804 (2013)

Adaptive optics corrected full-field OCT for 3D retinal imaging

Marie Glanc[1*], Marie Blavier[1*], R. Dembet[1], P. Fédou[1], Gérard Rousset[1],

[1] *LESIA, Observatoire de Paris, PSL Research University, CNRS, UPMC Univ. Paris 06, Sorbonne Universités, Univ. Paris Diderot, Sorbonne Paris Cité, 5 place Jules Janssen, 92190 Meudon, France*

marie.glanc@obspm.fr

* *These authors have equally contributed to this work.*

Keywords: Adaptive optics, full-field OCT, in vivo retinal imaging

1. INTRODUCTION

Adaptive optics (AO) is now a common technique to successfully perform in vivo 2D high-resolution imaging of the human retina. In retinal imaging, the main part of aberrations comes from the anterior segment of the eye. Unfortunately, AO imaging does not show tomographic capability, meaning that several layers in a 3D sample contribute to the actual image. Full-field optical coherence tomography (FF-OCT) is an en-face interferometric technique allowing for optical sectioning. Its z-resolution is given by the illuminating light spectrum, whereas the fringe contrast is linked to the optical quality of the eye and the instrument itself.
Coupling AO and FF-OCT shall provide ophthalmologists with 3D high-resolution retinal images: AO improves both 2D lateral resolution and fringe contrast and FF-OCT provides axial resolution. To couple these 2 techniques for in vivo imaging, we proceeded step by step: we first built a conventional AO retinal imager and obtained 2D high resolution retinal images of living subjects [1]; then we designed the coupled system, which included a λ/20 mirror in place of the AO deformable mirror (DM). In this configuration, we obtained 3D reconstructions of ex vivo thin biological samples by FF-OCT. We are currently working on coupling AO and FF-OCT ex vivo.

2. EXPERIMENTAL SETUP

The system is based on a Linnik interferometer performing FFOCT imaging, with a filtered supercontinuum laser (710-750 nm) as illumination source. Images field of view is 1°. The AO part is included in the sample arm of the interferometer in order to correct for the whole sample arm aberrations.

FF-OCT axial resolution is 5 microns. 2D in-depth images are obtained in the sample with a CCD camera at 50 Hz. An example of a 4 phases reconstruction of a part of rat cerebellum is provided in Figure 1. This image was obtained with the plane mirror in place of the DM (to test the capability of the tomographic FFOCT part alone).

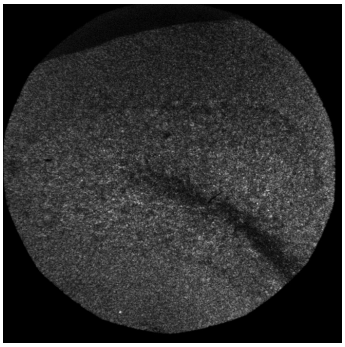

Figure 1: “Z-summation” of 10 OCT reconstructed layers in a ex vivo sample of rat cerebellum

Our current AO system is made of a 18 x 18 Shack-Hartmann wavefront sensor matched to a 97-actuator magnetic DM (ALPAO 97-15). AO system frequency is 100 Hz. The wavelength chosen for wavefront sensing is 830 nm (SLD point source formed in the sample, as a laser guide star). Imaging and WFS wavelengths are close to each other in order to reduce differential chromatism between imaging and AO correction. A shorter imaging wavelength could lead to a higher theoretical spatial resolution; however 730 nm penetrates better through biological samples and is much more comfortable for the subject. AO in the sample arm modifies the FFOCT illumination beam in double path, therefore: (i) light is well focused on the retina and, after passing through the eye, (ii) the backscattered wavefront from the retina is corrected (aberration free): lateral resolution is improved and retinal wavefront interferes correctly with the reference wavefront, providing a good fringe contrast.
Without AO, lateral resolution is worse than 20 microns and fringes contrast is degraded to a few percent in an eye.

3. COUPLING AO AND FF-OCT

The first step of coupling consisted in replacing the plane mirror by the DM without losing the accurate system alignment. This has been achieved by using information provided by the Real Time Computer and the preliminary setting of the interferometer at zero optical path difference.
The contrast measurement in closed loop on a mirror sample informs us on the highest performance of the system. The closed loop is designed to deal with the eye's aberrations, of large amplitude and dynamic. Therefore it hardly corrects for small residual aberrations in the setup. Proper calibrations have to be introduced in order to get this limit as high as possible: for instance, acquiring as accurately as possible the reference slopes for the AO with respect to FFOCT image quality and taking into account the system differential aberrations by a dedicated method. We registered interferometric fringes in the pupil plane to check the flatness of the DM (Figure 2). Fringe patterns are visible around the actuators, involving high spatial frequencies that can not be corrected by the AO loop. As it degrades image quality, we have to improve DM flatness by other calibrations. In a short term, a comparison of our system performance with others [2] shall be done.

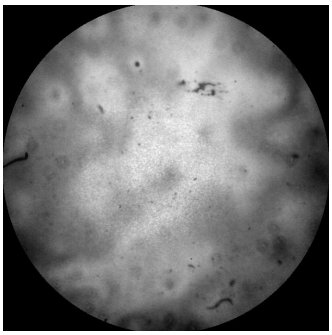

Figure 2: Fringes in the pupil plane showing the print-through of individual actuators.

Acknowledgements: The authors thank L. Bourdieu for the rat cerebellum sample. This work has been supported by Medicen Région IdF and PSL.

REFERENCES

[1] M. Glanc, L. Blanco, L. Vabre, F. Lacombe, P. Puget, G. Rousset, G. Chenegros, L. Mugnier, M. Pâques, J.-F. Le Gargasson, A. J. Sahel, "First adaptive optics images with the upgraded quinze-vingts hospital retinal imager" Adaptive Optics : Analysis and Methods, OSA, 2007. Conference date: June 18-20, 2007, Vancouver (Canada)

[2] C. Torti, B. Povazay, B. Hofer, A. Unterhuber, J. Carroll, P.K. Ahnelt, W. Drexler, "adaptive optics optical coherence tomography at 120,000 depth scans/s for non-invasive cellular phenotyping of the living human retina", *optics express*, vol. 17, no. 22, pp. 19382-19400, 2009

Wavefront engineering for imaging mammalian brain

Lingjie Kong[1], Jung Hoon Park[1], Meng Cui[1-4*]

[1] *School of Electrical and Computer Engineering, Purdue University, West Lafayette, USA*
[2] *Department of Biological Sciences, Purdue University, West Lafayette, USA*
[3] *Bindley Bioscience Center, Purdue University, West Lafayette, USA*
[4] *Purdue Imaging Cluster, West Lafayette, USA*

*mengcui@purdue.edu

Fluorescence microscopy has been widely used in biology for studying the cellular dynamics. In the field of neuroscience, with the advance of sensitive calcium indicator and laser scanning two-photon microscopy, fluorescence based calcium imaging has become the major workhorse in many labs worldwide. The noninvasiveness and high spatiotemporal resolutions are greatly desired in a variety of applications.

Despite its huge success, there are several limitations of optical fluorescence microscopy. A major drawback of optical measurement is the inherently limited penetration depth as compared to other modalities such as MRI. This has limited the calcium imaging to the superficial depth in mammalian brains. To date, most imaging studies are still performed for layer 2/3 neurons (up to ~400 μm). High resolution imaging of layer 5 or 6 neurons remains very challenging.

The fundamental cause of limited imaging depth is the inhomogeneous and random refractive index distribution. At large imaging depth, the aberration and scattering cause deteriorated focus and reduce the achievable Strehl ratio. As a result, imaging at large depth demands higher input power and yields reduced contrast, resolution and signal-to-noise ratio. A key character of linear wave propagation is that it is a time reversible process. In other words, a properly engineered optical wavefront can always cancel the wavefront distortion caused by the refractive index inhomogeneity and therefore achieve improved performance at large imaging depth, which is one of our major research directions. For practical imaging applications, there are two challenges. One is to obtain the correction wavefront information accurately and efficiently [1]. The other is to perform simultaneous correction over a large imaging field of view or imaging volume. In this talk, we will present our development for accurately measuring wavefront and increasing the correction field of view [2].

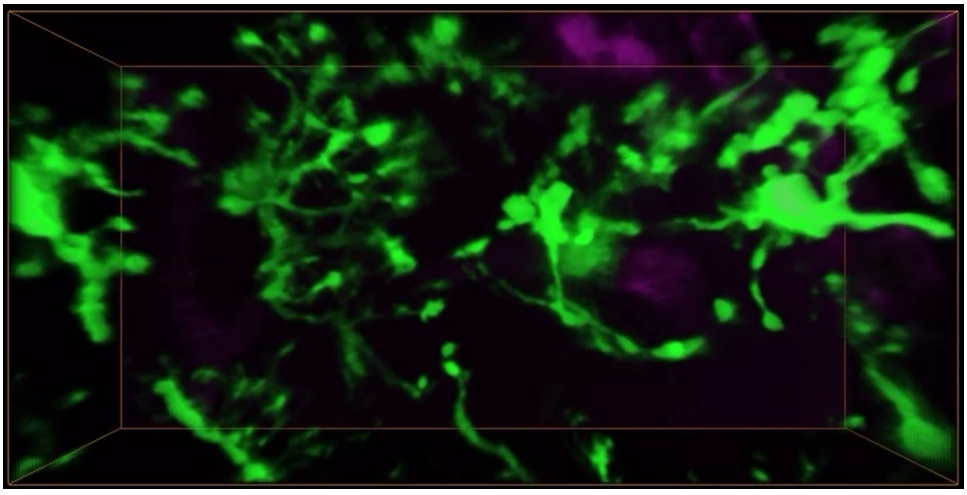

Figure 1: Volumetric imaging of cellular dynamics in mammalian brain. The microglial cells are activated by the blood-brain-barrier disruption (150 × 75 × 40 μm^3, at 100-140 μm depth under the dura). Green: microglia, magenta: blood plasma labeled with Qdot-655.

For calcium imaging of neuron networks, the other major challenge is the throughput. Within a cubic millimeter volume, the number of neurons can approach ~ 1 million. Even at a modest 10 Hz volume rate, this requires an overall throughput of ten million neuron×Hz, which is approximately three orders of magnitude greater than what current state-of-the-art solutions can provide. We will discuss our recent work [3] along this direction, which utilizes wavefront engineering for continuous volumetric imaging (Fig. 1).

REFERENCES

[1] J. Tang, Germain, R. N., & Cui, M. "Superpenetration optical microscopy by iterative multiphoton adaptive compensation technique," *Proceedings of the National Academy of Sciences*, 109(22), 8434-8439, 2012.

[2] J. H. Park, W. Sun, & M. Cui. (2015). High-resolution in vivo imaging of mouse brain through the intact skull. *Proceedings of the National Academy of Sciences*, 112(30), 9236-9241, 2015

[3] L. Kong, J. Tang, J. P. Little, Y. Yu, T. Lämmermann, C. P. Lin, R. N. Germain & M. Cui, "Continuous volumetric imaging via an optical phase-locked ultrasound lens," *Nature Methods*, 12(8), 759-762, 2015.

Light control in scattering medium via photoacoustic-guided wavefront shaping

Thomas Chaigne[1,2], Jérôme Gateau[1], Ori Katz[1,2], Emmanuel Bossy[1], Sylvain Gigan[2]

[1] *Institut Langevin, 1 rue Jussieu, 75005 Paris, France*
[2] *Laboratoire Kastler-Brossel, 24 rue Lhomond, 75005 Paris, France*

thomas.chaigne@espci.fr

Keywords: wavefront shaping, adaptive optics, scattering media, photoacoustic imaging

1. SCIENTIFIC CONTEXT

During the last decade, photoacoustic (PA) imaging emerged as a powerful technique to image biological structures with optical absorption contrast. Two techniques can be identified, operating at different depths and providing different spatial resolution. The first regime is explored with optical-resolution photoacoustic microscopy. The resolution here relies on optical focusing of the illumination (~1µm), which restricts this technique to shallow imaging depths (~100µm). Deeper, light scattering scrambles the optical focus. Hence, at large depth (up to a few centimeters), the resolution is limited by the acoustic wavelength of the detected ultrasound, which is typically of the order of tens to hundreds of micrometers.
In 2007, Vellekoop and Mosk introduced the concept of wavefront shaping to control multiply scattered light after propagation in a complex scattering sample. By shaping the phase of the incident wavefront by mean of a Spatial Light Modulator (SLM), they were able to focus light through an opaque, highly scattering sample [1]. A broad range of applications emerged, from image transmission through scattering samples to light control in multimode fiber. In any of these experiments, the one requirement is to provide a feedback signal monitoring the light intensity at the target location. Using a camera, this measurement is straight forward for outgoing light control. It is much more challenging if one wants to focus light within the scattering medium itself. In 2011, Kong and colleagues proposed to combine photoacoustic imaging and wavefront shaping to perform this task [2].

We demonstrate that using a photoacoustic feedback signal to monitor light intensity at the desired location, it is possible to measure a transmission matrix and to selectively focus on absorbing targets, as well as to retrieve scattering properties of the scattering medium [3,4]. These developments pave the way toward optical resolution photoacoustic imaging at unprecedented depth.

It appears also that coherent illumination itself without precise wavefront control can help overcoming inherent limitations of photoacoustic imaging. We demonstrate that visibility issues, caused by limited view detection or frequency mismatching, can be overcome by replacing the standard homogenous illumination by a fluctuating speckle illumination [5]. We also investigate the resolution enhancement that such a fluctuation imaging technique could provide.

2. RESULTS

Here, we report on the measurement of the transmission matrix of a scattering sample using photoacoustic feedback. The acoustic detection is performed with a linear ultrasonic array, providing a two-dimensional imaging capability. We exhibit both light focusing and imaging abilities.
On Fig.2.a-b, we show that we are able to focus light on an absorbing sample using the photoacoustic transmission matrix.

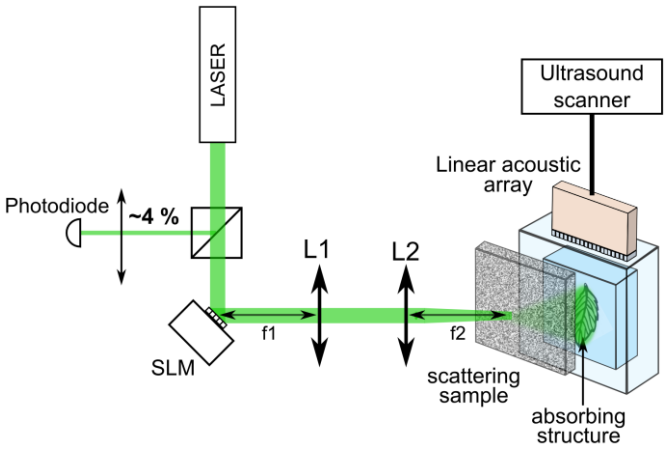

Figure 1: Experimental setup: a 5-ns laser pulse is shaped by an SLM before passing through a scattering sample and illuminating an absorbing structure. Photoacoustic signals are detected with an ultrasonic linear array, driven by an ultrasound scanner.

On Fig.2.c, the entire standard photoacoustic image is shown. Due to limited aperture detection, vertical structures cannot be imaged. On Fig.2.d, we show that using fluctuating speckle illumination, these structures can be revealed without changing the acoustic detection.

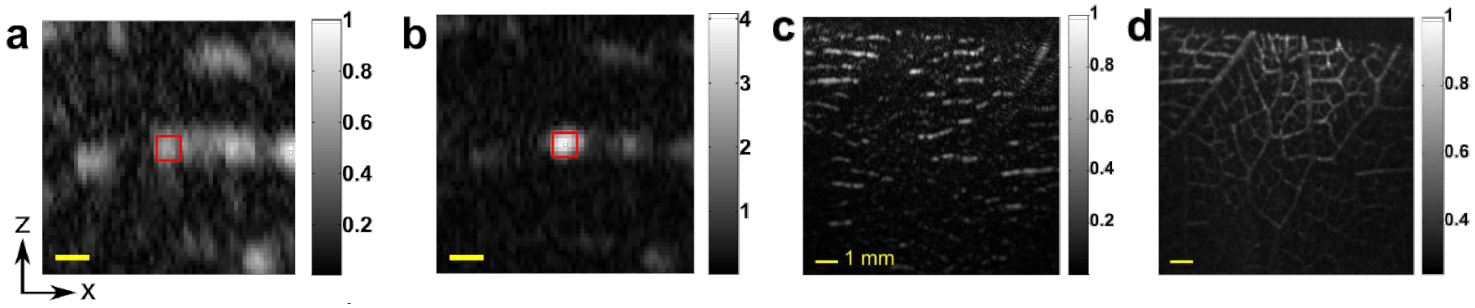

Figure 2: (a) PA image (envelope) when flat phase mask displayed on SLM, (b) PA image when focusing phase mask displayed on SLM, (c) PA image under homogenous illumination, (d) modulation image (obtained by averaging the transmission matrix over the input modes).

Further investigations are discussed about necessary improvements to apply these techniques in actual biological samples. Fast decorrelation of the tissue and wavelength mismatch between acoustics and optics are of particular interest. We address the latter by spectrally filtering the photoacoustic feedback signal, which enables us to focus to tighter regions.

REFERENCES

[1] Vellekoop, I.M. & Mosk, A.P. Focusing coherent light through opaque strongly scattering media. *Opt Lett* **32**, 2309-2311 (2007).
[2] Kong, F. *et al*. Photoacoustic-guided convergence of light through optically diffusive media. *Opt*. *Lett*. **36**, 2053-2055 (2011).
[3] Chaigne, T. *et al*. Controlling light in scattering media non-invasively using the photoacoustic transmission matrix *Nature Photonics* 8, 58–64 (2014).
[4] Chaigne, T. *et al*. Light focusing and two-dimensional imaging through scattering media using the photoacoustic transmission matrix with an ultrasound array. *Optics letters*, *39*(9), 2664-2667. (2014).
[5] Gateau, J. *et al*. Improving visibility in photoacoustic imaging using dynamic speckle illumination. *Optics letters* **38** (23), 5188-5191

A Random Matrix Approach of Optical Imaging and Detection through Turbid Media

Amaury Badon, Dayan Li, Geoffroy Lerosey, Albert C. Boccara, Mathias Fink, Alexandre Aubry

Institut Lagenvin, ESPCI ParisTech, PSL Research University,
CNRS UMR 7587, 1 rue Jussieu, 75005 Paris, France

alexandre.aubry@espci.fr

Keywords: Imaging, turbid media, reflection matrix, random matrix

The limit of conventional imaging techniques in inhomogeneous media can be derived from a physical parameter called the scattering mean free path l_s. It describes the average distance that a photon travels between two consecutive scattering events. Until a depth of one scattering mean free path, most of the collected photons originate from single scattering (SS) events and a direct image of the medium can be obtained with conventional microscopy. On the contrary, beyond one scattering mean free path, a photon undergoes several random scattering events before emerging from the scattering medium. Multiple scattering (MS) randomizes light directions. The image of the medium is blurred and no longer provides the reflectivity of the medium in the focal plane.

To cope with the fundamental issue of MS, several approaches have been proposed in order to enhance the SS contribution drowned into a predominant MS background. The first option is to spatially discriminate SS and MS as performed in confocal microscopy [1]. The second option consists in discriminating ballistic photons from MS photons in time with coherence time gating techniques [1]. Optical coherence tomography combines both approaches and allows to image a scattering medium until a depth of several scattering mean free paths. Inspired by previous works in acoustics [2,3] and the emergence of wave-font shaping techniques in optics [4,5], we propose a matrix approach of wave reflection by a turbid medium and demonstrate the detection and imaging of targets beyond a depth of 12 l_s.

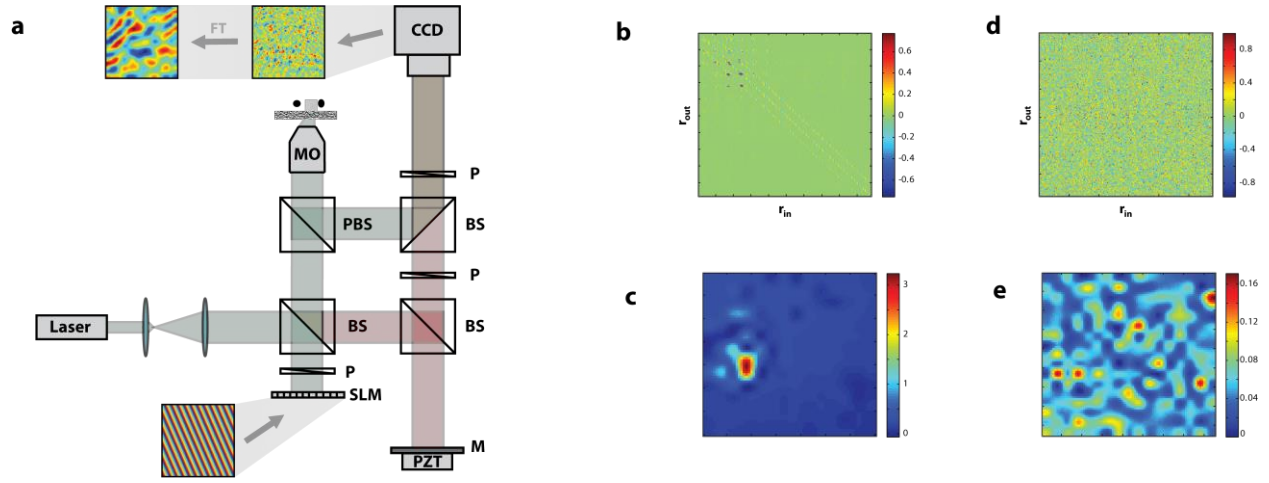

Fig 1. **(a)** Experimental set up used to record the time-resolved reflection matrix. **(b)** Reflection matrix of a 10 µm bead placed on a glass slide and **(c)** corresponding confocal image. **(d)** Reflection matrix with an highly scattering medium and **(e)** the corresponding confocal image.

To that aim, the experimental set up shown in Fig.1(a) is used to record the time-resolved reflection matrix associated to the scattering medium under investigation. The incident wave-front is controlled with a spatial light modulator (SLM) illuminated with a femtosecond laser. The scattered wave-field is recorded with a CCD camera at a given time of flight t controlled by the length of an interferometric arm. The reflection matrix $\mathbf{R}$ corresponds to the response between each point in the focal plane. $\mathbf{r}_{in}$ and $\mathbf{r}_{out}$ denote the

input and output points, respectively. A confocal image can be built from the diagonal elements of this matrix for which $\mathbf{r_{in}} = \mathbf{r_{out}}$. Fig.1(b) displays the reflection matrix measured for a 10µm diameter bead on a glass slide. We use 289 input plane waves leading to a field of view of 40x40µm^2 and a resolution of 2.5 µm. Not surprisingly, most of the backscattered intensity emerge along the diagonal and sub-diagonals elements of **R** for which $\mathbf{r_{in}} \sim \mathbf{r_{out}}$ [Fig.1(b)]. The confocal image built from **R** provides a reference image of the bead [Fig.1(c)]. Fig.1(d) displays the matrix **R** when a paper sheet is placed between the bead and the microscope objective. This scattering layer displays a thickness of 12.2 l_s, leading to an attenuation of the singly scattered light by a factor $e^{-24} \sim 10^{-11}$. In such a configuration, the single-to-multiple scattering ratio is theoretically estimated to be of 10^{-9}. Because of the highly predominant MS contribution, the corresponding reflection matrix exhibits a random feature [Fig.1(d)] and the corresponding confocal image is an image of speckle [Fig.1(e)], without any connection with the *true* reflectivity in the focal plane [see the comparison with Fig.1(c)].

The confocal image is formed by only considering the diagonal elements of **R**. However, due to the finite size of the object and the aberrations induced by the scattering layer, SS also emerges along the sub-diagonal elements. A matrix $\mathbf{R_s}$ is built from the measured **R** matrix by only considering these elements [Fig.2(a)]. In confocal microscopy, this would correspond to an enlargement of the pinhole aperture. The matrix $\mathbf{R_s}$ contains the whole SS contribution and a residual MS background. To get rid of the latter contribution, we apply the D.O.R.T method to $\mathbf{R_s}$ [5,6]. Derived from the theoretical study of the iterative time reversal process, this approach relies on the diagonalization of the time-reversal operator $\mathbf{RR}^*$. In the single scattering regime, a one-to-one association between each time-reversal invariant eigenstate and each scatterer allows focusing on each of them by transmitting the computed eigenvectors. Technically, a singular value decomposition (SVD) of the reflection matrix is used to compute the eigenstates of the time-reversal operator. The histogram of the singular values of $\mathbf{R_s}$ is shown in Fig.2(b). One singular value emerges from the distribution predicted by random matrix theory and associated to the MS background. This singular value is associated to the target and the corresponding eigenstate allows to retrieve the image of the target [Fig.2(c)] though the highly scattering layer.

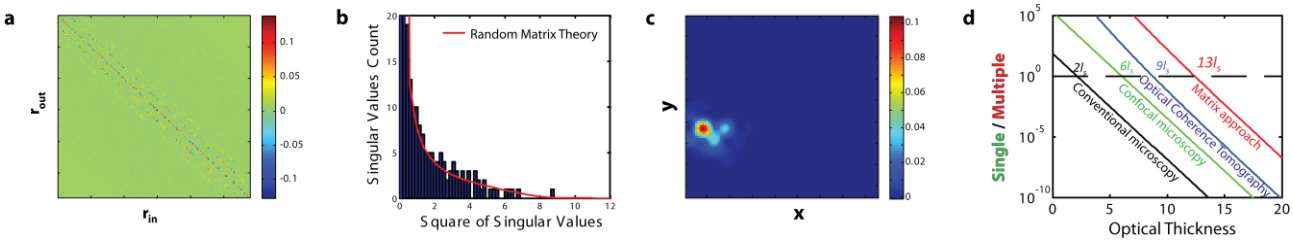

Fig 2. **(a)** Single scattering matrix $\mathbf{R_s}$ **(b)** Histogram of singular values of $\mathbf{R_s}$. **(c)** The eigenstate associated to the largest singular value directly provides an image of the target hidden behind the highly scattering layer. **(d)** Comparison of the ratio SS/MS for various imaging techniques.

In conclusion, this study demonstrates how a matrix approach of wave reflection by a turbid medium can be powerful for detection and imaging despite multiple scattering. Based on theoretical calculations, we show that our approach is capable of pushing back the current limit of OCT by a factor of 3/2 in depth [Fig.2(d)], which can be of great interest for imaging of biological tissues under the skin.

REFERENCES

[1] C. Dunsby, and P.M.W. French, *J. Phys. D: Appl. Phys.* **36**, R207–R2, 2003
[2] A. Aubry and A. Derode, *Phys. Rev. Lett* **102**, 084301, 2009
[3] A. Aubry and A. Derode, *J. Appl. Phys* **106**, 044903, 2009
[4] S. M. Popoff et al., *Phys. Rev. Lett* **104**, 100601, 2010
[5] S. M. Popoff et al., *Phys. Rev. Lett* **107**, 263901, 2011
[6] C. Prada and M. Fink, *Wave motion* **20**, 151, 1994

Spatio-temporal focusing of an ultrashort pulse through a scattering medium using the Multi Spectral Transmission Matrix

Mickael Mounaix[1], Daria Andreoli[1,2], Giorgio Volpe[1,2], Ori Katz[1,2], Samuel Grésillon[2], Sylvain Gigan[1]

[1] *Laboratoire Kastler Brossel, ENS-PSL Research University, CNRS, UPMC-Sorbonne universités, Collège de France ; 24 rue Lhomond, F-75005 Paris, France*

2 Institut Langevin, ESPCI ParisTech, PSL Research University, CNRS, 1 rue Jussieu, 75005, Paris, France

mickael.mounaix@lkb.ens.fr

Keywords: *wavefront shaping, scattering medium, ultrashort pulse*

1. INTRODUCTION

Imaging through scattering media remains a daily challenge. Indeed, phase and amplitude information of light are seemingly destroyed by the multiply scattering events during the propagation, limiting resolution, depth and contrast of most microscopy techniques. Previous work have proven that, using a Spatial Light Modulator (SLM) and a monochromatic coherent beam, the spatial speckle pattern can be controlled at the output of a scattering medium[1]. In particular, thanks to the measurement of the transmission matrix of a medium, these techniques allow focusing of light [2], or imaging through a scattering medium [3].

However, if the laser is broadband, such as an ultrashort pulse, the scattering medium can respond differently for different spectral components of the pulse [4-5] and the monochromatic approach breaks down. The transmitted pulse is temporally stretched.

Thanks to the measurement of the multi spectral transmission matrix (MSTM) of a medium, it is possible to spectrally control the propagation of a broadband source [6], but deterministic temporal control was still elusive. In our work, by adding the measurement of the phase relation between the different frequencies response of the medium, we can completely describe the temporal behavior of an ultrashort pulse through a scattering medium. Once the matrix is learnt, with wavefront shaping techniques we demonstrate control both spatial and spectral degrees of freedom of the output field. The spectral ones give access to a temporal control of the output pulse. We prove an experimental temporal compression of an ultrashort pulse close to its initial time-width after passing through a scattering medium, allowing a more intense excitation of a non-linear process.

2. MULTI SPECTRAL TRANSMISSION MATRIX

We present the analogue of the optical transmission matrix (TM) for a spectral broadband signal, the MSTM. The added dimension is the spectral response, allowing the characterization of the response in the wavelength domain of the medium with a broadband input signal. The first step is the measurement of the spectral correlation length of the medium (L_c), corresponding to difference in input wavelength that gives uncorrelated speckle patterns. The ratio between the spectral bandwidth of the pulse and L_c gives the number of spectral degrees of freedom (N), i.e. the number of monochromatic matrices one needs to measure to fully characterize both spatially and spectrally the propagation of a pulse. Therefore the MSTM is a 3D tensor, including N monochromatic TM separated by a distance L_c in wavelength.

To focus the pulse in time, one needs to know the spectral phase of each wavelength of the pulse at a given position at the output, and set them equal to compensate the dispersion induced by the scattering medium. This phase information can be learnt when learning the transmission matrices by interfering the output signal with an external reference and the modulation of the phase of the output field.

We use two different methods in order to prove the temporal compression : Fourier Transform Interferometry and two-photon fluorescence. The first one relies on an heterodyne detection, the interference between an ultrashort pulse used as a reference and the unknown one. A Fourier Transform of the signal allows to recover the temporal shape of the unknown pulse. The second one is a non-linear excitation process, here two-photon fluorescence, involving two incident photons at 800nm and emission of a fluorescent photon around 500nm. The total intensity of the fluorescent signal is proportional to the square of the excitation intensity. Therefore, with an equivalent spatial focusing, a temporal compression corresponds to a higher two-photon intensity.

3. EXPERIMENTAL RESULTS

The phase-only SLM (LCOS-SLM, Hamamatsu X10468-02) is subdivided in 16x16 macropixels. A Ti:Sa laser source produces a 100fs ultrashort pulse, centered at 800nm with a spectral bandwidth of 10nm FWHM. The scattering medium used is a thick layer of ZnO nanoparticles randomly deposited on a glass slide, characterized by a spectral correlation L_c =0.5nm. Therefore the MSTM to be measured is composed of 20 monochromatic matrices. The linear signal can be measured directly on a CCD camera, and a two-photon layer is fabricated: fluorescein diluted in ethanol, inside a glass capillary of thickness 20μm, allowing to record a "two-photon speckle" using a EMCCD camera, which carries information about the pulse compression.

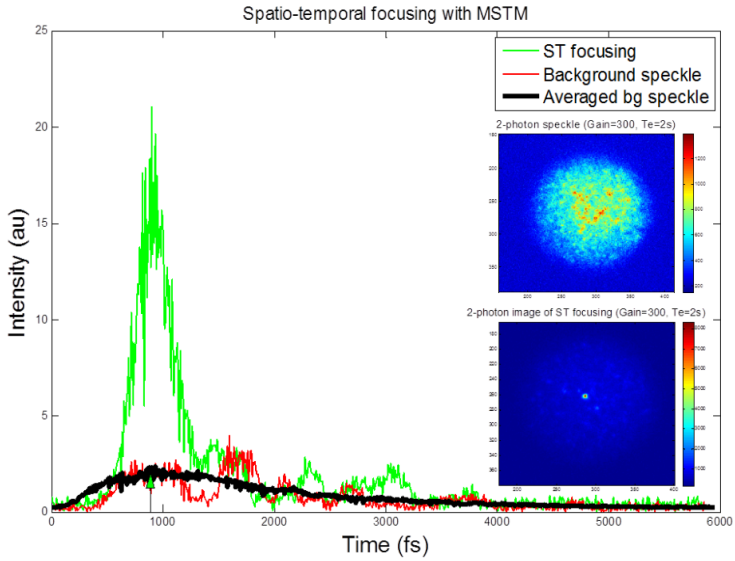

Figure 1: Spatio-temporal focusing with MSTM. (See text)

The main result is presented in Fig1. The 3 curves are the evolution of intensity over time, retrieved by Fourier transform interferometry using the linear CCD images, for three situations. The red curve is the temporal shape of one speckle grain : the intensity is fluctuating over time, and the input information of the ultrashort pulse seems to be lost. The black curve is an average over 100 different positions. Averaging over speckle realization, we retrieve the time of flight distribution, with an exponential decay time of 2ps, inversely proportional to and in good agreement with L_c. This time corresponds to the average temporal broadening of the output pulse. A 2-photon speckle image is the top inset, showing a rather homogeneous excitation. Controlling the MSTM and at the same time imposing a flatspectral phase for each wavelength of the output signal should yield spatio-temporal compression. The result is the green curve, and the corresponding two-photon image the down inset, where a sharp focus is observed at the chosen position.

The MSTM permits to measure the effect of the medium on both spatial and spectral degrees of freedom. We use this information for spatio-temporal focusing, but not only. We can perform more complex temporal shaping, such as adding a phase ramp to delay the pulse, adding a quadratic phase to control the dispersion, or generate arbitrary shapes. The MSTM should be beneficial for non-linear excitation of localized nano-objects in a scattering medium. In the long run, the interaction between the non-linear signal and the scattering medium may be useful for the study of light-matter interaction inside complex media.

REFERENCES

[1] S. Popoff et al, *Physical Review Letters*, 104, 100601, (2010)
[2] I. Vellekoop et al ,*Optics Letters*, 32 (16), 2309-2311, (2008)
[3] S. Popoff et al, *Nature Communications*, 1, 81, (2010)
[4] J. Aulbach et al., *Physical Review Letters,* 106, 103901, (2011).
[5] D. McCabe et al., *Nature Communications*, 2, 447 (2011)
[6] D. Andreoli et al., *Scientific Reports*, 5, 10347(2015)

Wavefront Shaping in the realm of Nonlinear Microscopy: prospects for label-free deep imaging in scattering media

Hilton B. de Aguiar[1], Sylvain Gigan[2], Sophie Brasselet[1]

[1] *Aix-Marseille Université, CNRS, Centrale Marseille, Institut Fresnel UMR 7249, 13013 Marseille, France*
[2] *Kastler Brossel, UMR 8552 of CNRS and Université Pierre et Marie Curie, 24 rue Lhomond, 75005 Paris, France*

h.aguiar@fresnel.fr

Keywords: nonlinear microscopy, wavefront shaping, multiple scattering, polarization-resolved microscopy.

1. INTRODUCTION

Nonlinear Microscopy is established as a powerful approach for biomolecular imaging with high sectioning capabilities and, depending on the process, high chemical specificity. It includes imaging lipid-containing specimens by coherent Raman microscopies, non-centrosymmetric biological structures by Second-Harmonic Generation (SHG), birefringent species or at the vicinity of interfaces by Third-Harmonic Generation, and fluorescently-labeled neuron activity monitoring by two-photon excited fluorescence (2PF) microscopy, to cite a few examples.

Despite tremendous impact in various fields in biophotonics and biomedical optics, Nonlinear Microscopy still faces challenges, among which, depth penetration is the major issue. Nonlinear Microscopy is remarkably superficial when imaging biological specimens, because nonlinear signals rapidly decreases at depths of typically 100 μm within biological tissues. This poor penetration (about one scattering mean free path) in the medium is mainly due to the loss of coherence of focused spots within aberrant and scattering media. This induces a rapid loss of the generated signals because of the nonlinear dependence on the excitation fields. Adaptive optics provides an interesting strategy to achieve deeper penetration depths, however it acts on the optimization of nonlinear signals arising from ballistic photons [1]. Even though certain "optical tricks", such as increasing the incident wavelength, might be used in highly scattering media [2] the maximum obtained penetration depth (in the mm-range) represents only 3 scattering mean free path. This means that far deeper regions in biological specimens could be imaged if one exploits the remaining scattered light instead of the ballistic one.

Wavefront Shaping, which manipulates scattered light based on control of high spatial frequencies, holds the promise of enabling deep imaging in scattering media. Although various demonstrations and beautiful examples have been made in the field using purely linear optics [3], just a few have been made in the context of Nonlinear Microscopy [4]. Despite their importance, a realistic experiment involving *imaging* a biological sample has been shown only for incoherent process (2PF) [4(c)].

In this contribution, we present our first results in exploiting the Wavefront Shaping approach for Nonlinear Microscopy, focusing on aspects relevant for coherent nonlinear processes. In a series of experiments, we address and discuss various properties that are commonly used in a typical nonlinear microscopy experiment: pulse bandwidth, scattering medium properties and depolarization effects. For that purpose, we use as a model system coherent SHG from nanocrystals (150 nm) of potassium titanyl phosphate (nanoKTP). We address in particular the question of the feedback mechanism used for enhancing a nonlinear signal through a scattering medium: while nonlinear signals are currently used as a feedback for optimization [4], we show that using the linear signal can present considerable advantages. Although we chose to use SHG as a nonlinear signature, our conclusions are general and applicable to any nonlinear contrast mechanism, since we mostly address the linearly scattered photons.

2. RESULTS

Fig. 1 summarizes the main results of our work. Fig. 1(a) shows the experimental layout in which we can switch between using a nonlinear feedback (emCCD) or a linear feedback (CMOS detection) for nonlinear

signal enhancements. In the nonlinear feedback scheme, published procedures [5] of Wavefront Shaping are applied to optimize the nonlinear SHG signal at the location of a nanoKTP crystal. Fig. 1(b) shows a SHG image of a single nanoKTP crystal without and with an optimal wavefront shape. Remarkably, high nonlinear signal enhancements (x500) are obtained by only using 64 controlled SLM segments. Nevertheless, since this result uses a nonlinear feedback, it is considerably time consuming to find the optimal wavefront (limited by photon noise). Therefore, we exploit the possibility of using the linearly scattered photons as a feedback for nonlinear signal enhancement. We then obtain similarly high nonlinear signal increase however at a much faster acquisition speed, only limited by the SLM speed (50 Hz). At last, this method works even for nonlinear imaging through an opaque medium (TiO_2 thin film).

As a last result, we showcase our approach in a realistic biological sample, namely SHG from rat tendon collagen (Fig. 1(c)), using the linear feedback approach. Highly contrasted images are obtained as shown by the fibers running along the diagonal of the image. This specific example illustrates the potential advantages of using a linear feedback over a nonlinear one: Although we show in Fig. 1(b) highly nonlinear signal enhancements using a nonlinear feedback, such a scheme could fail in the presence of strong backgrounds as found in biological samples.

These results show that wavefront shaping is a promising approach to overcome penetration depth limits in realistic scenarios of nonlinear microscopy, even where background signal is the limiting factor [2,6].

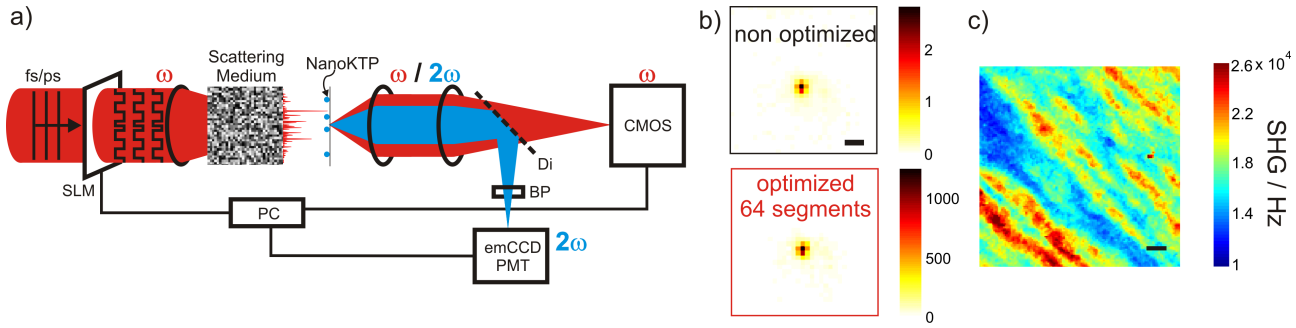

Figure 1: (a) Simplified experimental layout for performing nonlinear microscopy with wavefront shaping. (b) SHG images of a single nanoKTP crystal before (upper panel) and after wavefront shaping (lower panel). In this particular experiment we used a nonlinear feedback (emCCD) for optimization. Similar results are obtained from a linear feedback-based optimization. Scale bar: 0.9 µm. (c) SHG imaging of rat tendon collagen after a scattering medium. Before optimization, no discernable feature was visible. Scale bar: 2.3 µm.

REFERENCES

[1] Débarre *et al*., "Image-based adaptive optics for two-photon microscopy," *Opt. Express*, vol. 34, pp. 2495–2497, 2009; C. Wang *et al*., "Multiplexed aberration measurement for deep tissue imaging in vivo," *Nat. Method*., vol. 11, pp. 1037–1040, 2014.

[2] N. G. Horton *et al*., "In vivo three-photon microscopy of subcortical structures within an intact mouse brain," *Nat. Phot*., vol. 7, pp. 205–209, 2013.

[3] A. P. Mosk *et al*., "Controlling waves in space and time for imaging and focusing in complex media," *Nat. Phot*., vol. 6, pp. 283–292, 2012.

[4] (a) O. Katz *et al*., "Focusing and compression of ultrashort pulses through scattering media," *Nat. Phot*., vol. 5, pp. 372–377, 2011; (b) J. Aulbach *et al*., "Spatiotemporal focusing in opaque scattering media by wave front shaping with nonlinear feedback," *Opt. Express*., vol. 20, pp. 29237–29251, 2012; (c) J. Tang *et al*., "Superpenetration optical microscopy by iterative multiphoton adaptive compensation technique," *Proc. Natl Acad. Sci. USA*, vol. 109, pp. 8434–8439, 2012; (d) O. Katz *et al*., "Noninvasive nonlinear focusing and imaging through strongly scattering turbid layers," *Optica*, vol. 1, pp. 170–174, 2014.

[5] S. M. Popoff *et al*., "Measuring the Transmission Matrix in Optics: An Approach to the Study and Control of Light Propagation in Disordered Media," *Phys. Rev. Lett*., vol. 104, pp. 100601, 2010.

[6] P. Theer and W. Denk, "On the fundamental imaging-depth limit in two-photon microscopy," *J. Opt. Soc. Am. A*, vol. 23, pp. 3139–3149, 2006.

Exploiting the Time-Reversal Operator and the Van-Cittert Zernike theorem for Adaptive Ultrasonic Imaging

Mathias Fink

Institut Langevin, ESPCI ParisTech, CNRS, 1 rue Jussieu, 75238 Paris Cedex 05, France

mathias.fink@espci.fr

In this paper, we show how the measurement of the backscattering matrix from a medium containing a random distribution of scatterers allows to extract the Green's functions of the medium. This method can be used to compensate for wave-front distortions induced by aberrations from an inhomogeneous medium. This work was initially performed in the field of ultrasound and we will discuss the extension to optics for multiple illumination OCT.

We show that despite the fact that the backscattering matrix is a random matrix, the so called time-reversal operator associated to this matrix is a deterministic operator. This important theorem is linked to the connection that exists between the time-reversal operator (the covariance matrix associated to the backscattering matrix) and the Van-cittert Zernike theorem. Computing the eigenvalues and eigenvectors of this time-reversal operator allows to extract the focusing laws needed to correct aberrations.

Applications of this method in the field of in vivo medical ultrasonic imaging will be demonstrated.

Multimodal imaging through a capillary waveguide using digital phase conjugation

Nicolino Stasio[1], Atsushi Shibukawa[1], Ioannis N. Papadopoulos[1], Olivier Simandoux[2], Emmanuel Bossy[2], Christophe Moser[3] and Demetri Psaltis[1]

[1]*Laboratory of Optics, École Polytechnique Fédérale de Lausanne (EPFL), Route Cantonale, 1015 Lausanne, Switzerland*

[2] *ESPCI ParisTech, PSL Research University, CNRS, INSERM, Institut Langevin, 1 rue Jussieu, 75005 Paris, France*

[3]*Laboratory of Applied Photonics Devices, École Polytechnique Fédérale de Lausanne (EPFL), Route Cantonale, 1015 Lausanne, Switzerland*

nicolino.stasio@epfl.ch

Keywords: Endoscopic imaging, Phase conjugation, Digital holography

Optical imaging into biological tissue is an important tool for diagnostic purposes. Unfortunately, tissue is a highly scattering medium in the visible spectrum, which compromises the focusing capability of an imaging system as well as the collection of the optically generated signals.

One technique to overcome this issue is Photoacoustic Imaging (PAI), which allows to image absorbing media with scalable resolution and imaging depth by detecting acoustic waves generated by a pulsed laser [1]. In order to realize optical resolution photoacoustic imaging (OR-PAI) very deep in tissues, endoscopic approaches can be used, with device diameters ranging from 1 to a few mm.

Using Digital Phase Conjugation (DPC), optical resolution photoacoustic images were obtained using an ultrathin multimode fiber [2]. The ultrasound signal generated by the photoacoustic effect is collected using an ultrasound transducer right next to the interrogated sample, forming the photoacoustic image. OR-PAI, in fact, generates acoustic signal in the MHz range, which are difficult to detect externally because of the acoustic attenuation in tissues.

Recently, we showed that a 330 μm in diameter, water-filled silica capillary can guide high frequency ultrasound waves through a 3 cm thick fat layer, allowing OR-PAI. In this case, the photoacoustic signal was created by focusing light through a microscope objective placed on the sample side [3].

Here we demonstrate that using DPC, the same water-filled capillary (3 cm long) can be used as an endoscopic probe to obtain both fluorescence and optical resolution photoacoustic imaging. The annular part (NA= 0.22) of the capillary is used as an optical waveguide in order to focus light using DPC, and for fluorescence signal collection. The water-filled core is used as an acoustic waveguide to collect the ultrasound waves. The endoscope has to be calibrated first: a focus spot is raster scanned in a plane in front of the capillary (the *sample side*); on the other side of the capillary (the *proximal side*), for each position of the focus, a speckle pattern is generated and its hologram is digitally recorded with a CMOS. The conjugate distributions of the detected phases are used to drive a Spatial Light Modulator (SLM): phase-conjugated beams are sent back inside the waveguide, allowing the scanning of a focused spot on the sample side (Figure 1). After this calibration step, no optical element is needed on the sample side.

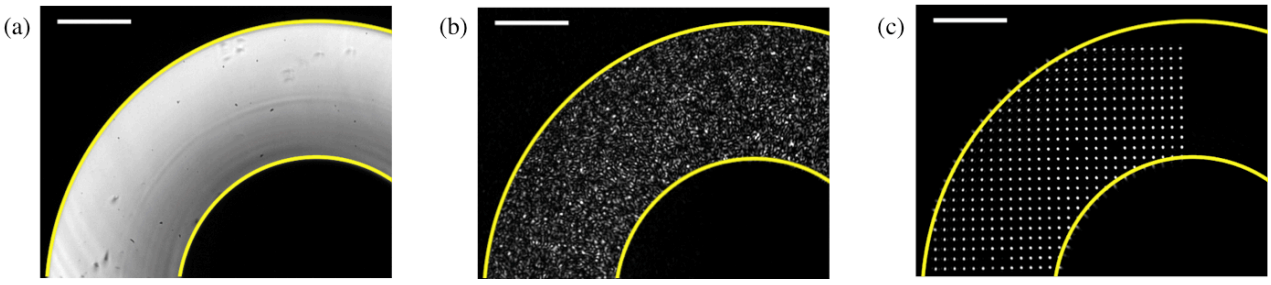

Figure 1: Images of the capillary waveguide facet, (a) incoherent light illumination, (b) speckle pattern generated by focused laser beam illumination, (c) phase conjugated spot scanned over the capillary waveguide facet. Scale bar: 50μm

At this point, thanks to the capillary waveguide, it is possible to guide back and detect on the proximal side both fluorescence using a photomultiplier tube and photoacoustic signal using a focused ultrasound transducer arranged in a particular geometry (as suggested in [3]).

In this work we show for the first time that a multimodal device is able to combine photoacoustic and fluorescence imaging capabilities. As a proof of principle, we show images of 2 μm fluorescent beads (Figure 2), and photoacoustic images of a 30 μm thick absorbing nylon thread (Figure 3) obtained by detecting ultrasound waves with a spectrum centered around 25MHz.

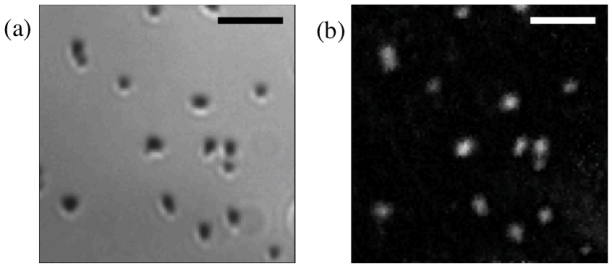

Figure 2: Fluorescence imaging using the capillary waveguide, (a) widefield image of 2µm fluorescent beads, (b) fluorescence image obtained using the capillary endoscope. Scale bar: 10µm

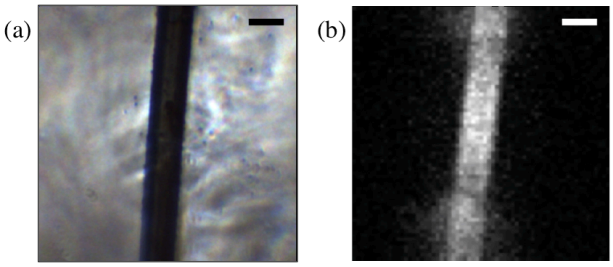

Figure 3: Photoacoustic imaging using the capillary waveguide, (a) widefield image of 30µm thick nylon thread, (b) photoacoustic image obtained using the capillary endoscope. Scale bar: 30µm

In conclusion, this kind of silica-capillary waveguide together with wavefront shaping techniques such as DPC, has the potential to enable minimally invasive multimodal endoscopy.

REFERENCES

[1] L. V. Wang and S. Hu, "Photoacoustic Tomography: In Vivo Imaging from Organelles to Organs," *Science*, vol. 335, no. 6075, pp. 1458–1462, 2012.

[2] I. N. Papadopoulos, O. Simandoux, S. Farahi, J. P. Huignard, E. Bossy, D. Psaltis, and C. Moser, "Optical-resolution photoacoustic microscopy by use of a multimode fiber," *Appl. Phys. Lett.*, vol. 102, no. 21, p. 211106, 2013

[3] O. Simandoux, N. Stasio, J. Gateau, J.-P. Huignard, C. Moser, D. Psaltis, and E. Bossy, "Optical-resolution photoacoustic imaging through thick tissue with a thin capillary as a dual optical-in acoustic-out waveguide," *Appl. Phys. Lett.*, vol. 106, no. 9, p. 094102, 2015

Two-photon lensless endoscope by controlling the wave front in a multi-core optical fiber

Siddharth Sivankutty[1], Esben Ravn Andresen[1], Géraud Bouwmans[2], Serge Monneret[1], and Hervé Rigneault[1,*]

[1] *Aix-Marseille Université, CNRS, Centrale Marseille, Institut Fresnel UMR7249, 13013 Marseille, France*
[2] *PhLAM CNRS, IRCICA, Université Lille 1, 59658 Villeneuve d'Ascq Cedex, France*

[*]herve.rigneault@fresnel.fr

Keywords: Wave front shaping, endoscopic imaging, fluorescence microscopy, nonlinear microscopy, Optical fiber, multi-core fiber.

1. INTRODUCTION

Typical endoscopes need optical or micromechanical components attached to their tip in order to form an image. These components limit miniaturization of the endoscope probe to around a few millimeters. Recently, there has been a surge in reports of so-called 'lensless endoscopes' [1-7], a term which denotes variations of the concept sketched in Fig. 1. The ability to control the wavefront at the distal end of a fiber allows the miniaturization of endoscope probes to the fundamental limit, the size of the optical fiber itself. This concept would enable imaging at depths inaccessible to conventional microscopes .

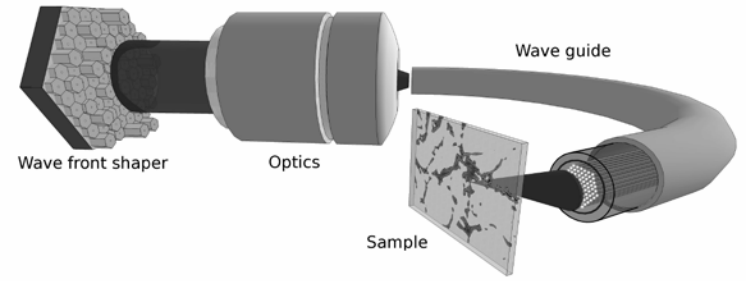

Figure 1: The concept of a lensless endoscope is to focus and point-scan the light emitted by a wave guide. To this end a wave front shaping element, *e.g.* a two-dimensional spatial light modulator (2D-SLM), is used to pre-shape the light injected into the wave guide.

2. LENSLESS ENDOSCOPE BASED ON MULTI-CORE FIBER

Our approach sets itself apart in two ways: (i) We strive for a lensless endoscope capable of nonlinear image contrast using two-photon fluorescence; and (ii) we strive for high image acquisition rates. Here, we show how our approach of employing wave front shaping methods with a specifically-designed multi-core fiber (MCF) as the wave guide can accommodate both.

We have developed an MCF specifically for our approach, (see Fig. 2.) It consists of 169 highly homogeneous single-mode cores which deliver a wave front to the sample; each core being one 'pixel' of the wave front. The composite waveform at the distal end is then generated by pre-shaping the beam before it is coupled into the fiber cores. Hence, the generation of a focal spot and its scanning can be performed without any opto-mechanical components on the fiber tip. The MCF is designed with a multi-mode inner cladding with a very high numerical aperture (NA) of 0.65. This permits the collection of the resulting fluorescence signal with a high efficiency.

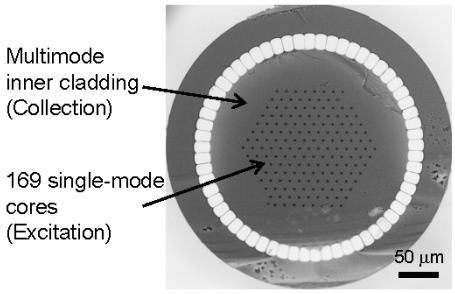

Figure 2 : Scanning electron micrograph of the endface of the specifically-designed MCF (inverted colors).

We have demonstrated a video-rate lensless endoscope capable of acquiring full-resolution images (896 x 640 pixels) at a rate of 12 fps [5], examples of images acquired are shown in Fig. 3. A spatial light modulator (SLM) is used to both characterize and correct the phase offset between individual cores of the MCF. With such compensation, any change in input wavefront gives rise to the same change in the output wavefront. So we can use a fast-scanning element, a pair of galvanometric scan mirrors, at the MCF input to induce rapid beam-scanning at the MCF output, enabling imaging rates not restricted by the update rates of the SLM.

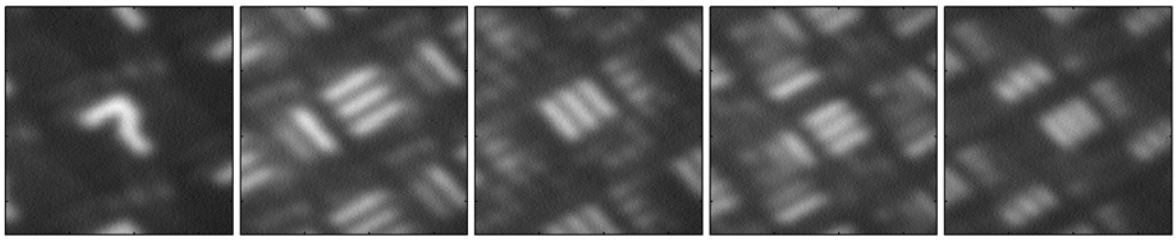

Figure 3: Video-rate imaging through a MCF. Frames from a video with a frame rate of 12 fps that was acquired as the sample, a 1951 USAF resolution target, was moved across the field of view. Smallest feature size of the sample was 2.8 microns.

In the context of two-photon fluorescence imaging, the constraints on the delivery of ultrafast pulses through the fiber become equally critical. The use of the MCF in conjunction with SLMs permits the generation of intense focal spots with ultrafast pulses, capable of invoking nonlinear contrast. We have demonstrated two-photon imaging with the lensless endoscope [6] Fig. 4(a) shows example images of a nonlinear crystal taken at different planes, demonstrating the optical sectioning that is inherent to nonlinear imaging. Here, wavefront shaping techniques are used to both generate and raster scan the focal spot on the sample. Imaging is performed in an endoscopic configuration with the epi-collected signal through the MCF. We reckon that lensless endoscopes based on MCF, with further improvements such as [7], could find potential in demanding deep tissue imaging applications where space is constrained and scattering high.

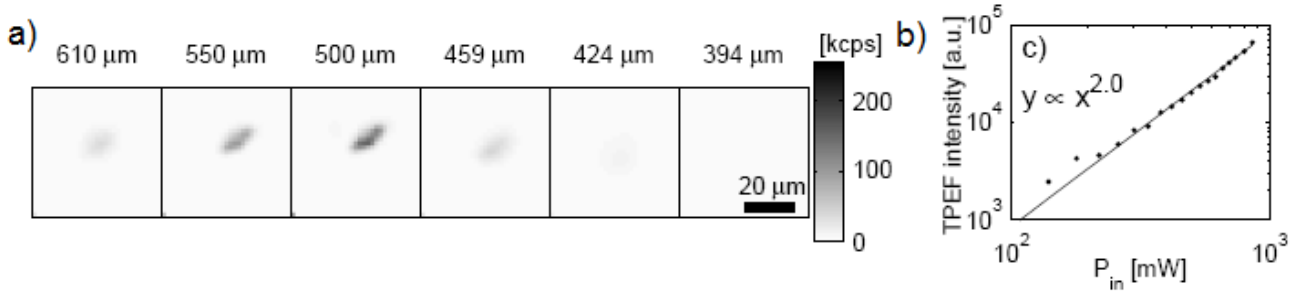

Figure 4: Two-photon imaging with the lensless endoscope. (a) Images of a Rh6G crystal acquired in different planes, *i.e.* for different focal lengths of the lensless endoscope, controllable with the wave front shaper. (b) Measured intensity of the two-photon signal as a function of input power (double-logarithmic scale).

REFERENCES

[1] Y. Choi *et al.*, "Scanner-free and wide-field endoscopic imaging by using a single multimode optical fiber", *Phys. Rev. Lett.*, vol. 109, no. 20, 203901, 2012.

[2] T. Cizmar and K. Dholakia, "Exploiting multimode waveguides for pure fibre-based imaging", *Nat. Commun.*, vol. 3, 1027, 2012.

[3] I. Papadopoulos *et al.*, "High-resolution, lensless endoscope based on digital scanning through a multimode optical fiber", *Biomed. Opt. Express*, vol. 4, no. 2, 260-270, 2013.

[4] A. J. Thompson *et al.*, "Adaptive phase compensation for ultracompact laser scanning endomicroscopy", *Opt. Lett.*, vol. 36, no. 9, 1707-1709, 2013.

[5] E. R. Andresen *et al.*, "Toward endoscopes with no distal optics: Video-rate scanning microscopy through a fiber bundle", *Opt. Lett.*, vol. 38, no. 5, 609-611, 2013.

[6] E. R. Andresen *et al.*, "Two-photon lensless endoscope", *Opt. Express*, vol. 21, no. 18, 20713-20721, 2013.

[7] E. R. Andresen *et al.*, "Measurement and compensation of residual group delay in a multi-core fiber for lensless endoscopy", *J. Opt. Soc. Am. B*, vol. 32, no. 6, 1221-1228, 2015.

Towards a multimode fiber two-photon endoscope

Edgar E. Morales Delgado[1], Salma Farahi[1,2], Ioannis Papadopoulos[2], Demetri Psaltis[2] and Christophe Moser[1]
[1]*Laboratory of Applied Photonics Devices, School of Engineering, École Polytechnique Fédéral de Lausanne (EPFL), Station 17, 1015, Lausanne, Switzerland*
[2]*Laboratory of Optics, School of Engineering, École Polytechnique Fédéral de Lausanne (EPFL), Station 17, 1015, Lausanne, Switzerland*
edgar.moralesdelgado@epfl.ch

Keywords: Wavefront shaping, Phase conjugation, Femtosecond pulses, Imaging through multimode fibers.

Multiphoton endoscopy through optical fibers has been traditionally based on a single mode fiber bundle or double clad fibers whose single mode core is used to deliver illumination. A lens placed at the distal tip of the fiber focuses the light on the specimen and the fluorescence is collected through the fiber bundle or the multimode cladding [1]. In the case of the fiber bundle, the image is pixelated by the bundles. For the dual clad fiber, a scanning mechanism is required at the distal tip to move the focused spot over the field of view.

The information capacity of multimode optical fibers, given by the large number of supported propagation modes, has allowed a new type of ultra-thin endoscopy in which point-scanning single-photon fluorescent imaging through multimode fibers without distal lenses or mechanical actuators have been demonstrated using wavefront-shaping, digital phase conjugation or the transmission matrix measurement [2-4].

Adding of multiphoton imaging capability to such methods is not straightforward. The transmission of ultrashort pulses through multimode fibers produces a scrambled intensity profile and a broad temporal pulse due to modal dispersion. Attempts have been made for two-photon lensless imaging through a custom fiber bundle [5]. However, simultaneous spatial and temporal control of light propagation through multimode fibers has not been demonstrated.

In this work, we have developed a method to deliver spatially focused femtosecond pulses through a multimode optical fiber, which can be used for two-photon endoscopy. We minimize modal dispersion by a time-gated mode-selective phase conjugation process, in which only a set of modes of similar group velocities is counter-propagated. The non-excitation of modes of different group velocities reduces modal dispersion. We use digital phase conjugation (DPC) to achieve selective mode launching by spatially modulating a phase conjugated reconstructed field on the proximal side, consisting of the selected time-sampled set of modes. We demonstrate that the spatial control provided by the selected set of modes is enough to generate a 500 fs ultrashort pulse spatially focused at the distal end of a 30 cm long fiber, as shown in Fig. 1. Moreover, we show that the delivered focused pulse can produce two-photon absorption in a Silicon-based detector, opening the possibility of ultra-thin lensless multiphoton imaging through multimode fibers.

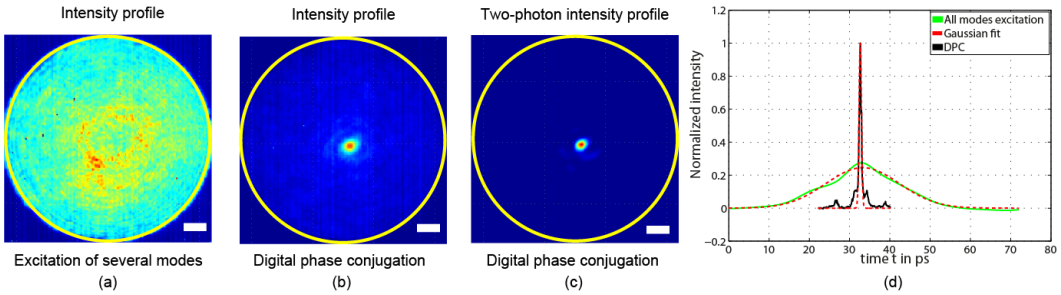

Fig. 1 Comparison between the excitation of several fiber modes and the proposed selective-mode excitation method. (a) Intensity when many fiber modes are excited. (b) Intensity of the delivered focused pulse using the proposed method. The spot size is 7 µm. The spot is 10 times more intense than the surrounding background. (c) Two-photon intensity of the delivered focused pulse. The spot size is 5 µm. The spot is 270 times more intense than the surrounding background. (d) Envelope of the second order autocorrelation trace of the delivered pulse for the case of excitation of several fiber modes (green curve) and for the proposed method (black curve). Dashed red lines are their respective Gaussian fits. The temporal duration of the phase conjugated spot is 500 fs, which is 30 times shorter than the duration of the broad pulse generated when many fibers modes are excited. The broad pulse (black curve) was scaled to enhance its visibility on the graph. Both pulses possess the same energy. Scale bars are 30 µm. Yellow circles indicate the edge of the core of the multimode fiber.

References

[1] B. A. Flusberg, E. D. Cocker, W. Piyawattanametha, J. C. Jung, E. L. M. Cheung, and M. J. Schnitzer, "Fiber-optic fluorescence imaging," Nature Methods 2, 941-950 (2005).

[2] Bianchi, S. & Di Leonardo, R. A multimode fiber probe for holographic micromanipulation and microscopy. *Lab Chip* **12,** 635–639 (2012).

[3] Čižmár, T. & Dholakia, K. Exploiting multimode waveguides for pure fibre-based imaging. *Nat. Commun.* **3,** 1027 (2012).

[4] I. N. Papadopoulos, S. Farahi, C. Moser, and D. Psaltis, "High-resolution, lensless endoscope based on digital scanning through a multimode optical fiber," Biomedical Opt. Express 4, 260 (2013).

[5] Andresen, E. R., Bouwmans, G., Monneret, S. & Rigneault, H. Two-photon lensless endoscope. *Optics Express* **21,** 20713–20721 (2013).

Wide-field adaptive optics without guide stars

Jerome Mertz[1,2], Jiang Li[1], Devin Beaulieu[2], Hari Paudel[2], Roman Barankov[1], Thomas Bifano[2]

[1] *Dept. of Biomedical Engineering, Boston University, Boston, MA USA*
[2] *Photonics Center, Boston University, Boston, MA USA*

jmertz@bu.edu

Keywords: Adaptive Optics, Phase retrieval, Microscopy.

1. INTRODUCTION

Sample-induced aberrations generally lead to reduced image quality in optical microscopy. A standard approach to counter such aberrations is to use adaptive optics (AO), which was first developed in astronomy but is now gaining traction in microscopy. The basic idea of AO is to insert an active optical correction element, typically a deformable mirror, in the optical path of the microscope to compensate for the aberrations produced by sample. The most common placement of this correction element, by far, is in a pupil plane of the microscope optics, called pupil AO. However, as first recognized by the astronomy community, a placement of the correction element in a plane conjugate to a primary sample aberration plane can lead to a significant field of view (FOV) advantage when these aberrations are spatially varying [1]. More recently this advantage of conjugate AO has been recognized by the microscopy community both in simulation studies and in experiment. In this paper we describe a novel implementation of conjugate AO, bearing in mind that our results can be equally applied to pupil AO.

2. TECHNIQUE

We demonstrate an implementation of widefield microscopy with sensor-based AO that does not require the use of guide stars [2]. Wavefront sensing is performed using illumination provided directly by the object itself, over the entire FOV of the wavefront correction. Since our implementation here involves conjugate AO (as opposed to pupil AO), the correction FOV is almost as large as the full FOV of our microscope. The development of our technique addressed two key challenges. The first challenge was the development of a wavefront sensor that exhibits large dynamic range capable of operating with relatively uncollimated light. For this we used a technique called partitioned aperture wavefront (PAW) sensing, previously developed in our lab for quantitative wavefront sensing [3]. The second challenge was to modify PAW sensing to enable it to work with an arbitrarily distributed extended source, namely the object itself. As we will see, this required supplementing PAW sensing with additional information provided by the science camera in our system (i.e. the imaging camera focused on the object), and applying a phase retrieval algorithm based on the Van Cittert-Zernike theorem.

We provide proof of principle demonstrations of our technique

REFERENCES

[1] J. Mertz, H. Paudel, T. G. Bifano, "Field of view advantage of conjugate adaptive optics in microscopy applications," Appl. Opt. 54, 3468-3506 (2015).

[2] J. Li, D. R. Beaulieu, H. Paudel, R. Barankov, T. G. Bifano, J. Mertz, "Conjugate adaptive optics in widefield microscopy with an extended-source wavefront sensor," http://arxiv.org/abs/1506.03463 (2015).

[3] A. B. Parthasarathy, K. K. Chu, T. N. Ford, and J. Mertz, "Quantitative phase imaging using a partitioned detection aperture," Opt. Lett. 37, 4062–4064 (2012).

Wavefront Control by GPC

Jesper Glückstad[1], Andrew Banas[2], Mark Villangca[1], Darwin Palima[1]

[1] *DTU Fotonik, Dept. Of Photonics Engineering, DK-2800 Kgs. Lyngby, Denmark*
[2] *OptoRobotix ApS, SCION DTU, Diplomvej 381, DK-2800 Kgs. Lyngby, Denmark*

jesper.gluckstad@fotonik.dtu.dk www.ppo.dk www.OptoRobotix.com www.GPCphotonics.com

Keywords: Generalized Phase Contrast, Binary Phase Modulation, Wavefront Control

1. GENERALIZED PHASE CONTRAST (GPC)

Sculpting the wavefronts of light in both fixed and programmable shapes has a variety of applications in both research, industry and medicine. With the widespread use of lasers that lend themselves to efficient reshaping due to their high spatial coherence, the versatility of wavefront control is further increased. Therefore, laser beam shaping based on photon-efficient phase-only methods are extensively applied in research such as in advanced adaptive and active microscopy and contemporary optical micro-manipulation [1,2] to mention a few typical uses. Phase-only light shaping and wavefront control is also finding its use in new and exciting applications such as for emerging neurophotonics applications and in fully parallel two-photon optogenetics [3] which applies the most advanced optical tools for exploring neuro-scientific challenges. Beyond the research laboratories, efficient light shaping is also desirable for applications such as laser machining, lithography and future laser-based digital cinemas to name a few. These diverse applications all require light to be shaped in a plurality of ways [4]. For example, the illuminated optical window of spatial light modulators, used for both optics research and consumer display projectors, have a rectangular form factor. A variety of shapes bounded by steep edges and particular point spread functions are desirable in laser cutting and engraving. In two-photon optogenetics [5], it is a key aim to selectively illuminate intricate patterns of dendrites or axons within neurons, preferably with minimal loss of light and maintaining speckle-free light excitations even within turbid media.

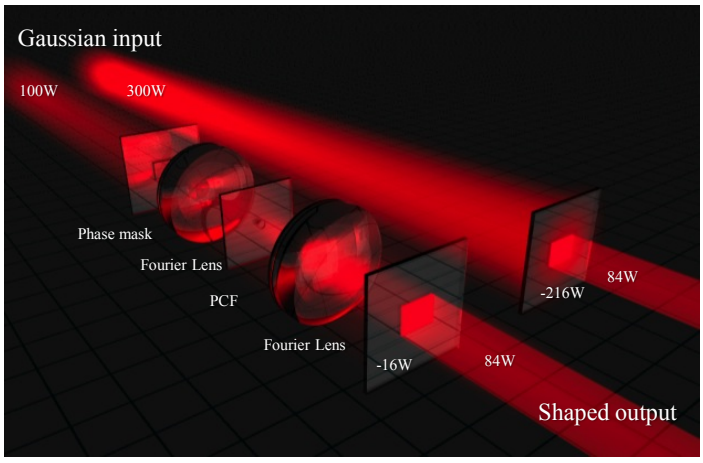

Figure 1: GPC efficiently transforms an incident Gaussian beam into a bright shaped output using only simple binary spatial phase modulation. For comparison an amplitude masking configuration is shown besides a GPC Light Shaper to illustrate the significant difference in energy utilization when aiming for the same shaped output. (Figure adapted from [6])

Laser sources typically exhibit a Gaussian intensity profile. Shaping such a beam with the commonly applied hard truncation is inherently highly inefficient. It is well known that more than two thirds of an incident power will be lost when homogenously illuminating a rectangular aperture with an expanded Gaussian beam [6-8]. To complicate things, this lost light power will inherently contribute to device heating that can either shorten device lifespan or require additional power for active cooling. Besides the obvious disadvantages of light inefficiency, the high price tag of advanced laser sources, such as femtosecond lasers or supercontinuum sources, used for multi-photon excitation, multi-spectral biophotonics and other state-of-the-art experiments, demands efficient use of the available photons

GPC (for Generalized Phase Contrast) belongs to the class of non-absorbing common-path architectures [9]. A phase-only aperture directly representing the desired output intensity is mapped through the interference of its high and phase-shifted low spatial frequencies. This is achieved by phase shifting the lower spatial frequencies through a binary phase contrast filter (PCF) at the optical Fourier plane (cp. Fig. 1). GPC can thus be implemented with binary phase plates that are inherently simple to mass-produce with standard foundry processes common for silicon devices or microelectronics. The use of a one-to-one mapping geometry in GPC avoids dispersion effects which makes it advantageous for use with multiple wavelengths [10,11], spectrally broad light sources or for temporal focusing which can effectively confine light along the axial direction. Recently GPC also demonstrated its inherent adaptivity for boosting computer holographic reconstructions encoded on reconfigurable spatial light modulators [12].

REFERENCES

1) J. Glückstad, “Optical manipulation: scupting the object”, Nature Photonics, Vol. 5, 7-8 (2011).
2) D. Palima, A. R. Bañas, G. Vizsnyiczai, L. Kelemen, P. Ormos, and J. Glückstad, "Wave-guided optical waveguides," Opt. Express 20, 2004–14 (2012).
3) E. Papagiakoumou, F. Anselmi, A. Bègue, V. de Sars, J. Glückstad, E. Y. Isacoff, and V. Emiliani, "Scanless two-photon excitation of channelrhodopsin-2," Nature Methods 7, 848–854 (2010).
4) D. Palima, C. A. Alonzo, P. J. Rodrigo, and J. Glückstad, "Generalized phase contrast matched to Gaussian illumination," Opt. Express 15, 11971–7 (2007).
5) D. Palima and J. Glückstad, "Gaussian to uniform intensity shaper based on generalized phase contrast," Opt. Express 16, 1507–16 (2008).
6) A. Bañas, D. Palima, M. Villangca, T. Aabo, and J. Glückstad, "GPC light shaper for speckle-free one- and two- photon contiguous pattern excitation," Opt. Express 7102, 5299–5310 (2014).
7) A. Bañas, O. Kopylov, M. Villangca, D. Palima, and J. Glückstad, "GPC Light Shaper: static and dynamic experimental demonstrations," Opt. Express (2014).
8) S. Tauro, A. Bañas, D. Palima, and J. Glückstad, "Experimental demonstration of Generalized Phase Contrast based Gaussian beam-shaper," Opt. Express 19, 7106–11 (2011).
9) J. Glückstad and P. C. Mogensen, "Optimal phase contrast in common-path interferometry.," Appl. Opt. 40, 268–82 (2001).
10) D. Palima and J. Glückstad, "Multi-wavelength spatial light shaping using generalized phase contrast," Opt. Express 16, 1331–42 (2008).
11) O. Kopylov, A. Bañas, M. Villangca, and D. Palima, "GPC light shaping a supercontinuum source," Opt. Express 23, 1894–1905 (2015).
12) M. Villangca, A. Banas, D. Palima, and J. Glückstad, “GPC-enhanced read-out of holograms,” Opt. Comm. 351, 121-127 (2015).

Remote axial positioning of temporally focused holographic patterns

Oscar Hernandez[1,*], Ben Leshem[2,*], Eirini Papagiakoumou[1], Valentina Emiliani[1] and Dan Oron[2]

[1] *Wavefront Engineering Microscopy, Group, Neurophotonics Laboratory, University Paris Descartes, Sorbonne Paris Cité, Paris, France*
[2] *Department of physics of Complex Systems, Weizmann Institute of Science, Rehovot 76100, Israel*
* *Equal contributors*

dan.oron@weizmann.ac.il

Keywords: wavefront shaping, light patterning, nonlinear microscopy, temporal focusing

Two-photon excitation with temporally focused pulses can be combined with phase-modulation approaches, such as computer-generated holography and generalized phase contrast, to efficiently distribute light into two-dimensional, axially confined, user-defined patterns [1,2]. These light patterns are extremely robust against the effects of scattering and can propagate through hundreds of microns into brain tissue without significant degradation [3,4] . However, thus far these approaches were limited to the generation of patterns focused at the objective focal plane.

For temporally focused Gaussian beams, it was shown both theoretically and experimentally that the temporal focal plane can be axially shifted by applying a quadratic spectral phase to the incident beam (Group Velocity Dispersion, GVD) [5]. However, the case for complex wavefronts is not straightforward. Here, present an analytical, numerical and experimental study of this phenomenon and the conditions that enable remote axial control of temporally focused holographic patterns.

Remote axial displacement of holographic patterns enables coupling of holographic illumination with a second imaging or stimulation channel, providing independent control of their respective focal planes, as well as remote volume scanning.

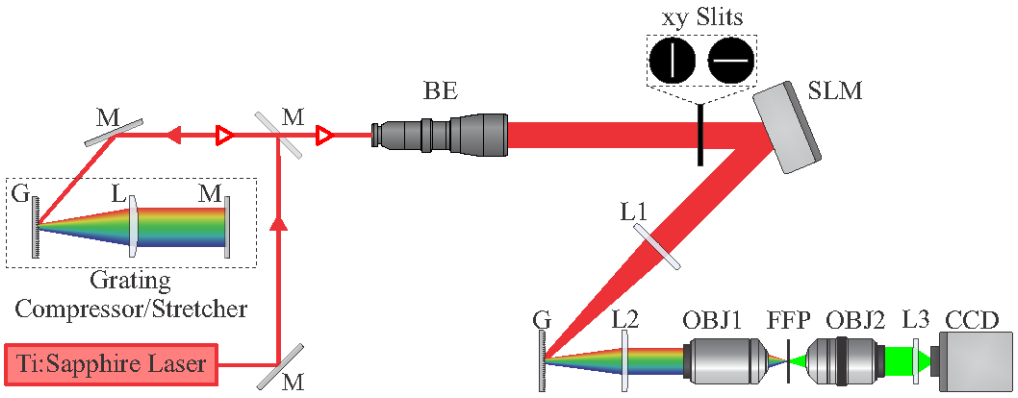

Figure 1: Schematic of an experimental setup for remote axial displacement of temporally focused holographic patterns. Laser beam from a Ti:Sapphire laser is passed through a grating compressor/stretcher where GVD is applied. The beam then impinges on an SLM and focused into the TF setup, constituted of a diffraction grating, G, and an imaging system. L: Lens, M: Mirror, BE: Beam Expander, OBJ: microscope Objectives, FFP: Front Focal Plane.

REFERENCES

[1] D. Oron, E. Tal, and Y. Silberberg, "Scanningless depth-resolved microscopy," Opt. Express 13, 1468–1476, 2005.

[2] E. Papagiakoumou, F. Anselmi, A. Bègue, V. de Sars, J. Glückstad, E. Y. Isacoff, and V. Emiliani, "Scanless two-photon excitation of channelrhodopsin-2," Nature methods 7, 848–854, 2010.

[3] A. Bègue, E. Papagiakoumou, B. Leshem, R. Conti, L. Enke, D. Oron, and V. Emiliani, "Two-photon excitation in scattering media by spatiotemporally shaped beams and their application in optogenetic stimulation" Biomed. Opt. Express 4 (12), pp. 2869, 2013.

[4] E. Papagiakoumou, A. Bègue, B. Leshem, O. Schwartz, B.M. Stell, J. Bradley, D. Oron and V. Emiliani, "Functional patterned multiphoton excitation deep inside scattering tissue", Nature Photon 7 (4), pp. 274–278, 2013.

[5] M.E. Durst, G. Zhu and C. Xu, "Simultaneous spatial and temporal focusing for axial scanning". Opt. Express 14 (25), p. 12243, 2006.

Super-resolution in marker-free optical far-field microscopy using numerical reconstruction

Ting Zhang, Charan Godhavarti, G. Maire, K. Belkebir, H. Giovannini, M. Allain, P. Chaumet , Anne Sentenac

Fresnel Institute, faculté de St Jérôme, 13013 Marseille, France

Anne.sentenac@fresnel.fr

The resolution of marker-free microscopy is fundamentally limited by the elastic light-matter interaction which states that, in the single scattering regime, the far-field scattered by an object illuminated under propagative waves conveys information on the object permittivity spatial frequencies up to $2/\lambda$ at most (where λ is the illumination wavelength in the background medium). In addition, this information is poorly restored with conventional analogical microscopes (such as brightfield or confocal) as the observed standard resolution limit, seen as the full width at half maximum of a point-like object is usually about 0.6 λ instead of the theoretical reachable diffraction limit of 0.3λ [1].

A widely explored solution for improving the resolution consists in taking advantage of evanescent waves for the illumination or the detection via near-field probes or metamaterial lenses [2-4]. These techniques ameliorate the resolution, albeit seldom beyond 0.3λ in practice, but at the expense of an increase in the experimental complexity and a restriction to surface imaging.

Another research avenue consists in extracting the most out of the sample scattered field using numerical reconstructions based on an accurate model of the sample-light interaction. This quantitative imaging approach has been implemented in a specific far-field microscope configuration, known as Tomographic Diffraction Microscopy (TDM), synthetic aperture holography or phase nanoscopy, in which the phase and amplitude of the scattered field are recorded for many angles of incidences via an interferometric mounting [3]. It has been shown experimentally to achieve the best possible resolution of 0.3λ [4-6] in the single scattering regime and even much better for certain samples in the multiple scattering regime (when the theory subtending the notion of diffraction-limited resolution does not hold) [7].

An additional advantage of quantitative TDM compared to analogical microscopes is that it can take advantage of *a priori* information on the sample to restrain the possible solutions of the inverse problem and possibly recover object spatial frequencies beyond the physically accessible domain. The most widespread constraint is the positivity of the sought parameter. Studied in numerous applications, from fluorescence microscopy to TDM or microwave and acoustic imaging, it has been shown to improve the readability of the images, in particular by suppressing the deconvolution-induced oscillating behavior of the background, but has seldom brought any significant amelioration of the resolution [8].

In this work, we push forward the performance of TDM by imposing a binary behavior on the permittivity. Contrary to positivity, binary constraint is expected to have a major influence on the resolution by raising the indetermination between small objects of similar optical volume. We demonstrate experimentally that it permits a spectacular improvement of the TDM resolution on complex samples.

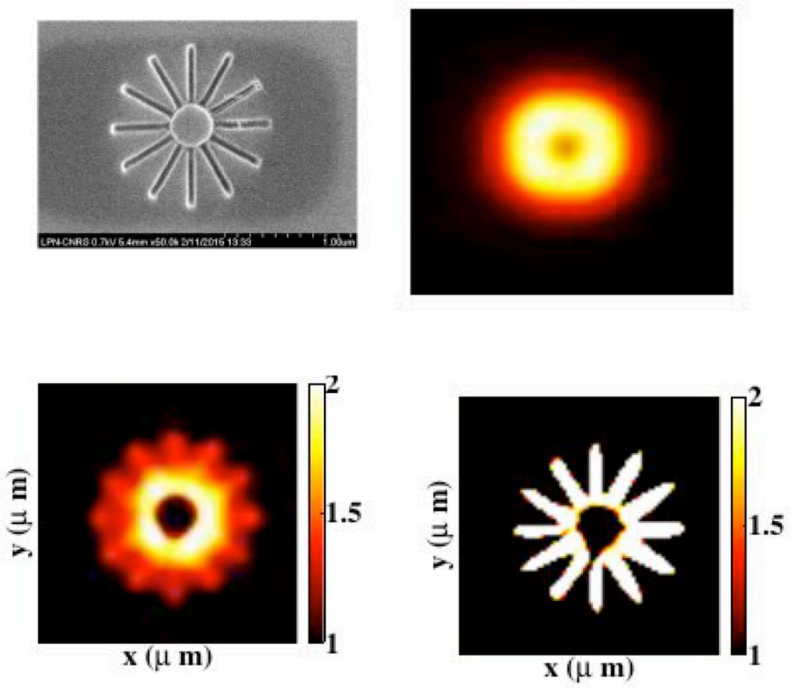

Top left: TEM image of a sample made of resin rods of width 66 nm and length 475 nm deposited on a Si substrate. Top right: darkfield image of the sample. Bottom left: TDM reconstruction using the positivity constraint. Bottom right: TDM reconstruction using the binarity constraint. The TDM experiment is conducted at a wavelength of 475 nm. The observed resolution in the bottom right figure is about one sixth of the wavelength.

References

[1] D. W. Pohl, U. Ch. Fischer and U. T. Dürig 'Scanning near-field optical microscopy', J. of Microscopy, 152, 853-861, (1988)

[2] Liu Z, Lee H, Xiong Y, Sun C, Zhang' far-field optical hyperlens magnifying sub-diffraction-limited objects' Science 315, 1686, (2007)

[3] O. Haeberlé, K. Belkebir, H. Giovannini and A. Sentenac, 'Tomographic Diffractive Microscopy, basics, techniques and perspectives', 57, 686-699, (2010) and references therein

[4] M. Debailleul, V. Georges, B. Simon, R. Morin, and O. Haeberlé 'High-resolution three-dimensional tomographic diffractive microscopy of transparent inorganic and biological samples'Optics Letters Vol. 34, Issue 1, pp. 79-81 (2009)

[5] Yann Cotte, Fatih Toy, Pascal Jourdain,Nicolas Pavillon, Daniel Boss,Pierre Magistretti, Pierre Marquet and Christian Depeursinge, 'marker-free phase nanoscopy', Nature Photonics, 7, 113, (2013)

[6] T. Zhang, Y. Ruan, G. Maire, D. Sentenac, A. Talneau, K. Belkebir, P. C. Chaumet, and A. Sentenac, 'Full-polarized tomographic diffraction microscopy achieves a resolution about one fourth of the wavelength ', Physical review letters, 11, 243904 (2013)

[7] J. Girard, G. Maire, H. Giovannini, A. Talneau, K. Belkebir, P. C. Chaumet and A. Sentenac, Nanometric resolution using far-field optical tomographic microscopy in the multiple scattering regime, Phys. Rev. A 82, 061801(R) (2010)

[8] R. Heintzmann 'Estimating missing information by maximum likelihood deconvolution', micron 38, 136-144, (2007)

Tomographic diffractive microscopy combining sample and illumination rotation delivers 3-D isotropic resolution in the 100 nm range

Jonathan Bailleul, Bertrand Simon, Matthieu Debailleul and Olivier Haeberlé

Laboratoire MIPS EA2332 Université de Haute-Alsace
IUT Mulhouse, 61 rue Albert Camus, 68093 Mulhouse Cedex, France

olivier.haeberle@uha.fr

Keywords: microholography, tomographic diffractive microscopy, Fourier imaging

Microscopy techniques, which permit to observe unlabeled samples, have recently known a regain of interest. In particular, techniques, which allow for recording both the amplitude and phase of the light diffracted by the specimen, have experienced intensive developments. Tomographic diffractive microscopy (TDM) is a numerical technique, which relies on inversion methods to reconstruct from the diffracted field an image of the observed sample. For weakly diffractive specimens, the diffracted field simply depicts a subset of the 3-D Fourier transform of the observed specimen permittivity distribution [1-3].

In Fourier space, the diffracted wave depicts the so-called Ewald sphere. Because of the microscope objective's limited numerical aperture, only a cap of sphere can be recorded. In digital holographic microscopy with a single illumination, one can therefore record only very limited information about the sample [4,5]. In order to improve the resolution, TDM makes use of a large number of tilted illuminations, and a numerical synthetic aperture process permits to accumulate information in Fourier space. As a result, an enlarged and filled frequency support is obtained: Fig. 1(left) [4-7]. In this approach the resolution is strongly anisotropic, because of a dissymmetric Optical Transfer Function (OTF), and the so-called "missing cone", characteristic of transmission microscopes, induces poor sectioning capabilities [4,7].

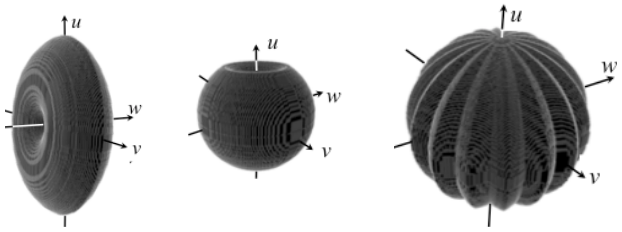

Figure 1: Optical Transfer Functions achievable in TDM with illumination rotation (left), sample rotation (middle), and combining illumination and sample rotation (right)

On the contrary, TDM with specimen rotation permits a quasi-isotropic resolution (Fig. 1(middle)) [8]. A possible limitation of this approach is its lower resolution. Furthermore, it often requires a large number of acquisitions (typically one per degree [9]) to deliver a precise reconstruction of the observed sample, while maintaining a high precision rotation, compatible with interferometric measurements, is very difficult.

Several configurations have been proposed in order to combine the high resolution permitted by TDM with illumination rotation with the isotropic resolution permitted by TDM with specimen rotation [10]. We have built a TDM microscope incorporating a dedicated specimen rotation stage in the aim of combining several OTFs from TDM with illumination rotation, so as to obtain a symmetric final synthetic OTF, but with very few rotations compared to classical TDM with specimen rotation. Figure 1(right) shows the final achievable OTFs for 8 acquisitions: note the wider *and* missing-cone free OTF, which indicates that a high-, isotropic resolution should be achievable in this configuration.

Figure 2 shows experimental results. An optical fiber was tapered by the heat-and-pull technique, which permits to obtain very sharp tips, with diameter below 100 nm. Figure 2(a) shows (x-y), (x-z), and (y-z) cuts of the 3-D image of the fiber tip, obtained in TDM with one angle of view (without object rotation). Note that the lateral resolution permits to observe the fiber tip on the (x-y) view, but the resolution along the optical axis (z) is lower: the sharp tip is not visible in the (x-z) view, and the fiber itself is not seen as a cylindrical object, but is deformed along the optical axis.

Figure 2(b) shows the same fiber, after combining 5 views. The section of the fiber now depicts a disc, as expected, and the sharp tip is visible on both (x-y) and (x-z) views, indicating that an isotropic resolution is indeed obtained (in the 100nm range, with $\lambda = 475$ nm, $NA_{obj} = NA_{cond} = 1.4$).

Figures 2(c-e) shows a pollen grain observed with our system. Figures 2(c,d) show (x-y) and (x-z) views. Note the pollen spikes, visible on the (x-y) view, but hardly noticeable on the (x-z) view. Figure 2(e) shows a 3-D recombination of three views, in three different colors: spikes along quasi-orthogonal directions are now visible (in green and red). Note also that precise recombination of data is possible only when a numerical correction of the aberrations is performed [11]. This aberration correction constitutes an equivalent of adaptative optics, but performed numerically, thanks to the recording of the diffracted field in both amplitude and phase, and not in intensity only as in fluorescence microscopy.

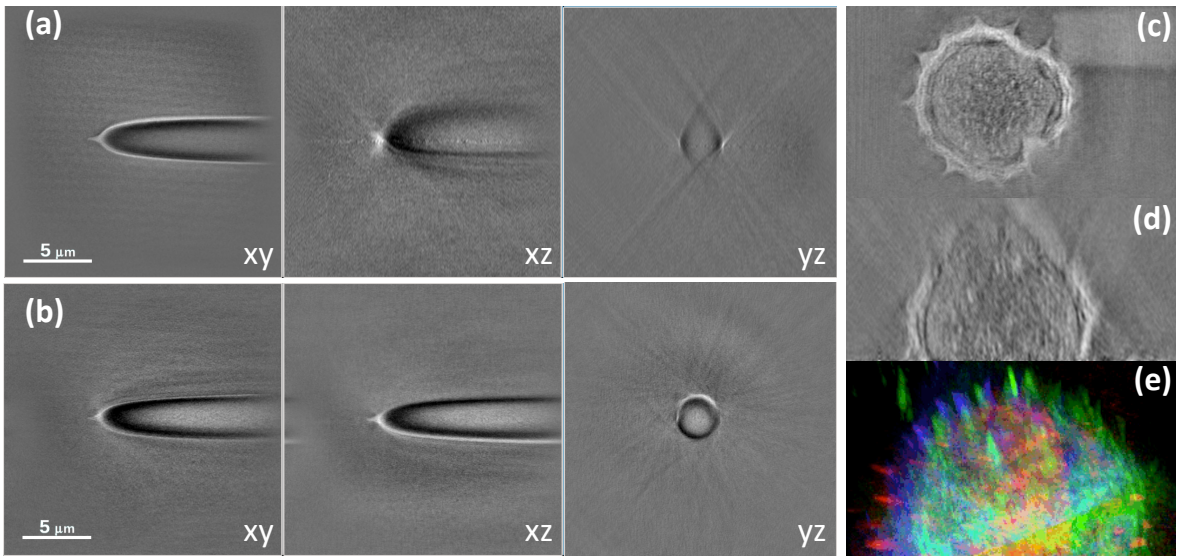

Figure 2: Optical fiber and pollen grain observed in TDM with sample and illumination rotation.

REFERENCES

[1] E. Wolf, "*Three-dimensional structure determination of semi-transparent objects from holographic data*", Opt. Commun. **1**, pp. 153-156 (1969)

[2] V. Lauer, "*New approach to optical diffraction tomography yielding a vector equation of diffraction tomography and a novel tomographic microscope*"J. Microscopy **205**, pp. 165-176 (2002)

[3] O. Haeberlé *et al*. "Tomographic Diffractive Microscopy: Basics, Techniques and Perspectives", J. Mod. Opt. **57**, 686-699 (2010)

[4] B. Simon, *et al*., *"Tomographic diffractive microscopy of transparent samples*", Eur. Phys. J. Appl. Phys. **44**, pp. 29-35 (2008)

[5] M. Debailleul, *et al*., *"High resolution three-dimensional tomographic diffractive microscopy of transparent inorganic and biological samples*", Opt. Lett. **34**, pp. 79-81 (2009)

[6] B. Simon, *et al*., "*High resolution tomographic diffractive microscopy of biological samples*", J. Biophoton. **3**, pp. 462-467 (2010)

[7] Y. Cotte, *et al*., *"Marker-free phase nanoscopy"*, Nature Phot. **7**, pp. 113–117 (2013)

[8] S. Vertu, J.-J. Delaunay, I. Yamada, and O. Haeberlé, *"Diffraction microtomography with sample rotation: influence of a missing apple core in the recorded frequency space"*, Centr. Eur. J. Phys. **7**, pp. 22-31 (2009)

[9] A. Kuś, M. Dudek, B. Kemper, M. Kujawińska, and A. Vollmer, *"Tomographic phase microscopy of living three-dimensional cell cultures"*, J. of Biomed. Opt. **19**, 046009 (2014)

[10] S. Vertu, J. Flügge, J.-J. Delaunay, and O. Haeberlé, "Improved and isotropic resolution in tomographic diffractive microscopy combining sample and illumination rotation," Central Eur. J. Phys. **9**, pp. 969-974 (2011)

[11] H. Liu, *et al*., *"Tomographic diffractive microscopy and multiview profilometry with flexible aberration correction"*, Appl. Opt. **53**, pp. 748-755 (2014)

Depth of field extension for fast volumetric imaging using light-sheet microscopy

Jordi Andilla[1], Omar E. Olarte[1], Jacob Licea[1], David Artigas[1,2], and Pablo Loza-Alvarez[1]

[1] ICFO-Institut de Ciencies Fotoniques,
Av.Carl Friedrich Gauss, 3, 08860 Castelldefels (Barcelona), Spain
[2] Department of Signal Theory and Communications, Universitat Politècnica de Catalunya,
Jordi Girona 1-3,08034 Barcelona, Spain
Pablo.loza@icfo.es

Keywords: Fast Imaging, Light-Sheet Microscopy, Wavefront Coding.

1. INTRODUCTION

Microscopy is one of the fundamental sources of information for modern biology. Current demands on this field are the visualization of large 3D samples, with increased sensitivity, higher resolutions and at faster speeds. Several developments based on different techniques like point-scanning, light-sheet and pointillist strategies have been designed to tackle some of these demands. Although successful, all these possess an important requirement: The illuminated sections need to be tightly coupled with the detection optics in order to accomplish efficient optical sectioning. In this work, we demonstrate a method that breaks this paradigm. This is done by extending the depth of field (DoF) of the detection optics using wavefront coding [1] in combination with light-sheet microscopy [2]. As a consequence, the light-sheet can be freely accommodated to any place within the extended DoF while maintaining the optical sectioning capabilities. This gained degree of freedom allows for a quick scan of the light-sheet along the extended DoF, without the need of any other moving element.

2. DESCRIPTION OF THE WORK

In this work, we present the actual implementation of a system that implements the combination of wavefront coding with light sheet microscopy techniques. We also present a complete characterization of the system that determines the performances and limits of the implementation. Finally, we demonstrate capabilities of the system when imaging biological samples and the acquisition of volumetric images faster than 2x volumetric video-rate (>70 volumes/second).

REFERENCES

[1] J. Dowski and W.T. Cathey, "Extended depth of field through wave-front coding." Appl. Opt. 34, 1859–1866, 1995.

[2] J. Huisken, J. Swoger, F. Del Bene, J. Wittbrodt and E. H. K. Stelzer, "Optical Sectioning Deep Inside Live Embryos by Selective Plane Illumination Microscopy." Science 305, 1007–1009, 2004.

New perspectives for Ultrasound in the brain: fUltrasound imaging and Ultrasound Localization Microscopy

Mickaël Tanter

Institut Langevin, ESPCI ParisTech, CNRS, INSERM, Paris, France

mickael.tanter@espci.fr

In the last fifteen years, the introduction of plane or diverging wave transmissions rather than line by line scanning focused beams has broken the conventional barriers of ultrasound imaging. By using such large field of view transmissions, the frame rate reaches the theoretical limit of physics dictated by the ultrasound speed and an ultrasonic map can be provided typically in tens of micro-seconds (several thousands of frames per second). Interestingly, this leap in frame rate is not only a technological breakthrough but it permits the advent of completely new ultrasound imaging modes, including shear wave elastography, electromechanical wave imaging, ultrafast doppler, ultrafast contrast imaging, and even functional ultrasound imaging of brain activity (fUltrasound) introducing Ultrasound as an emerging full-fledged neuroimaging modality.

At ultrafast frame rates, it becomes possible to track in real time the transient vibrations – known as shear waves – propagating through organs. Such "human body seismology" provides quantitative maps of local tissue stiffness whose added value for diagnosis has been recently demonstrated in many fields of radiology (breast, prostate and liver cancer, cardiovascular imaging...). Today, Supersonic Imagine company is commercializing the first clinical ultrafast ultrasound scanner, Aixplorer® with real time Shear Wave Elastography. This is the first example of an ultrafast Ultrasound approach surpassing the research phase and now widely spread in the clinical medical ultrasound community with an installed base of more than 1000 Aixplorer systems in 54 countries worldwide. Beyond clinical applications, it leads also to better fundamental understanding of the influence of tissue mechanics on carcinogenesis.

For blood flow imaging, ultrafast Doppler permits high-precision characterization of complex vascular and cardiac flows. It also gives ultrasound the ability to detect very subtle blood flow in very small vessels. In the brain, such ultrasensitive Doppler paves the way for **fUltrasound** (functional ultrasound imaging) of brain activity with unprecedented spatial and temporal resolution compared to fMRI.

Finally, we recently demonstrated that Ultrafast Ultrasound Localization could provide a first *in vivo* and non-invasive imaging modality at microscopic scales deep into organs combined with contrast agents. Many of these ultrafast modes should lead to advancements in prevention, diagnosis, and therapeutic monitoring.

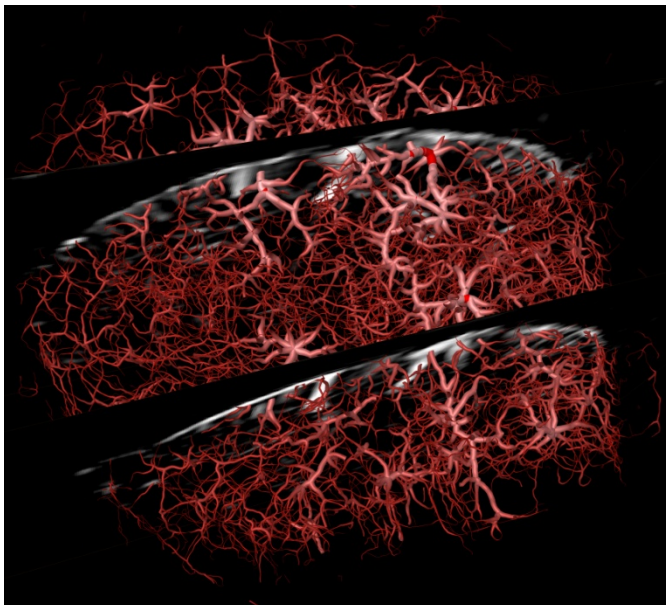

3D Ultrafast Doppler Imaging of the rat brain (C.Demene et al)

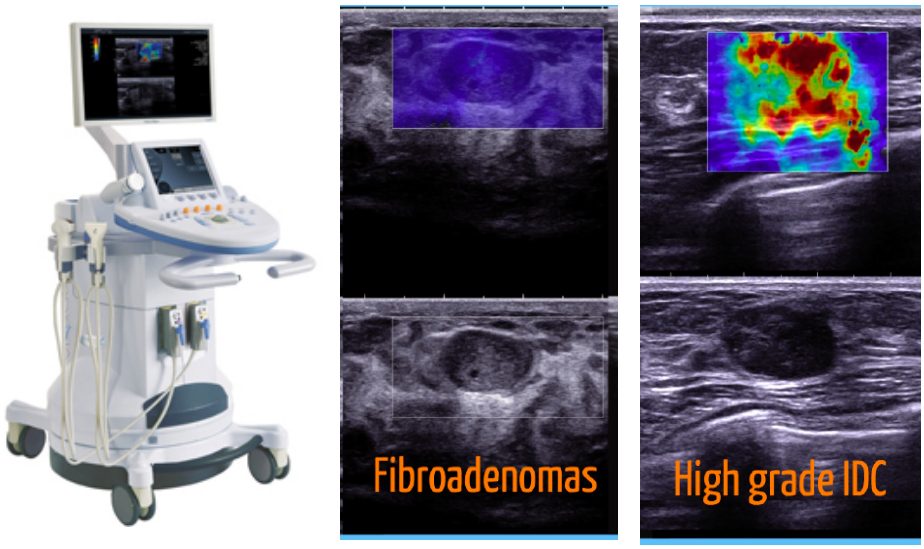

Quantification of biomechanical properties of organs using Shear Wave Elastography (Breast lesions examples)

POSTER SESSION

Quantitative Phase Tomographic Imaging to Investigate Label-free Biological Tissues before Applying Adaptive Optics

S. Aknoun[1], Pierre Bon[2], J. Savatier [3], B. Wattellier[1], S. Monneret[3]

[1] *Phasics S.A, Espace technologique de Saint Aubin, Route de l'Orme des Merisiers, 91190 Saint Aubin, France*

[2] *CNRS, Institut d'Optique (LP2N), UMR 5298, Bordeaux Univ. Talence, France*

[3] *Aix-Marseille Université, CNRS UMR 7249, Institut Fresnel, Campus de Saint-Jérôme, 13013 Marseille, France*

aknoun@phasics.fr

Keywords: quantitative phase imaging, optical tomography, adaptive optics

INTRODUCTION

It is known that for high numerical aperture high magnification microscopy, images are degraded by optical aberrations for depths of more than tens of micrometers. Microscope objectives are optimized to image samples close to the coverslip. When the object plane is set far from the coverslip, the index mismatches between the medium, coverslip, immersion oil and objective glass generate spherical aberration at the image center and off-axis aberrations at the edges. These aberrations are predictable since they mostly depend on the imaging depth and the sample mean index. However the optical rays emitted or diffracted by the sample are refracted also by the sample inhomogeneities. This distorts the image wave front and degrades the image quality. Both effects are now one of the limiting factors for deep imaging, scattering being another one.

In this paper, we will focus on the tissue-self-induced aberrations. Spherical aberration or associated off-axis aberrations (astigmatism and coma) are predictable with respect to the imaging depth or at least reproducible for different sample locations. Tissue self-induced aberrations by definition depend on the sample location and need to be evaluated prior to imaging. In preliminary studies, it is interesting to evaluate the refractive index 3D structure to make statistical models for adaptive optics. In analogy with multi-conjugate adaptative optics, it is interesting to know whether the refractive index is mostly homogeneous or if specific layers have more influence on the image aberrations. Knowing the location of these layers will help optimize the deformable mirror conjugation.

To generate the refractive index 3D structure maps, we have applied a new technique for tomographic phase imaging, called TIPI.

TOMOGRAPHIC INCOHERENT PHASE IMAGING (TIPI)

Quantitative phase imaging (QPI) is a powerful method to visualize a semi-transparent sample in a quantitative manner. Plenty of techniques for QPI have been developed in the last decade but the majority of them only work under spatially coherent illumination. However, coherent illumination leads to noisy (speckle), poor resolution (especially in the axial direction) images, which limits the use of QPI for biological tissue imaging.

Using a spatially incoherent illumination rather than a coherent one has multiple advantages: (i) axial sectioning is achieved with a doubled lateral resolution compared to coherent QPI; (ii) a 3D reconstruction of the sample can be obtained simply by scanning it in the axial direction; and (iii) this approach can also be applied on highly scattering samples, usually not compatible with QPI because of the coherence loss.

We propose to use spatially incoherent illumination combined with axial scanning of the sample (z-scan) and a numerical 3D deconvolution to achieve QPI with the same 3D resolution as fluorescence imaging. Indeed, we have shown that quadri-wave lateral shearing interferometry (QWLSI) is one of the few

techniques able to retrieve QPI under spatially incoherent illumination [1,2]. Moreover, incoherent QPI is achieved without any microscope modification: QWLSI is used as conventional camera directly plugged onto the microscope with its native Köhler illumination.

We will show quantitative 3D reconstruction of complex structures (such as brain tissue, see Figure 1) and discuss the applications of this technique combined with regular fluorescence imaging.

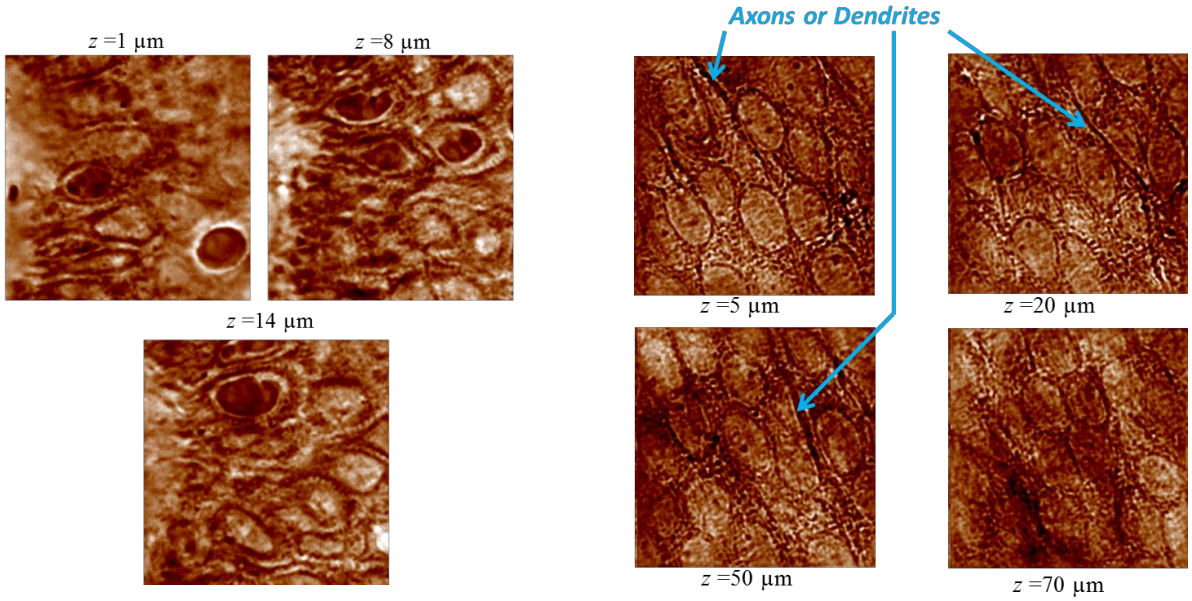

Figure 1: (left) tomographic phase images of a 14-µm thick mouse skin. The different cell layers are clearly resolved (right) Tomographic images of a 100-µm thick mouse brain biopsy at different depths (z)

REFERENCES

[1] Bon, Maucort, Wattellier, and Monneret, "Quadriwave lateral shearing interferometry for quantitative phase microscopy of living cells," *Opt. Express* 17, 13080-13094 (2009)

[2] Bon, Aknoun, Monneret, Wattellier, "Enhanced 3D spatial resolution in quantitative phase microscopy using spatially incoherent illumination", *Opt. Express*, 22(7), 8654-8671 (2014)

[3] Bon, Lécart, Fort, Lévêque-Fort, "Fast Label-Free Cytoskeletal Network Imaging in Living Mammalian Cells", *Biophysical J.*, 106, 1588 - 1595 (2014)

Fast wavefront shaping for focusing through biological tissue

Baptiste Blochet[1, 2], David Martina[1], Laurent Bourdieu[2], Sylvain Gigan[1]

[1] *Laboratoire Kastler Brossel, ENS-PSL Research University, CNRS, UPMC-Sorbonne universités, Collège de France ; 24 rue Lhomond, F-75005 Paris, France*

[2] *Ecole Normale Supérieure, Institut de Biologie de l'ENS (IBENS), and Inserm U1024, and CNRS UMR 8197, Paris, F-75005 France*

Baptiste.blochet@lkb.ens.fr

Keywords: Wavefront shaping, Complex media, Non-linear microscopy

INTRODUCTION

The propagation of light in biological tissues is dominated by multiple scattering: ballistic light is exponentially attenuated and scattering limits the penetration depth of conventional microscopy techniques. For coherent light, the recombination of the different scattered paths creates a complex interference known as a speckle pattern. Recently, different techniques of wavefront shaping have been developed to manipulate this speckle pattern. This technical breakthrough opens the possibility to focus light through complex media and eventually to image in them [1, 2], provided the medium can be considered stationary. We study here the possibility to focus in and through dynamical biological tissue. Their intrinsic temporal dynamics creates a fast decorrelation of the speckle pattern. Therefore, focusing trough biological tissues requires a fast wavefront shaping device and fast sensors. We investigate the use of MEMS-based spatial light modulator (SLM) and a fast photodetector, combined with different algorithms for fast focusing through thin slices of fixed and fresh biological tissues.

1. EXPERIMENTAL SETUP

A spatial light modulator (SLM) based on micro-mirrors MEMS (segmented Boston Kilo DM) controls locally the reflected phase of a green laser light (532 nm). The laser beam is focused on a biological scattering tissue by a microscope objective (4x/0,10). The multiply-scattered light is collected by a second objective (10x/0,30), which allows us to image the transmitted speckle pattern with either a camera or a photomultiplier tube (PMT). The 32x32 independent micro-mirrors SLM can work at a frequency of 32 kHz. Each mirror controls locally the phase between 0 and 2π. The signal detected by the PMT is used to control the focusing process. A computer controls the SLM and the detector to implement an optimization process with the smallest possible response time. Focusing of the light through biological samples is obtained with an optimization algorithm [3] in open loop with the photomultiplier signal as feedback.

2. ALGORITHM

The open loop algorithm works as follows. A set of spatial modes (Hadamard basis) is sent to the SLM. For each mode, four relative global phases are applied (0, $\pi/2$, π, $3\pi/2$) and the respective resulting intensities on the PMT are recorded. The intensity variation as a function of the applied phases is interpolated to determine its maximum and the optimal phase for the corresponding spatial mode. The phase mask that maximizes the focusing is built by adding up the modes with their optimal phase. In open loop, the algorithm takes approximately two seconds for 1024 modes. The resulting focus can be monitored with the CCD camera.

3. RESULTS

Two biological samples have been investigated : a fixed, strongly scattering thick skull of adult rat and a more dynamic, anisotropic scattering slice of fixed mouse brain (decorrelation time: 10s). The optimization technique was successful for the two samples.

The characteristic time of decorrelation has been measured as follows: after focusing, the phase mask is kept constant on the SLM. The variation of the intensity is recorded in time. As the media changes across time, the applied phase mask is no longer the optimal phase mask, and the intensity decreases at the focus. The characteristic time of this decrease is the decorrelation time.

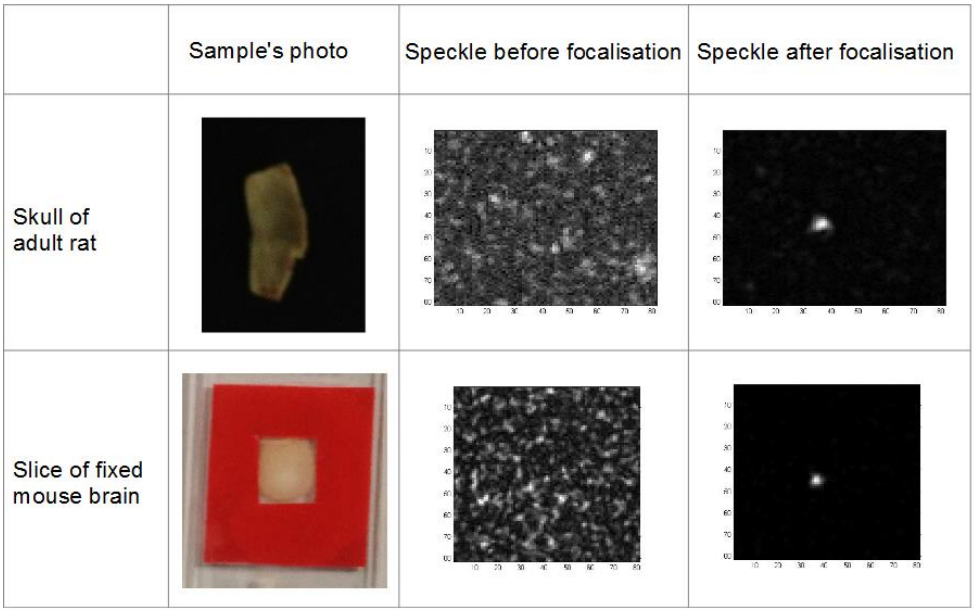

Figure 1: Sample pictures and CCD images of the speckle before and after focusing through an adult's rat skull and a fixed mouse brain's slice.

4. CONCLUSIONS AND PERSPECTIVE

The SLM's maximum frame rate is 34 kHz. We are currently developing an FPGA electronic (module NI FlexRIO FPGA) to interface faster the SLM and the detector to reach the ultimate speed and be able to study in vivo tissues with faster decorrelation time (in the range of few hundreds of millisecond). It will also allow us to implement close-loop optimization that will allow us to use more advanced algorithms.

Our experimental set-up fulfills the required characteristics (speed, number of actuators) to study ex-vivo biological tissues. Using close loop optimization at the maximum speed of the SLM, we will be able to study more dynamical sample such as acute brain slices, thus making it possible to extend these techniques to non-linear microscopy to obtain two-photon fluorescence images deep inside the mouse brain.

REFERENCES

[1] Vellekoop, I. M., & Mosk, A. P. (2007). Focusing coherent light through opaque strongly scattering media. *Optics letters*, *32*(16), 2309-2311.

[2] Popoff, S. M., Lerosey, G., Carminati, R., Fink, M., Boccara, A. C., & Gigan, S. (2010). Measuring the transmission matrix in optics: an approach to the study and control of light propagation in disordered media. *Physical review letters*, *104*(10), 100601.

[3] Vellekoop, I. M., & Mosk, A. P. (2008). Phase control algorithms for focusing light through turbid media. *Optics Communications*, *281*(11), 3071-3080.

Adaptive Biology: Refractive index matching using novel mounting media improves axial resolution

Coralie Fouquet[1,3], Jean-François Gilles[1], Nicolas Heck[1,4], Marc Dos Santos[1,4], Richard Schwartzmann[1], Alain Trembleau[1,3] and Susanne Bolte[1]

[1] *Institute of Biology Paris-Seine, CNRS FR3136, Sorbonne Universités, UPMC Univ Paris 06, Paris, France*
[3]*Lab. "Neuroscience Paris Seine" CNRS UMR8246, Inserm U1130, UPMC UM CR18, Team Development and Plasticity of Neural Networks, Paris, France*
[4]*Lab. "Neuroscience Paris Seine" CNRS UMR8246, Inserm U1130, UPMC UM CR18, Team Neuronal Signaling and Gene Regulation, Paris, France*

susanne.bolte@upmc.fr

Keywords: refractive index matching, mounting media, resolution, transparency

1. PART ONE

Resolution, high signal intensity and elevated signal to noise ratio are key issues for biologists who aim to study the localisation of biological structures on the cellular and subcellular level with confocal microscopy. The resolution required to separate sub-cellular biological structures is often near to the resolving power of the microscope. When optimally used, confocal microscopes may reach resolutions of 150 nm laterally and 500 nm axially, however, axial resolution is often impaired by spherical aberration that may occur due to refractive index mismatches (1, 2). Spherical aberration results in broadening of the point-spread function (PSF), a decrease in peak signal intensity when imaging in depth and a focal shift that leads to the distortion of the image along the z-axis and thus in a scaling error.

In this study, we use novel high refractive index mounting media to eliminate the effects of spherical aberration. These mounting media are compatible with most common fluorochromes and fluorescent proteins. We compare their performance with conventional mounting media by estimating lateral and axial resolution with subresolution fluorescent beads. We show furthermore, that the use of our high refractive index media renders fixed brain tissue transparent and improves considerably the axial resolution and imaging depth in immuno-labelled or fluorescent protein labelled fixed mouse brain (Fouquet et al., 2015). We propose thus to use those novel high refractive index mounting media, whenever optimal axial resolution is required.

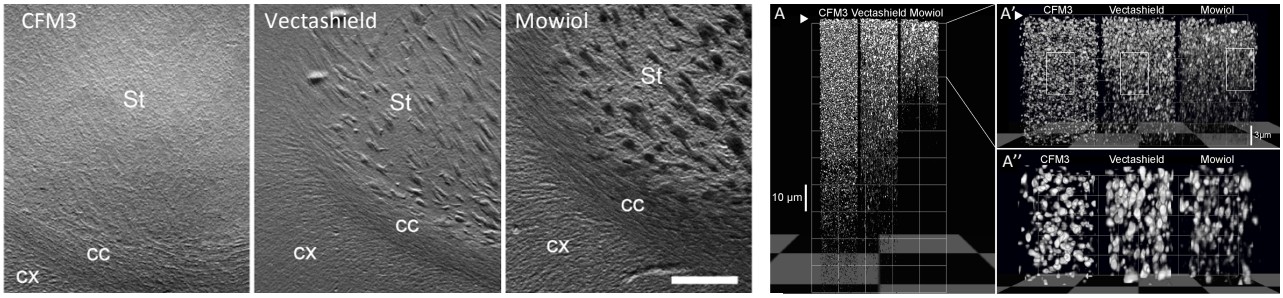

Figure 1. modified from (3)

Transparency, depth penetration and resolution improvement mouse brain sections: 100µm vibratome sections of brain of adult transgenic mice (VGLUT1^{Venus}) were mounted in CFM3 (ri=1.518), Vectashield (ri=1.458) or Mowiol (ri=unknown).

Left panels: Bright field images were taken in relief-contrast mode at equal light levels with a 1.0

objective (Zeiss Axiozoomer) to visualise contrast changes in the striatum (S), corpus callosum (CC) and cortex (C) when using different mounting media. Note that in CFM3 medium (refractive index = 1.518), the contrast of the brain section is very low, indicating refractive index matching between the fixed brain and the mounting media. Scale bars=500µm.

Right panels: Equivalent sections were imaged using the 514nm laser line. Imaging was carried out in the cortex using optimal z-sectioning. 3D-reconstructions of the entire z-stack (A) and of the first 20µm (A') of VGLUT1^{Venus}-labelled synaptic boutons demonstrate depth penetration in the different media (arrowhead = coverslip position). Note that depth penetration is best with CFM3-medium. (A'') is a magnified view of the insert in (B) showing synaptic boutons in a depth of 5-15µm. Note that the boutons mounted in Vectashield and Mowiol appear elongated in comparison to CFM3 mounted sections.

2. PART TWO

Further developments: We currently extent our study and develop novel mounting media in collaboration with our industrial partner Robert S. Davidson from Citifluor Limited. We follow two axes of development: Firstly, we aim at improve our high refractive index mounting media for the use in super-resolution microscopy (STED, Structured illumination and STORM). Secondly, we will develop tunable CFM-variants to establish refractive index matching with several tissues (brain, retina, intestine, pancreas, etc), organs and whole embryos (mouse, zebrafish, drosophila, etc.) and for imaging modes adapted to thick samples such as multiphoton microscopy and lightsheet microscopy.

REFERENCES

(1) S. Hell, G. Reiner, C. Cremer and K. Stelzer: Aberrations in confocal fluorescence microscopy induced by mismatches in refractive index. *J Microscopy*. 169, Pt 3, pp391-405, 1993

(2) A. Diaspro, F. Federici and M. Robello: Influence of refractive index mismatch in high-resolution three-dimensional confocal microscopy. *Appl Opt*. 41 (4): 685-90, 2002

(3) C. Fouquet, J.-F. Gilles, N. Heck, M. Dos Santos, R. Schwartzmann, V. Cannaya, M.-P. Morel, R. S. Davidson, A. Trembleau and S. Bolte: Improving axial resolution in confocal microscopy with new high refractive index mounting media, *Plos One*, DOI: 10.1371/journal.pone.0121096, 2015

Full-Field Optical Coherence Microscopy of human donor cornea, a quantitative study

Marie Borderie[1], Kate Grieve[1], Cristina Georgeon[1], Andreiuolo Felipe[1], Laurent Laroche[1], Djida Ghoubay[1], Celine Desousa[2], Vincent Borderie[1]

[1] *Vision Institute/CIC 503, UPMC Université Paris 06, UMR_S 968 / INSERM, U968 / CHNO des XV-XX / CNRS, UMR_7210, Paris, France*
[2] *Etablissement Français du Sang – Ile-de-France, Paris, France*

marie.borderie@sfr.fr

Keywords: cornea, optical coherence tomography, graft, cell density.

Introduction: Full Field Optical Coherence Microscopy (FFOCM) is a new approach to quantify normal donor cornea. The aim of the study was to compare cell density of diseased and healthy corneas assessed with FFOCM, confocal microscopy (CM) and histology.

Methods: Epithelial, stromal and endothelial cell density and inter-keratocyte distance of 12 corneas of 12 keratoconus patients, 5 corneas of 5 patients with stromal scar after infectious keratitis, 10 normal human donor corneas and 10 normal corneas from 10 healthy patients were assessed.

Results: Keratocyte density was significantly higher in the very anterior stromal layer than in the remaining stroma ($p<0.0001$). Epithelial and keratocyte density was significantly lower in diseased groups ($p<0.005$). Keratocyte density correlated in FFOCM ($r=0.75$; $p=0.001$) and in CM ($r=0.64$; $p=0.003$) with that measured in histology. In FFOCM cross- sections, the different groups featured different morphological characteristics.

Discussion: FFOCM seems to be an appropriate technique to quantify cellular density and stromal morphology of human donor tissue. The cell counting and correlation methods developed could be applied to other imaging modalities, including retinal images from OCT and adaptive optics.

Towards dynamic supercritical angle fluorescence microscopy

Clément Cabriel[1,2], Nicolas Bourg[1,2], Guillaume Dupuis[2], Emmanuel Fort[3], Sandrine Lévêque-Fort[1,2]

[1] Institut des Sciences Moléculaires d'Orsay (ISMO), Université Paris Sud, CNRS UMR 8214, F91405 Orsay, France

[2] Université Paris Sud, Centre de Photonique BioMédicale (CPBM), Férération LUMAT, CNRS FR 2764, F91405 Orsay, France

[3] Institut Langevin, EPSCI ParisTech, CNRS, PSL Research University, 1 rue Jussieu, F-75005 Paris, France

Mail : Sandrine.leveque-fort@u-psud.fr

Keywords: microscopy, fluorescence, super-resolution, supercritical.

1. SUPERCRITICAL FLUORESCENCE EMISSION

Membrane imaging is of major importance to understand cell motility and adhesion or protein trafficking. Total Internal Reflection Fluorescence microscopy is commonly used to confine the excitation to the basal membrane region. However, it suffers from loss of confinement and inhomogeneous excitation. Supercritical Angle Fluorescence (SAF) emission is an alternative dual depth wide field imaging which takes advantage of evanescent waves at the detection rather than at the excitation.

The near field components of a fluorophore placed in the vicinity of the glass/cell interface can become propagative and collected at supercritical angles [1]. This SAF emission appears as a ring beyond the critical angle in the objective back focal plane (BFP). This emission sharply decays with the fluorophore/surface distance *z* over a characteristic length of about the fluorophore wavelength. Specific detection of SAF emission was initially developed to perform a wide field axial filtering in dense samples [2,3]. More recently it has been also successfully coupled to single molecule superlocalization microscopy to access nearly isotropic absolute 3D localization [4] .

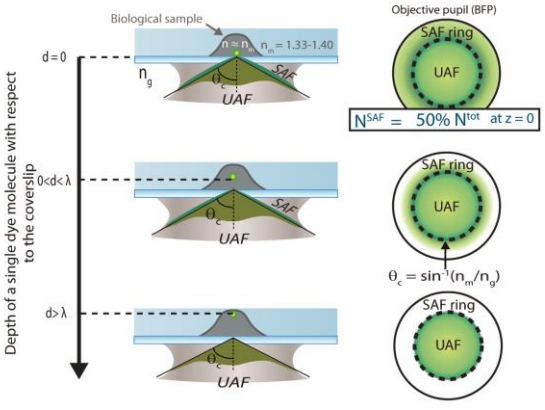

Fig. 1 Principle of Supercritical fluorescence emission

2. DETECTING SAF EMISSION

To retrieve the axial information held by SAF emission we have developed different strategies based on a static modulation (amplitude or phase) in a conjugated plane of the BFP of the objective. So far, SAF detection has been coupled with a wide field microscope to provide simultaneous dual depth investigation of membrane and intracellular events, with a confocal

microscope to add a selective membrane imaging, and to a super-resolution microscope (dSTORM) for isotropic localization. Our current goal is to implement a dynamic selectivity of the SAF emission for these various configuration, in order not only to precisely modulate the whole SAF emission area, but also to axially discriminate within this emission. We will present our current proposed setup to dynamically retrieve supercritical information.

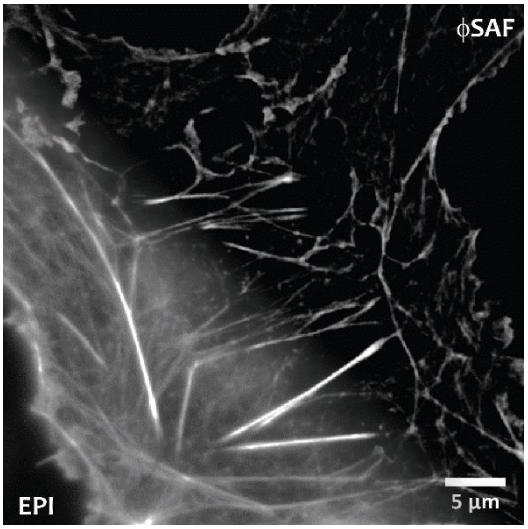

Fig. 2 Simultaneous epifluorescence and phase modulated SAF (ϕSAF) of the Actin network of a CHO cell

REFERENCES

[1] T. Ruckstuhl et al.,Forbidden light detection from single molecules, Analytical chemistry, 2000

[2] T. Barroca, K. Balaa, J. Delahaye, S. Lévêque-Fort and E. Fort, "Full-field supercritical angle fluorescence microscopy for live cell imaging", Optics letters **36,** 3051 (2011).
[3] T. Barroca et al., Full-field Near-Field Optical Microscope for Cell Imaging, PRL, 2012

[4] N. Bourg, C. Mayet, G. Dupuis, T. Barroca, P. Bon, S. Lécart, E. Fort, S. Lévêque-Fort, « Direct Optical Nanoscopy wiht Axially Localized detection « , Nat. Photon. Aout 2015.

Wavefront optimized microscopy for imaging neural activity

Dorian Champelovier[1,2], Arnaud Malvache[1,2], Thomas Tressard[2],Joel Teixeira[3], Jean-Marc Conan[3], Laurent Mugnier[3], Serge Meimon[3], Hervé Rigneault[1], Rosa Cossart[2], Serge Monneret[1]

[1] *Aix-Marseille Université, CNRS, Centrale Marseille, Institut Fresnel UMR 7249, 13013 Marseille, France*
[2] *Institut de Neurobiologie de la Méditerranée, INSERM U901, BP13 13273 Marseille Cedex 09, France*
[3] *Onera - the French Aerospace Lab, F-92322 Châtillon, France*

dorian.champelovier@fresnel.fr

Keywords: Two photon microscopy, adaptive optics, neuroscience.

1. TWO-PHOTON MICROSCOPE WITH ADAPTIVE OPTICS

Imaging neural activity has been a recent breakthrough in neuroscience. The combined use of calcium probes and two-photon microscopy allows the simultaneous recording of the activity of hundreds of neurons. However the use of this technique is currently limited by the accessible imaging depth which reduces the potential of such technique especially in *in vivo* experiments. Here we show how adaptive optics can help for imaging the hippocampus of living mice. We built a two-photon microscope that includes a deformable mirror and we adapted the modal-based [1] method to *in vivo* imaging of the hippocampus.

We designed the microscope (Figure 1) to be as close as the one used in the partner neuroscience lab: large field imaging up to 400x400μm, high NA objective (Nikon 16x/0.8 WD3mm). The laser source is a femtosecond Chameleon (Coherent) with an emission wavelength tuned on 920nm. The wavefront correction device is a segmented deformable mirror with 37 segments (IrisAO), imaged on the galvanometer mirrors (Cambrigde Technology). The scanners are imaged on the microscope objective. A photon counting photomultiplier (Hamamastu) is used for detecting the fluorescence photons emitted by the calcium probes (GAD-GFP or GCAMP).

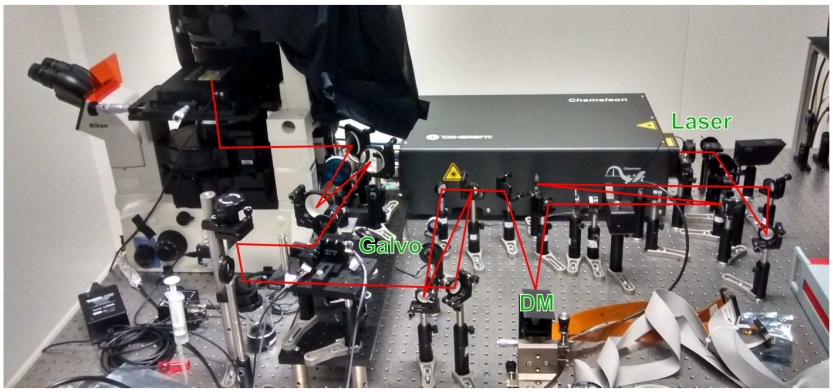

Figure 1: Experimental setup

2. INDIRECT WAVEFRONT MEASUREMENT

We use an optimized scheme of the modal-based method [2] in order to measure and correct the aberrations induced by the biological sample to the exciting laser beam. This sensorless method is based on scanning a set of aberration modes and finding the optimal amplitudes using a metric that quantifies imaging quality. We therefore investigated different image-based metrics in order to found a metric providing a good contrast in the different environments encountered in brain tissue. We compared the performance of standard metrics (mean intensity, intensity variance,…) versus metrics adapted to the sample such as pattern recognition filters. We show that the latter can be much more reliable in noisy conditions.

The modal-based method requires the use of an orthogonal basis of wavefront aberration modes. For two-photon imaging, the standard Zernike basis is not orthogonal due to non-linear coupling. We thus define experimentally a new orthogonal basis adapted to two-photon imaging using the method proposed in [3]: for

each pair of Zernike modes, we measured the metric evolution when applying different amplitudes to these modes under the constraint of constant total aberration (Figure 2). To enhance the contrast of the results, the metric used was based on pattern recognition.

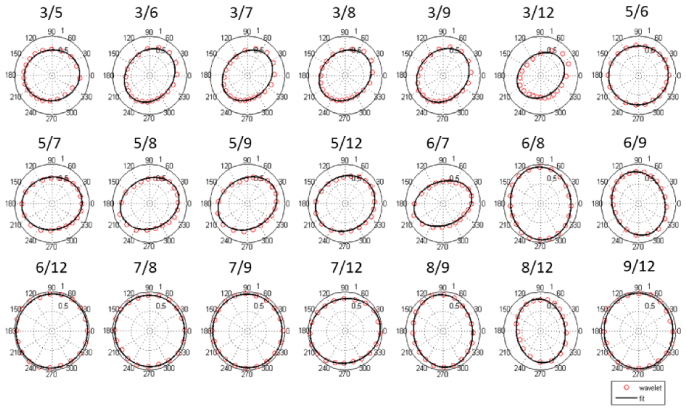

Figure 2: For each pair of modes (7 Zernike modes considered), the metric is plotted using a polar representation, the radial distance r is the metric value and the angle θ is the parameter that defines the amplitudes applied to the modes (cos θ and sin θ, respectively).

We then used this optimized metric and new basis in different brain samples. We first studied the aberration map induced by a thick volume of brain tissue using fixed brain slices. In such sample, we achieved increasing the intensity of imaged neurons (Figure 3). Finally we applied this method to *in vivo* experiments (anaesthetized mouse).

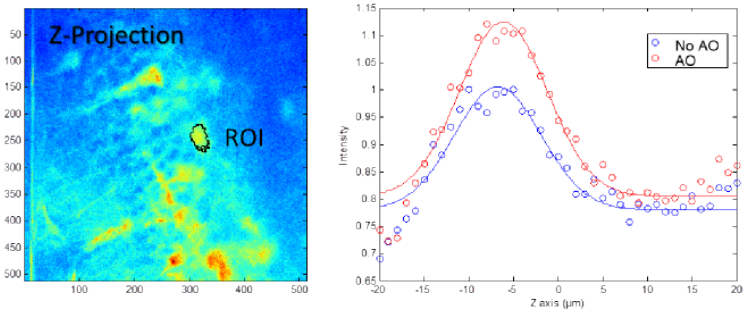

Figure 3: Left, z-projection of a 40μm image stack, 350μm deep in a brain slice; right, Intensity plot of the ROI with and without AO

We will next compare this modal-based method to the pupil segmentation method [4]. Using a combination of these two methods we expect increasing the accessible imaging depth for *in vivo* imaging of hippocampal activity.

Acknowledgments: This research is partly funded by Fondation pour la Recherche Médicale

REFERENCES

[1] D. Débarre, E. J. Botcherby, T. Watanabe, S. Srinivas, M. J. Booth, and T. Wilson, "Image-based adaptive optics for two-photon microscopy", Opt. Lett., 34, 2495-2497 (2009).

[2] J. Zeng, P. Mahou, M-C Schanne-Klein, E. Beaurepaire and D. Débarre, "3D resolved mapping of optical aberrations in thick tissues", Biom. Opt. Expr. 3(8), 1898-1913 (2012).

[3] D. Débarre, E. J. Botcherby, M. J. Booth, and T. Wilson, "Adaptive optics for structured illumination microscopy", *Opt. Express, 16, 13, pp. 9290-9305*, (2008)

[4] N. Ji, D. E. Milkie, and E. Betzig, "Adaptive optics via pupil segmentation for high resolution imaging in biological tissues", Nature Methods, 7(2), 141-147 (2009).

Unraveling synapse plasticity using several microscopy approaches

Agathe Verraes [1], Matthieu Trigano [1], Olivier Pascual [2], Thomas Freret [3], Thibault Lagache [4], Philippe Rostaing [5], Orestis Faklaris [6], Sébastien Nola [1], Marteen Loos [7], Jean-Christophe Olivo-Marin [4], Matthijs Verhage [7], Antoine Triller [5], Michel Boulouard [3], Thierry Galli [1]*, Lydia Danglot [1]*.

[1] Institut Jacques Monod, Inserm U950, Membrane traffic in Health & Disease, Université Paris-Diderot, Sorbonne Paris-Cité, Paris, France
[2] Centre de Recherche de Neurosciences de Lyon - Oncoflam - Lyon, France
[3] Groupe Mémoire et plasticité comportementale, Université Caen - Basse Normandie, Caen, France
[4] Institut Pasteur, Paris, France
[5] Institut de Biologie de l'ENS (IBENS), Paris, France
[6] Institut Jacques Monod, « Imagoseine » Imaging facility, Paris, France
[7] Center-for-neurogenomics-and-cognitive-research (cncr) - Synaptologics – Amsterdam, Netherlands
* *co-senior authors*

lydia.danglot@inserm.fr

Keywords: synapse, plasticity, super-resolution microscopy, SIM, STORM, brain tile imaging.

The establishment, maintenance and plasticity of the synapse require the transport, recycling and degradation of membrane-associated synaptic molecules via membrane trafficking mechanisms. Vesicular and target-SNAREs play a central role in all membrane trafficking pathways. Neurons express several v-SNAREs including TI-VAMP/VAMP7 which is involved in Golgi to plasma membrane transport particularly of membrane microdomains, presynaptic exocytosis, lysosomal secretion and autophagosome biogenesis and secretion. We previously found that TI-VAMP/VAMP7 KO mice are viable and characterized by decreased brain weight, increased ventricle volume as measured by MRI, and increased anxiety suggesting a role for VAMP7 in higher brain functions [1]. In addition, VAMP7 was previously found to be particularly enriched in the hippocampus, a brain structure involved in learning and memory, its expression being both pre- and post-synaptic. Here we found that VAMP7 KO mice showed increased memory performance and a decreased memory decline in old animals compared to wild-type. We are now deciphering at the tissular, cellular and molecular level what could explain such increased performances.

We investigated the neuronal morphology *in situ* by tile imaging of the entire brain (Golgi staining) to realized mosaic image at a good resolution in order to discriminate dendritic arbors. Those results indicated profuse dendritic pyramidal arborization in specific regions of the KO brain suggesting altered morphological and potentially functional post-synaptic properties. This was further established by electron microscopy which unravelled both pre and post-synaptic structural modifications in the KO.

We found altered synaptic biochemical content in glutamatergic receptors and associated molecules by biochemical approaches. We further investigate the localization of the glutamate receptor clusters by multicolor super-resolution microscopy (SIM and STORM). We found that the glutamate receptor was indeed less present at synaptic contacts in dissociated hippocampal neurons. We are currently developing image analysis software in collaboration with T. Lagache and JC. Olivo Marin (Institut Pasteur) to analyze precise distance between coupled synaptic molecules by robust statistical approaches [2]. One further step would be to unravel this synaptic organization by super resolution microscopy in brain slices. We now plan to add adaptive optics on our STORM set up to investigate this phenomenon deep into the tissue.

We conclude that VAMP7-dependent traffic is important for synaptic function particularly in glutamatergic post-synaptic domains. The contribution of this membrane trafficking pathway to synapse formation and maintenance which could result from a role of VAMP7 in transport, recycling and/or degradation of post-synaptic components, appears to play an important role in learning during aging.

REFERENCES

[1] L. Danglot, et al."Absence of TI-VAMP/Vamp7 leads to increased anxiety in mice.," *J. Neurosci.*, vol. 32, no. 6, pp. 1962-1968, 2012.

[2] T. Lagache, N. Sauvanet, L. Danglot and JC. Olivo-Marin, "Statistical analysis of molecule colocalization in bioimaging.," *Cytometry par A*, vol. 87, no. 6, pp. 568–79, 2015.

Zero-order suppression for holographic photo-excitation

Oscar Hernandez[1], Marc Guillon[1], Eirini Papagiakoumou[1] and V. Emiliani[1]

[1] *Wavefront Engineering Microscopy, Group, Neurophotonics Laboratory, University Paris Descartes, Sorbonne Paris Cité, Paris, France*

marc.guillon@parisdescartes.fr

Keywords: wavefront shaping, light patterning, nonlinear microscopy, spatial light modulators, temporal focusing

Wavefront shaping via computer generated holograms encoded on liquid crystal Spatial Light Modulators (SLMs) has been introduced in neuroscience at the end of the last decade as a flexible way to photostimulate neurons [1,2]. However, its use is frequently hindered by the remaining fraction of undiffracted light from the SLM, the so-called "zero-order" [3,4]. Here we propose to suppress the contribution of the zero-order by introducing aberrations in holographic systems based on non-linear excitation mechanisms. Aberrations are then corrected for the excitation spot by the SLM, except for the zero-order component that remains aberrated. A decrease by 4 orders of magnitude in zero-order-induced two-photon fluorescence intensity is demonstrated with a simple cylindrical lens as an aberrating optical element, at the moderate expense of a 12% decrease in diffraction efficiency of the SLM. Combination with temporal focusing [5] is shown to further decrease zero-order fluorescence by a factor of 10.

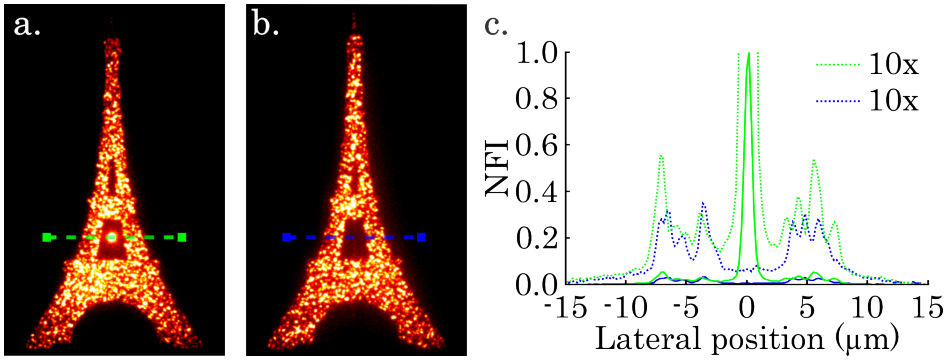

Figure 1: Comparison between a computer-generated holographic image of the Eiffel tower without (a) and with (b) a single 1 m cylindrical lens aberrating the zero order in the optical path. (c) Two-Photon Normalized Fluorescence Intensity (NFI) profiles along the lines drawn in (a) (green) and (b) (blue).

REFERENCES

[1] Lutz, C. et al. Holographic photolysis of caged neurotransmitters. Nat. Methods 5, 821–827, 2008.

[2] Nikolenko, V. et al. SLM Microscopy: Scanless Two-Photon Imaging and Photostimulation with Spatial Light Modulators. Front. Neural Circuits 2, 5, 2008.

[3] Palima, D. & Daria, V. R. Holographic projection of arbitrary light patterns with a suppressed zero-order beam. Appl. Opt. 46, 4197–201, 2007.

[4] Zahid, M. et al. Holographic photolysis for multiple cell stimulation in mouse hippocampal slices. PLoS One 5, e9431 (2010).

[5] Papagiakoumou, E., de Sars, V., Oron, D. & Emiliani, V. Patterned two-photon illumination by spatiotemporal shaping of ultrashort pulses. Opt. Express 16, 22039–47 (2008).

TRANSPARENT FILM THICKNESS MEASUREMENT BY OPTICAL COHERENCE TOMOGRAPHY

Aïssa Manallah, Mohamed Bouafia

Institute of Optics and Precision Mechanics, University of Sétif 1, Algeria

manallah_aissa@yahoo.fr

Keywords: Optical coherence tomography, Optical metrology, Nondestructive testing, Film thickness.

1. INTRODUCTION

Optical coherence tomography is a powerful optical method, noninvasive and noncontact diagnostic method. Although it is usually used for medical examinations, particularly in ocular exploration; it can also be used in optical metrology as measure technique. In this work, we use OCT to measure thicknesses of transparent films.

In OCT, depth profiles are constructed by measuring the time delay of back reflected light by interferometry measurements. Reflection is caused by refraction index changes at boundaries (i.e., air-film interface). OCT signals only contain information about the depth of reflecting surfaces. This process is attributed to a depth dependent amplitude reflectivity profile $r(z)$.

The interference between reflected light from the reference and the sample arm is limited to optical path differences (OPD) inferior at the round trip coherence length of the broadband laser source.

$$\delta z = l_c = \frac{2ln(2)}{\pi}\frac{\lambda_m^2}{\Delta\lambda} \tag{1}$$

In Fourier Domain OCT (FD-OCT), the reflectivity profile is obtained by a Fourier transformation, and the difference in position between two successive peaks of the resulting spectrum gives the film thickness with high accuracy.

2. EXPERIMENTAL

The typical OCT measuring head consists of a collimator, a scanning unit and an objective lens. It is a confocal system with the SM fibre tip acting as a point-like light source and as a spatial filter for the detection system.

The axial resolution of an OCT system is,

$$\delta x = \delta y = \frac{\sqrt{2ln(2)}}{\pi N_{A\ fib}}\frac{f_{ob}}{f_{col}}\lambda \quad , \quad \delta z = \frac{2ln(2)}{\pi}\frac{\lambda_m^2}{\Delta\lambda} \tag{2}$$

Here f_{ob}, f_{col} are the objective and collimator focal length respectively, λ the central wavelength and $N_{A\ fib}$ the numerical aperture of the fibre. The principle of the experimental setup, based on the Michelson interferometer, is shown in Figure 1.

A Source for spectrometer based FD-OCT of center wavelength 820 nm and bandwidth 120 – 240 nm is used.

By moving the reference arm the interference signal is created. Thus the resulting OCT signal is the source signal modulated by the interference pattern. The Fourier transform is used to detect the peaks positions in the spectral domain.

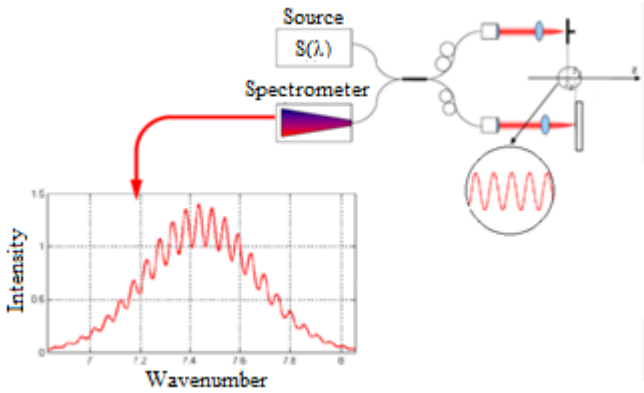

Figure 1: OCT principle.

The graphs of the figure below illustrate the different signals of OCT, starting with the signal source, through the interference signal in the time domain and then the signal in the Fourier domain which are clearly distinguished two peaks relating to positions of the surfaces of the film, and therefore the required thickness

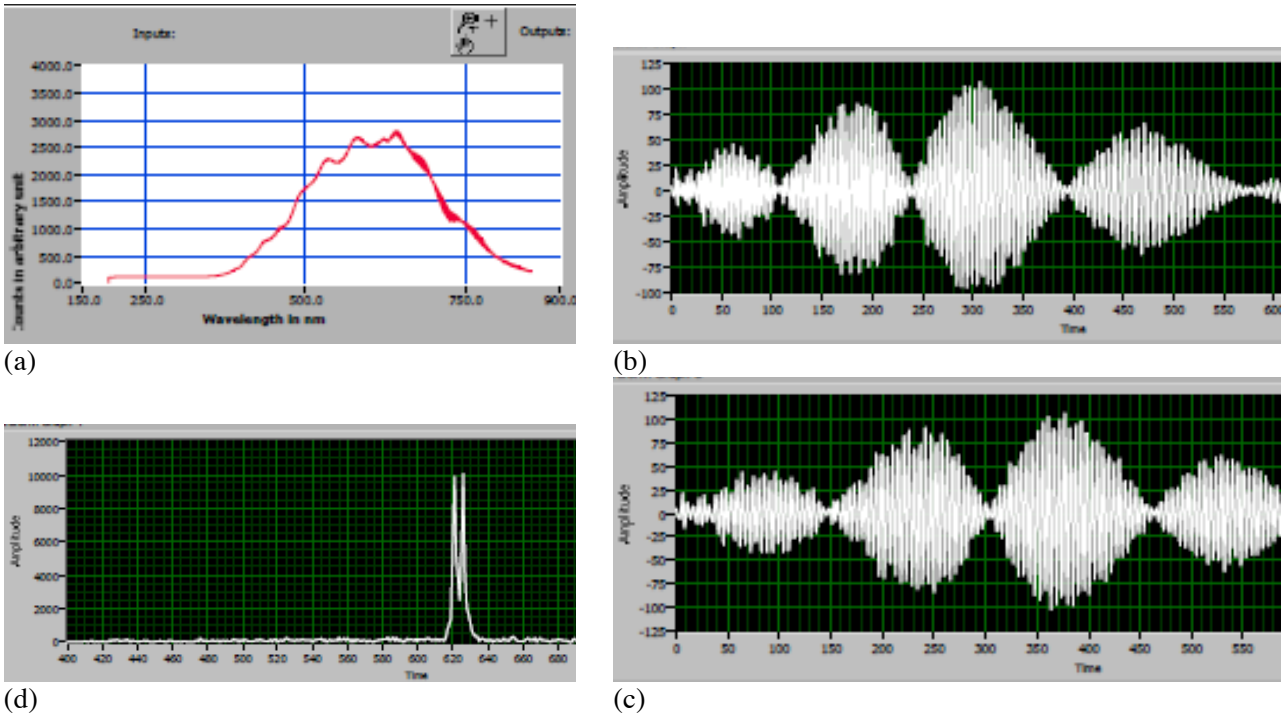

Figure 2: OCT signals.

REFERENCES

[1] Drexler, W., Optical Coherence Tomography, Springer-Verlag Berlin Heidelberg, (2008).

[2] Fercher, A. F., 2009, "Optical coherence tomography - development, principles, applications", Z. Med. Phys. (20) 251–276, (2010).

[3] Leitgeb, R.; Hitzenberger, C. K. & Fercher, A. F. (2003), 'Performance of Fourier domain vs. time domain optical coherence tomography', Optics Express 11(8), 889-894.

[4] Koprowski, R., Image Processing in Optical Coherence Tomography using Matlab, Dr Sosnowiec, Poland,

Autofocusing for whole-brain imaging in light-sheet microscopy

Caroline Müllenbroich[1,2], Ludovico Silvestri[1,3], Leonardo Sacconi[1,3], Francesco Pavone[1,2,3,4]

[1] *European Laboratory for Non-Linear Spectroscopy, Via Nello Carrara,1 50019 Sesto Fiorentino (FI), Italy*
[2] *Department of Physics and Astronomy, University of Florence, Via Sansone,1 50019 Sesto Fiorentino (FI), Italy*
[3] *National Institute of Optics, National Research Council, Via Nello Carrara,1 50019 Sesto Fiorentino (FI), Italy*
[4] *International Center for Computational Neurophotonics, Via Nello Carrara,1 50019 Sesto Fiorentino (FI), Italy*

muellenbroich@lens.unifi.it

Keywords: Light-sheet microscopy, single-plane illumination microscopy, whole-brain imaging, autofocusing

1. ABSTRACT

The imaging of structurally intact mouse brains for the mapping and quantification of neuronal projections requires microscopic resolution over large volumes [1]. Light-sheet fluorescence microscopy (LSFM) [2] is particularly suited for this task as it allows for the acquisition of cm-sized data sets with a resolution that is high enough to identify dendritic and axonal features in time scales which are no longer the bottle neck of high-throughput imaging. Here we describe an autofocusing routine which adjusts the focal plane of the detection objective in a light-sheet microscope for whole-mouse brain imaging [3]. An image-based sharpness metric is evaluated at various focus positions through motorisation of the detection objective and a search algorithm is used to determine optimal focus position. This routine is repeated at regular checkpoints throughout the image stack by moving the sample through the static light sheet with a xyz-sample translation stage. Intermediate focus positions are deduced by a linear fit of the values at the checkpoints. This approach represents a trade-off between increased acquisition time as stage motion is effectively doubled for every stack and enhanced image quality.

2. INTRODUCTION

In our setup, a transgenic mouse brain, roughly encompassed in a volume of 0.9 cm^3, is imaged with many hundreds of overlapping stacks of up to 8 mm depth. The brain is rendered transparent with an optical clearing method based on refractive index matching [4,5], yet nevertheless, significant aberrations degrade image quality; even after optical clearing, the large brain size means that also comparatively small heterogeneities in the refractive index matching sum up to large optical path differences and therefore strong aberrations at large imaging depth. The effect of optical aberrations can severely obscure features even above the resolution limit and is particularly detrimental for whole-brain 3D imaging because the size of data sets amounts to 2-3 TB and therefore warrants the application of fully automated analytical software to extract meaningful, quantifiable information, e.g. automated cell counting [6]. Adaptive optics [7] provides a means to compensate for optical aberrations and has recently been applied to LSFM [8]. Sample induced aberrations are hereby most difficult to correct at run-time due to their modal complexity, large amplitude and high spatial variability [9]. Traditional adaptive optics applications are operated in a closed loop between the wavefront sensor and the wavefront actuator. In order to reduce the amplitude of the necessary aberration correction to a level that can be compensated by the limited stroke of the wavefront actuator, high-amplitude, lower-order aberrations like defocus need to be addressed with an alternative strategy.

3. SHARPNESS MEASURE

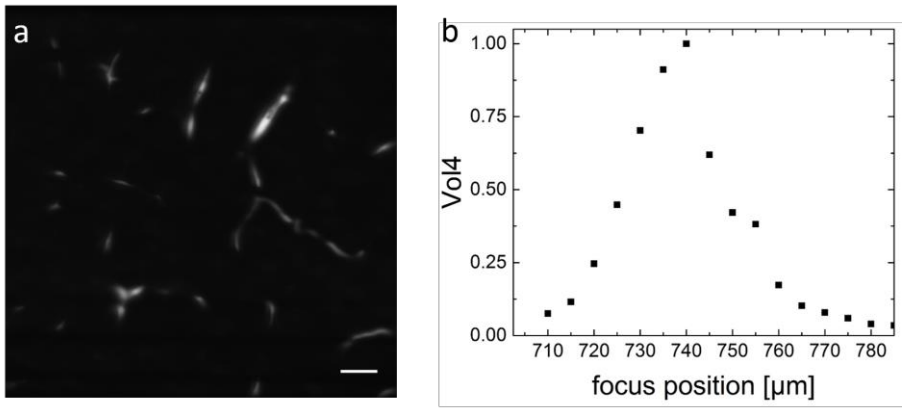

Figure1: (a) FITC-albumin labelled vasculature in clarified rat brain imaged with a Olympus objective (25X, 1.0NA, 8 mm WD) designed for high refractive index immersion, scale bar: 100µm, (b) focus curve, (c) Vollath-4 sharpness metric [11].

The choice of sharpness function is highly dependent on the kind of sample and microscopy technique used [10]. We tested several sharpness functions published in literature for their suitability to our fluorescently labelled brains (Fig 1a) and light-sheet imaging modality. A focus curve (Fig 1b) was acquired over a focusing range of 80 µm and using the Vollath-4 function [11] (Fig 1c) as sharpness metric. This routine was repeated throughout the image stack and intermediate focus positions were deduced by a linear fit. The image stack was then re-acquired with a 2 µm step size of the sample translation stage and a concurrent movement of the detection objective to adjust focus at run time. By correcting for defocus in this way the total amount of aberration is reduced opening the possibility of correcting for higher order aberrations with a wavefront actuator at run time.

REFERENCES

[1] L. Silvestri *et al*., "Confocal light-sheet microscopy: micron-scale neuroanatomy of the entire mouse brain," *Opt. Express*, vol. 20, no. 18, pp. 20582-20598, 2012.

[2] J. Huisken *et al*., "Optical sectioning deep inside live embryos by selective plane illumination microscopy," *Science*, vol. 305, no. 5686, pp. 1007–1009, 2004.

[3] C. Müllenbroich *et al*., "Comprehensive optical and data management infrastructure for high-throughput light-sheet microscopy of whole mouse brains," *Neurophotonics*, in press, 2015.

[4] K. Chung *et al*., "Structural and molecular interrogation of intact biological systems," *Nature*, vol. 497, no. 7449, pp. 332-337, 2013.

[5] I. Costantini *et al*., "A versatile clearing agent for multi-modal brain imaging," *Sci. Rep.*, vol. 5, no. 9808, pp. 1-9, 2015.

[6] P. Frasconi *et al*., "Large-scale automated identification of mouse brain cells in confocal light sheet microscopy images," *Bioinformatics*, vol. 30, no. 17, pp. i587-i593, 2014.

[7] M. Booth *et al*., "Adaptive optics in microscopy," *Trans. R. Soc. A*, vol. 365, no. 1861, pp. 2829-2843, 2007.

[8] R. Jorand *et al*., "Deep and clear optical imaging of thick inhomogeneous samples," *PLoS One*, vol. 7, no. 4, pp. e35795, 2012.

[9] K. Wang *et al*., "Rapid adaptive optical recovery of optimal resolution over large volumes," *Nat. Methods*, vol. 11 no. 6, pp. 625-628, 2014.

[10] O. Santos *et al*., "Evaluation of autofocus functions in molecular cytogenetic analysis," *J. Microsc*, vol. 188 no. 3, pp. 264-272, 1997.

[11] C. Gu *et al*., "Region sampling for robust and rapid autofocus in microscope," *Microsc. Res. Techniq.*, vol. 78 no. 5, pp. 382-390, 2015.

Optimization of indirect wavefront sensing methods for two photon scanning microscopy

Joel Teixeira[1], Jean-Marc Conan[1], Serge Meimon[1], Laurent Mugnier[1], Dorian Champelovier[2,3], Serge Monneret[3], Hervé Rigneault[3], Thomas Tressard[2], Rosa Cossart[2], Arnaud Malvache[2,3]

[1] *Onera - the French Aerospace Lab, F-92322 Châtillon, France*
[2] *Institut de Neurobiologie de la Méditerranée, INSERM U901, BP13 13273 Marseille Cedex 09, France*
[3] *Aix-Marseille Université, CNRS, Centrale Marseille, Institut Fresnel UMR 7249, 13013 Marseille, France*

jean-marc.conan@onera.fr

Keywords: adaptive optics, wave-front sensing, two-photon microscopy, modal sensorless

1. ADAPTIVE OPTICS FOR TWO PHOTON SCANNING MICROSCOPY

Two photon scanning microscopy is a powerful and mature tool used in biological imaging. This technique has been for instance applied to *in vivo* dynamic calcium imaging of the mouse hippocampus and has led to pioneering results [1-2]. However, in most applications, optical aberrations induced by the sample prevent imaging at large depth. Adaptive optics can correct for these aberrations, provided that one is able to perform an accurate and reliable wavefront sensing.

Two-photon microscopy requires indirect wavefront sensing. Two families of approaches have been proposed so far: the modal sensorless technique [3] and a method based on pupil segmentation [4]. Our recent qualitative analysis [5] has underlined the complementarities of these techniques.

This paper presents a quantitative analysis of these approaches based on realistic numerical simulations. Possible limitations are underlined and optimization strategies are studied. Preliminary experimental validations are also presented.

2. INDIRECT WAVEFRONT SENSING: LIMITATIONS AND OPTIMIZATION

Whatever the wavefront sensing strategy the key parameter is the two photon return flux. Our analysis is based on the evaluation of return flux with a precise modeling of the interaction between the fluorescent sample and the illuminating laser beam in the presence of aberrations, and for various values of the numerical aperture (NA).

We recall for instance that modal sensorless approach [3] optimizes the deformable mirror shape so as to maximize the mean return flux in a given field of view (FoV). One can show that this metric can be expressed as a function of the FoV averaged axial object distribution $\overline{\eta}(z)$ in the form:

$$F_r(a) = \int_{FoV} F(x_0, y_0; a)\,\mathrm{d}x_0\,\mathrm{d}y_0 = \int \bar{\eta}(z) \left(\iint \left| \tilde{h}_{z,a}(v_x, v_y) \right|^2 \mathrm{d}v_x\,\mathrm{d}v_y \right) \mathrm{d}z \qquad (1)$$

where $\widetilde{h}_{z,a}$ is the optical transfer function at a given depth z, and *a* represent the optical aberrations. In order to study the behavior of this metric with respect to the optical aberrations, we compute the return flux using Eq. 1 with an aberrated optical transfer function $\widetilde{h}_{z,a}$ derived from a diffractive scalar simulation. In our tutorial case study the object is localized in a unique plane at z_0. Figure 1 shows the return flux as a function of spherical aberrations for various object axial localizations. One can see that, for an object out of the focal plane, the mean return flux is maximized for non zero aberrations, hence a non diffraction limited PSF. Despite one of course forbids acting on tip-tilt and focus, adaptive optics still offers the possibility to distort the focal volume to capture the fluorophores where they are.

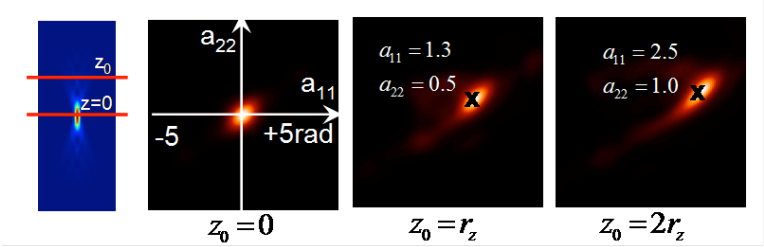

Figure 1: Focal volume and return flux as a function of the spherical aberrations Z11 et Z22 (Zernike radial order 4 and 6) for three object axial localization z_0 (expressed in units of depth of field r_z, typically a few microns).

One has therefore to be careful with interpretation of the apparent measured aberrations since a slight axial shift of the object can lead to significant aberration biases. Besides, one can see that the quadratic approximation may be questionable; this approximation is also challenged in the presence of strong aberrations. This may be an issue since efficient optimization generally relies on such a quadratic approximation. The interest of using other metrics (contrast and pattern recognition criteria) is also analyzed.

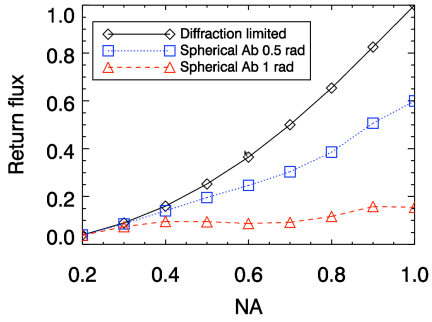

Figure 2: Return flux as a function of NA in the presence of spherical aberration (Zernike radial order 4); effective laser power is kept constant for all NA values.

In the presence of strong aberrations one may think of starting with a reduced aperture [6], or more generally of using pupil segmentation type sensing [4], especially since one can show that in the presence of significant aberrations the return flux is not severely reduced when using a smaller numerical aperture (see Figure 2). Based on these simulations and on first experimental demonstrations obtained on our adaptive two photon scanning microscope (including a 37 segment IRISAO deformable mirror), we will present optimized control strategies, aiming especially at in vivo calcium imaging of the mouse hippocampus.

Acknowledgment: This research is partly funded by Fondation pour la Recherche Médicale.

REFERENCES

[1] M. Lovett-Barron, P. Kaifosh, MA Kheirbek, N. Danielson, JD Zaremba, TR Reardon, *et al.*, "Dendritic inhibition in the hippocampus supports fear learning." *Science* 343 (6173), (2014).

[2] V. Villette, A. Malvache, T. Tressard, N. Dupuy, and R. Cossart, "Internally recurring hippocampaal sequences as a population template of spatio-temporal information", *Neuron in review*.

[3] D. Débarre, E. J. Botcherby, T. Watanabe, S. Srinivas, M. J. Booth, and T. Wilson, "Image-based adaptive optics for two-photon microscopy", *Opt. Lett.*, 34, 2495-2497 (2009).

[4] N. Ji, D. E. Milkie, and E. Betzig, "Adaptive optics via pupil segmentation for high resolution imaging in biological tissues", *Nature Methods*, 7(2), 141-147 (2009).

[5] S. Meimon, J.-M. Conan, L. M. Mugnier, V. Michau, R. Cossart, and A. Malvache, "Adaptive optics for in vivo two-photon calcium imaging of neuronal networks", *Proc. SPIE*, 8978, (2014).

[6] J.-M. Conan, J. Teixeira, S. Meimon, L. M. Mugnier, D. Champelovier, S. Monneret, R. Cossart, and A. Malvache, "Indirect wavefront sensing for adaptive optics assisted in vivo two-photon calcium imaging of neuronal networks," *Focus on Microscopy Program and Abstract Book*, 2015, p. 460.

Where to eat (well) near the institute?

The institute is situated in the middle of the Latin Quarter, literally full of restaurants, from the cheapest sandwich/crepe shop to the most gastronomic tables.
Below a list of some of our favourites (in no particular order), but many more choices are available if you walk down rue Linné, rue Monge, or rue Mouffetard, for instance.

1 La Baleine http://restaurant-la-baleine.com/fr/Le-restaurant-4.html
Type: French restaurant
Address: across the street
Distance: 10m
Price range: 15-30€

2 La Fontaine
Type: brasserie
Address: 20 rue Cuvier
Distance: 200m
Price range: 8-20€

3 Le Jardin des Pâtes http://www.lafourchette.com/restaurant/le-jardin-des-pates/16407
Type: organic homemade pasta restaurant
Address: 4 Rue Lacépède
Distance: 280m
Price range: 10-15€

4 La Mosquée de Paris http://www.restaurantauxportesdelorient.com/restaurant.html
Type: Moroccan cuisine – oriental tea house
Address: 39 Rue Geoffroy-Saint-Hilaire
Distance: 400m
Price range: 20-30€

5 L'Epsilon
Type: brasserie
Address: 24 Rue Linné
Distance: 260m
Price range : 10-15€

6 Girasole
Type: Italian
Address: 5 Rue Linné
Distance: 200m
Price range: 10-20€

7 Le Buisson Ardent http://www.lebuissonardent.fr
Type: gastronomic French
Address: 25 Rue Jussieu

Distance: 290m
Price range: 20-30€

8 Les Arènes
Type: brasserie
Address: 16 Rue Linné
Distance: 240m
Price range: 12-20€

9 L'Arbre à Cannelle
Type: Homemade pies and salads
Address: 14 rue Linné
Distance: 180m
Price range: 10-15€

10 Chez Lilane http://lilane.com (closed on Monday)
Type: gastronomic French
Address: 8 rue Gracieuse
Distance: 650m
Price range: 20-30€

11 El Picaflor http://www.picaflor.fr/la-carte/?carte=16 (closed on Monday)
Type: Peruvian
Address: 9 rue Lacépède
Distance: 350m
Price range: 20-30€

12 Mina Express
Type: Lebanese wraps (take away)
Address: 17 Rue Guy de la Brosse
Distance: 170m
Price range: 5-10€

13 Bonvivant http://www.bonvivant.paris/
Type: bistrot, café and sandwichs
Address: 7 rue des Écoles
Distance: 300m
Price range: 16-35€

14 Restaurant Kathmandu http://restaurantkathmandu.fr/en
Type: Nepalese restaurant
Address: 22 rue des Boulangers
Distance: 220m
Price range: 15-30€ (lunch menu starting at 10€)

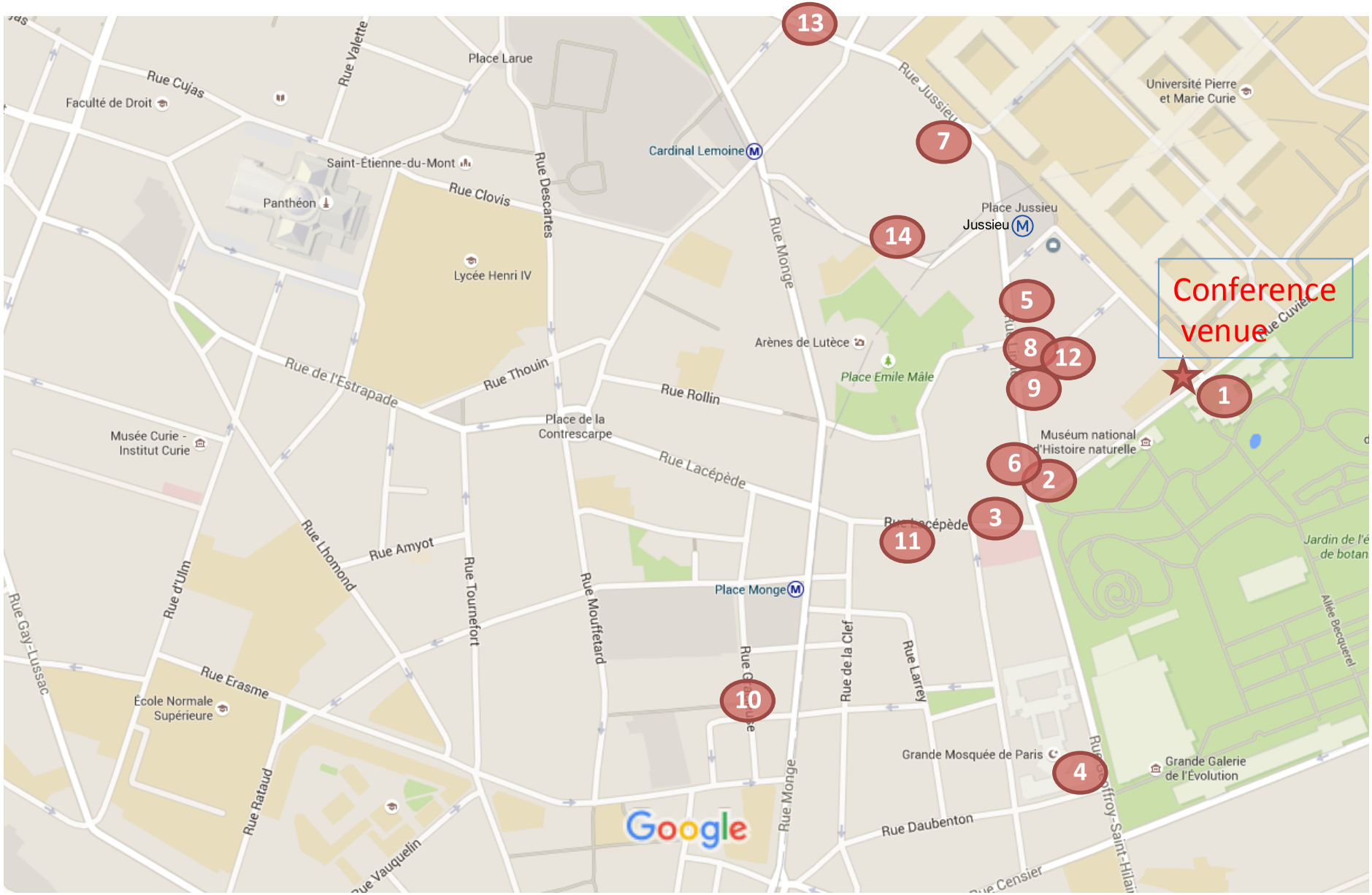
13
7
14
5
8
12
9
1
6
2
3
11
10
4
Conference venue
Rue Jussieu
Université Pierre et Marie Curie
Cardinal Lemoine
Place Jussieu
Jussieu
Rue Monge
Rue Descartes
Rue Clovis
Saint-Étienne-du-Mont
Panthéon
Lycée Henri IV
Rue Cujas
Faculté de Droit
Rue Valette
Place Larue
Arènes de Lutèce
Place Émile Mâle
Rue de l'Estrapade
Rue Thouin
Rue Rollin
Place de la Contrescarpe
Rue Lacépède
Musée Curie - Institut Curie
Muséum national d'Histoire naturelle
Rue Lhomond
Rue Amyot
Rue d'Ulm
Rue Tournefort
Rue Mouffetard
Place Monge
Rue de la Clef
Rue Larrey
Rue Gay-Lussac
Rue Erasme
École Normale Supérieure
Rue Rataud
Grande Mosquée de Paris
Grande Galerie de l'Évolution
Rue Daubenton
Rue Censier
Allée Becquerel
Google

CONFERENCE SPONSORS

ALPAO

ALPAO manufactures a complete range of adaptive optics products for use in research and industry, including very rapidly deformable mirrors with large strokes, wavefront sensors, and adaptive optics loops. These products are specially designed for astronomy, ophthalmology, microscopy, wireless optical communications, and laser applications. Our product's unrivalled performance allows users to recover very high-resolution images.

Boston Micromachines

Founded in 1999, Boston Micromachines Corporation (BMC) is the leading provider of advanced microelectromechanical systems (MEMS) - based mirror products for use in commercial adaptive optics systems. The company's suite of award-winning compact deformable mirror (DM) products is the most cost-effective, highest performance mirror technology in the market today. They are widely used to drive scientific discovery in astronomy, laser beam shaping, microscopy, vision science, and support a variety of defense applications.

DIM Nano-K

The Domaine d'Intérêt Majeur (DIM) Nano-K "From cold atoms to nanosciences" is a Key Areas of Interest labeled by the regional council of Paris Region for the period 2012-2015. It gathers the Skills Center in Nanosciences Ile-de-France (C'Nano IdF) and the Research Institute on Cold Atoms of Ile-de-France (IFRAF).

Fondation Pierre Gilles de Gennes

The Foundation's purpose is to promote the emergence of concrete applications of research, principally in the field of health and biology. It manages a network of academic research teams from ENS (Ecole Normale Superieure), ENSCP (Ecole Nationale Superieure de Chimie de Paris), ESPCI (Ecole Superieure de Physique et de Chimie Industrielles), and Institut Curie. This network represents 1% of the French academic researchers (150 teams, 1600 physicians, researchers, and PhDs). FPGG initiates interdisciplinary, inter-institutional programs at the chemistry/physics/biology/medicine interface with an objective of generating innovative breakthroughs for global Health Care.

France-BioImaging

France-BioImaging is a large-scale national research infrastructure and pluridisciplinary project with participants in Biology, Physics, Chemistry, Computer science and engineering. At the frontier between molecular and cell biology, biophysics and engineering, mathematics and bioinformatics, France-BioImaging gathers several outstanding biological Imaging Centers supported by state of the art R&D teams with the aim to cover recent advances in microscopy, spectroscopy, probe engineering and signal processing.

Groupement de Recherche 2588 "Microscopie et Imagerie du Vivant"

The purpose of GdR MIV (Research Group in Microscopy and Imaging in Living subjects) is to promote the sharing of expertise between research teams, with the aim to develop new strategies up to overcome technological and methodological limitations in the study of gene expression, nuclear organization in territories, network signaling, the membrane trafficking … This GdR gathers teams in biology, physics, chemistry, image processing, computing and applied mathematics .

Hamamatsu

Hamamatsu Photonics is a leading company of light technology and products. We design, manufacture and sell high level solutions for photometry systems, light sources & cameras. Hamamatsu has been working with the Photon for more than 50 years. We have established ourselves as the top company of photoelectron conversion technologies in the world.

Imagine Optic

Wavefront sensors and adaptive optics for optical metrology, lasers and microscopy. Imagine Optic is one of the world's leading providers of Shack-Hartmann wavefront sensing hardware and software, adaptive optics technologies and professional services in applied optics. We work with scientists and industrials in domains including pure science, industrial quality control, space and defense, semiconductors and many others. Since 1996, we've been supplying industry leaders around the world with the high-quality products and services that they need to perform.

Investments for the Future

Launched in 2009 by the French Government, the Investments for the Future programmes are strategic initiatives which aim to boost French competitiveness by investing in research, higher education and vocational training, in industry and SMEs, in sustainable development and in expanding sectors such as digital technology, biotechnology and nuclear energy.

Laser 2000

Laser 2000 is your expert in Europe for components and systems for Photonics, Fiber Optics & Networks and Laser Systems & Solutions. We provide „customer-specific solutions from a single source" for sophisticated applications, e.g. laser safety and protection, or in the area of microscopy & spectroscopy. Our employees' in-depth experience insures expert consulting in the area of material processing with short laser pulses and meets the highest demands for high-end lighting and cameras for image processing.

LESIA

LESIA (Laboratory of Space Studies and Instrumentation in Astrophysics) is one of the largest French laboratories of research in astrophysics (approximately 12% of the discipline). It is one of the five Scientific Departments of the Paris Observatory and also a CNRS Laboratory. LESIA's primary role consists in the design and implementation of scientific instrumentation in space and on the ground, analysis and interpretation of scientific observations and development of advanced techniques applied in ground-based and space instruments. LESIA is also involved in technology transfer from astrophysics to medical imaging.

Paris Sciences et Lettres

Founded in 2010, Paris Sciences & Lettres Research University brings together 25 prestigious establishments in the very heart of Paris, all united by their common intent to create an entity comparable in performance to the greatest universities worldwide. With their exceptional diversity, these institutions share a common culture based on scientific excellence and the very strong potential of their students. As a new federal type of university, and winner of a national Investments for the Future award in 2011, PSL Research University is implementing an ambitious program of research, training, and development.

Phasics

Specialized in high resolution wavefront sensing, Phasics offers a full range of high performance wavefront analyzers and integrated test benches for laser beam characterization and control, lens testing and biology imaging. Phasics solutions are all based on its unique patented technology, the quadriwave lateral shearing interferometry. Developed to overcome the Shack Hartmann limitations, this technology offers ultra-high resolution (up to 400x300 measurement points), high sensitivity and large dynamic. In more, it is compact, achromatic and able to measure diverging beam with no relay lens, for an easy implementation.

Région Ile-de-France

When it comes to research, the Paris Region features world-class fields. Examples include life sciences, healthcare and the environment. However, to rise to its full potential and strengthen its international visibility, the key is coordinating and fostering cooperation among the different actors. Key Areas of Interest (Domaines d'intérêt majeurs or DIM) are research networks created around strategic topics. For DIMs, regional support makes it possible to finance equipment for a particular area of interest, as well as research grants, feedback commissions, network coordination and scientific events.

Société Française d'Optique

The Société Française d'Optique (SFO) is the French branch of the European Optical Society (EOS). The purpose of EOS is to contribute to progress in optics and related sciences, and to promote their applications at the European and international levels, by bringing together individuals and legal entities involved in these disciplines and their applications. With about 1500 individual members and 40 groups, SFO gathers all French players in optics-photonics. As an independent association, SFO promotes the development of optics in its broadest sense.

58 Tour Eiffel Restaurant

9pm on Tuesday, 6 October

The restaurant is located on the 1st floor of the Eiffel Tower. At 57 meters above the ground, add a meter (the height of the kitchen stove) and you are there at 58 Tour Eiffel.

How to get the lift ticket to reach the restaurant?

The restaurant is only accessible by the lift. The lift ticket for the 1st floor of the Eiffel Tower will be either given on Tuesday afternoon at the conference venue or at **8.30pm** near the welcome desk located on the esplanade between the north and east pillars of the Eiffel Tower (near the BNP Paribas ATM). The kiosk can be noticed by a flag « 58 Tour Eiffel ».

Your lift ticket gives you priority access to the 1st floor of the Eiffel Tower from 8.30pm. Feel free to enjoy the terrace on the 1st floor before or after your meal.

Please bring your badge with you.

Important:

- Expect an hour to get there from the conference venue.
- A formal dress code is required (no jean, no trainers).
- Smoking is not allowed in the Eiffel Tower.
- The restaurant does not have coat-check facilities. Oversized luggage cannot be allowed into the tower. There are no luggage lockers.

How to get there?

The Eiffel Tower is located on the Champ de Mars, in the 7th arrondissement of Paris

Address: Eiffel Tower – 5, Avenue Anatole France – Champ de Mars – 75007 – Paris

By subway

- Line no.6, "Bir-Hakeim" station
- Line no.9, "Trocadéro" station
- Line no.8, "Ecole militaire" station

By RER

Line C : « Champs de Mars - Tour Eiffel » station

By bus

- Bus 82, stops : « Tour Eiffel » or « Champ de Mars »
- Bus 42, stop : « Tour Eiffel »
- Bus 87, stop : « Champ de Mars »
- Bus 69, stop : « Champ de Mars »

By boat

You can also get to the Eiffel Tower by boat with Batobus (Eiffel Tower stop). An original and pleasant way of exploring the heart of Paris with all the magic that lines the Seine on your way to the Eiffel Tower.

By car

We recommend you park in any of the nearest underground car parks to the Eiffel Tower, a good choice being the Quai Branly car park located less than 300 metres from the Tower.

By bike

Self-hire bikes are available 24 hours a day, 7 days a week at any of the Vélib' stations. A pleasant way of exploring the Parisian streets by bike on your way to the Eiffel Tower.

From the conference venue:

By bus 87 from « Institut du Monde Arabe » stop to terminus « Champ de Mars » stop (45 min – 10 min walk, 30 min bus, 5 min walk/1,80€).

By subway lines 10 and 6 : line 10 from « Jussieu » station to « La-Motte-Picquet-Grenelle » station then line 6 from « La-Motte-Picquet-Grenelle » to « Bir Hakeim » (40 min – 5 min walk, 20 min subway, 15 min walk/1,80€).

By RER line C from « Gare d'Austerlitz » or « Saint-Michel-Notre-Dame » stations to « Champ-de-Mars/Tour Eiffel » station (45 min -15 min walk, 15 min RER, 15 min walk/1,80€).

By Batobus from « Notre-Dame » or « Jardin des Plantes/Cité de la mode et du design » stations to « Eiffel Tower » stop (55 min/16€).

Participants list

Name	Institution	Mail
Walther AKEMANN	IBENS, Ecole Normale Supérieure, Paris, France	akemann@biologie.ens.fr
Sherazade AKNOUN	PHASICS, Saint-Aubin, France	aknoun@phasics.fr
Arjen AMELINK	TNO, Delft, Netherlands	arjen.amelink@tno.nl
Jordi ANDILLA	ICFO - Institut de Ciències Fotòniques, Barcelona, Spain	jordi.andilla@icfo.es
Alexandre AUBRY	Institut Langevin, Paris, France	alexandre.aubry@espci.fr
Amaury BADON	Institut Langevin, Paris, France	amaury.badon@espci.fr
Pedro BARAÇAL DE MECÊ	ONERA, Châtillon, France	pedro.baracal_de_mece@onera.fr
Emmanuel BEAUREPAIRE	Laboratoire d'Optique et Biosciences, Ecole Polytechnique, Palaiseau, France	emmanuel.beaurepaire@polytechnique.edu
Xavier BERTHELON	Institut de la Vision, Paris, France	xavier.berthelon@inserm.fr
Nazim BHARMAL	Durham University, Durham, UK	n.a.bharmal@durham.ac.uk
Thomas BIFANO	Boston University, Boston, MA, USA	tgb@bu.edu
Marie BLAVIER	LESIA, Observatoire de Paris, Meudon, France	marie.blavier@obspm.fr
Baptiste BLOCHET	Laboratoire Kastler Brossel & IBENS, Ecole Normale Supérieure, Paris, France	baptiste.blochet@lkb.ens.fr
Claude BOCCARA	Institut Langevin, Paris, France	claude.boccara@espci.fr
Susanne BOLTE	Institut de Biologie Paris-Seine, Paris, France	susanne.bolte@upmc.fr
Marco BONAGLIA	INAF Osservatorio Astrofisico di Arcetri, Florence, Italy	mbona@arcetri.astro.it
Marie BORDERIE	Institut de la Vision, Paris, France	marie.borderie@sfr.fr
Jonathan BOULANGER-WEILL	IBENS, Ecole Normale Supérieure, Paris, France	jonathan.boulanger-weill@ens.fr
Laurent BOURDIEU	IBENS, Ecole Normale Supérieure, Paris, France	laurent.bourdieu@ens.fr
Guy BOUVIER	IBENS, Ecole Normale Supérieure, Paris, France	guy.bouvier@ens.fr
Sophie BRASSELET	Institut Fresnel, Marseille, France	sophie.brasselet@fresnel.fr
Olena BRAZHNIKOVA	Institut de la Vision, Paris, France	elena.brazhnikova@inserm.fr
Lorenzo BUSONI	INAF Osservatorio Astrofisico di Arcetri, Florence, Italy	lbusoni@arcetri.astro.it

Corey BUTLER	Interdisciplinary Institute for Neurosciences & Imagine Optic, Bordeaux, France	corey.butler@etu.u-bordeaux.fr
Clement CABRIEL	Institut des sciences moléculaires d'Orsay, Université Paris-Sud, Orsay, France	ccabriel@ens-cachan.fr
Alessia CANDEO	IBENS, Ecole Normale Supérieure, Paris, France	candeo@biologie.ens.fr
Dino CARPENTRAS	LAPD, Ecole Polytechnique Fédérale de Lausanne, Lausanne, Switzerland	dino.carpentras@epfl.ch
Rémy CARRASSET	LASER 2000, Bordeaux, France	carrasset@laser2000.fr
Thomas CHAIGNE	Institut Langevin & Laboratoire Kastler Brossel , Paris, France	thomas.chaigne@espci.fr
Dorian CHAMPELOVIER	Institut Fresnel & INMED, Marseille, France	dorian.champelovier@fresnel.fr
Jean-Marie CHASSOT	Institut Langevin, Paris, France	jean-marie.chassot@espci.fr
Guillaume CHENEGROS	Institut de la Vision, Paris, France	Guillaume.Chenegros@obspm.fr
Grégory CLOUVEL	Imagine Optic, Orsay, France	gclouvel@imagine-optic.com
Jean-Marc CONAN	ONERA, Châtillon, France	jean-marc.conan@onera.fr
Donald CONKEY	LO, Ecole Polytechnique Fédérale de Lausanne, Lausanne, Switzerland	donald.conkey@epfl.ch
Meng CUI	ECE, Purdue University, West Lafayette, IN, USA	cuim10@janelia.hhmi.org
Chris DAINTY	University College London, London, UK	c.dainty@ucl.ac.uk
Eugénie DALIMIER	LLTech, Paris, France	edalimier@lltech.fr
Lydia DANGLOT	Institut Jacques Monod, Paris, France	lydia.danglot@inserm.fr
Hilton B. de AGUIAR	Institut Fresnel, Marseille, France	h.aguiar@fresnel.fr
Delphine DÉBARRE	LIPhy, Université J. Fourier, Grenoble, France	delphine.debarre@ujf-grenoble.fr
Hugo DEFIENNE	Laboratoire Kastler Brossel, Paris, France	Hugo.defienne@lkb.ens.fr
Julie DÉGARDIN	Institut de la Vision, Paris, France	julie.degardin@inserm.fr
Antoine DELON	LIPhy, Université J. Fourier, Grenoble, France	antoine.delon@ujf-grenoble.fr
Jacques DEROUARD	LIPhy, Université J. Fourier, Grenoble, France	jacques.derouard@ujf-grenoble.fr
Nicholas DEVANEY	National University of Ireland, Galway, Ireland	nicholas.devaney@nuigalway.ie
Stephane DIEUDONNE	IBENS, Ecole Normale Supérieure, Paris, France	dieudon@biologie.ens.fr
David DIGREGORIO	Institut Pasteur, Paris, France	david.digregorio@pasteur.fr
Niek DOELMAN	Leiden University & TNO, Leiden, Netherlands	niek.doelman@tno.nl

Ivan DOUDET	PHASICS, Saint-Aubin, France	doudet@phasics.fr
Wolfgang DREXLER	Medical University Vienna, Vienna, Austria	wolfgang.drexler@meduniwien.ac.at
Clara DUSSAUX	IBENS, Ecole Normale Supérieure, Paris, France	clara.dussaux@ens-lyon.fr
Bruno EMICA	Hamamatsu, Massy, France	bemica@hamamatsu.fr
Valentina EMILIANI	Neurophotonics Laboratory, Paris Descartes University, Paris, France	valentina.emiliani@parisdescartes.fr
Elric ESPOSITO	Institut de la Vision, Paris, France	elric.esposito@inserm.fr
Michael FEINBERG	Boston Micromachines Corp, Cambridge, MA, USA	mrf@bostonmicromachines.com
Mathias FINK	Institut Langevin, Paris, France	mathias.fink@espci.fr
Jozsua FODOR	IBENS, Ecole Normale Supérieure, Paris, France	jozsua.fodor@ens.fr
Alexandra FRAGOLA	LPEM, ESPCI, Paris, France	alexandra.fragola@espci.fr
Raphaël GALICHER	LESIA, Observatoire de Paris, Meudon, France	raphael.galicher@obspm.fr
Joseph GALLAGHER	LIPhy, Université J. Fourier & ALPAO, Grenoble, France	joseph.gallagher@ujf-grenoble.fr
Rémi GALLAND	Interdisciplinary Institute for Neurosciences, Bordeaux, France	remigalland38@gmail.com
Rachel GENTHIAL	LIPhy, Université J. Fourier, Grenoble, France	rachel.genthial@ujf-grenoble.fr
Sylvain GIGAN	Laboratoire Kastler Brossel, Paris, France	sylvain.gigan@lkb.ens.fr]
Marie GLANC	LESIA, Observatoire de Paris, Meudon, France	marie.glanc@obspm.fr
Jesper GLÜCKSTAD	DTU Fotonik , Lyngby, Denmark	jesper.gluckstad@fotonik.dtu.dk
Elena GOFAS SALAS	ONERA, Châtillon, France	elena.gofas-salas14@imperial.ac.uk
Kate GRIEVE	Institut de la Vision, Paris, France	kategrieve@gmail.com
Olivier HAEBERLÉ	Laboratoire Modélisation Intelligence Processus Systèmes, Mulhouse, France	olivier.haeberle@uha.fr
Vincent HARDY	ALPAO, Grenoble, France	vincent.hardy@alpao.fr
Laurent HÉLIOT	Laboratoire de Physique des Lasers, Atomes et Molécules, Lille, Paris	laurent.heliot@iri.univ-lille1.fr
Michael HELMBRECHT	Iris AO, Inc., Berkeley, CA, USA	michael.helmbrecht@irisao.com
Oscar HERNANDEZ	Neurophotonics Laboratory, Paris Descartes University, Paris, France	oscar.hernandez-cubero@parisdescartes.fr
Kristina IRSCH	The Johns Hopkins School of Medicine & Institut de la Vision, Baltimore, MD, USA & Paris, France	kristina.irsch@gmail.com
Ignacio IZEDDIN	Institut Langevin, Paris, France	ignacio.izeddin@espci.fr

Na JI	Janelia Farm Research Campus, Ashburn, VA, USA	jin@janelia.hhmi.org
Paul KIRKBY	University College London - NPP, London, UK	p.a.kirkby@ucl.ac.uk
Alexandr KLIOUTCHNIKOV	Research Center CAESAR, Bonn, Germany	alexandr.klioutchnikov@caesar.de
Caroline KULCSAR	Laboratoire Charles Fabry de l'Institut d'Optique, Palaiseau, France	Caroline.kulcsar@institutoptique.fr
Timothé LAFOREST	LAPD, Ecole Polytechnique Fédérale de Lausanne, Lausanne, Switzerland	timothe.laforest@epfl.ch
Jean-François LÉGER	IBENS, Ecole Normale Supérieure, Paris, France	leger@biologie.ens.fr
Mickaël LELEK	Institut Pasteur, Paris, France	mickael.lelek@pasteur.fr
Christophe LEROY-DOS SANTOS	Institut de la Vision, Paris, France	christophe.leroy-dos-santos@inserm.fr
Sandrine LÉVÊQUE-FORT	Institut des sciences moléculaires d'Orsay, Université Paris-Sud, Orsay, France	sandrine.leveque-fort@u-psud.fr
Arnaud MALVACHE	Institut Fresnel & INMED, Marseille, France	arnaud.malvache@inserm.fr
Aissa MANALLAH	Institute of Optics and Precision Mechanics, University of Setif 1, Setif, Algeria	manallah_aissa@yahoo.fr
Xavier MARQUES	IBENS, Ecole Normale Supérieure, Paris, France	marques@biologie.ens.fr
Aurore MASSON	Institut des Technologies Avancées en sciences du Vivant, Toulouse, France	aurore.masson@itav.fr
Benjamin MATHIEU	IBENS, Ecole Normale Supérieure, Paris, France	benjamin.mathieu@ens.fr
Serge MEIMON	ONERA, Châtillon, France	meimon@onera.fr
Jerome MERTZ	Boston University, Boston, MA, USA	jmertz@bu.edu
Oriane MOLLET	Optitec, Marseille, France	oriane.mollet@pole-optitec.com
Gael MONERON	Institut Pasteur, Paris, France	moneron@pasteur.fr
Serge MONNERET	Institut Fresnel, Marseille, France	serge.monneret@fresnel.fr
Edgar MORALES	LAPD, Ecole Polytechnique Fédérale de Lausanne, Lausanne, Switzerland	edgar.moralesdelgado@epfl.ch
Mickael MOUNAIX	Laboratoire Kastler Brossel, Paris, France	mickael.mounaix@lkb.ens.fr
Caroline MUELLENBROICH	European Laboratory for Non-Linear Spectroscopy, Florence, Italy	muellenbroich@lens.unifi.it
Laurent MUGNIER	ONERA, Châtillon, France	mugnier@onera.fr
Thu-Mai NGUYEN	Institut Langevin, Paris, France	thu-mai.nguyen@espci.fr
Satoshi NISHIMURA	Jichi Medical University, Shimotsuke, Japan	snishi-tky@umin.ac.jp
Jonas OGIEN	Laboratoire Charles Fabry de l'Institut d'Optique, Palaiseau, France	jonas.ogien@institutoptique.fr

Eirini PAPAGIAKOUMOU	Neurophotonics Laboratory, Paris Descartes University, Paris, France	eirini.papagiakoumou@parisdescartes.fr
Michel PAQUES	Institut de la Vision, Paris, France	michel.paques@gmail.com
Mélanie PEDRAZZANI	Laboratoire Aimé Cotton, Université Paris-Sud, Orsay, France	melanie.pedrazzani@gmail.com
Enrico PINNA	INAF Osservatorio Astrofisico di Arcetri, Florence, Italy	pinna@arcetri.astro.it
Rory POWER	Max Planck Institute of Molecular Cell Biology & Genetics, Dresden, Germany	power@mpi-cbg.de
Matthieu REFREGIERS	SOLEIL Synchrotron, Gif-sur-Yvette, France	refregiers@synchrotron-soleil.fr
Arnaud REHEL	PHASICS, Saint-Aubin, France	rehel@phasics.fr
Hervé RIGNEAULT	Institut Fresnel, Marseille, France	herve.rigneault@fresnel.fr
Gérard ROUSSET	LESIA, Observatoire de Paris, Meudon, France	Gerard.Rousset@obspm.fr
Jürgen SAWINSKI	Research Center CAESAR, Bonn, Germany	juergen.sawinski@caesar.de
Anne SENTENAC	Institut Fresnel, Marseille, France	anne.sentenac@fresnel.fr
Isabelle SERRE	Imagine Optic, Orsay, France	iserre@imagine-optic.com
Bertrand SIMON	Laboratoire Modélisation Intelligence Processus Systèmes, Mulhouse, France	bertrand.simon@uha.fr
Manuel SIMONUTTI	Institut de la Vision, Paris, France	manuel.simonutti@inserm.fr
Siddharth SIVANKUTTY	Institut Fresnel, Marseille, France	siddharth.sivankutty@fresnel.fr
Nicolino STASIO	LO, Ecole Polytechnique Fédérale de Lausanne, Lausanne, Switzerland	nicolino.stasio@epfl.ch
Mickaël TANTER	Institut Langevin, Paris, France	mickael.tanter@espci.fr
Joel TEIXEIRA	ONERA, Châtillon, France	joel.teixeira@onera.fr
Olivier THOUVENIN	Institut Langevin, Paris, France	olivier.thouvenin@espci.fr
Cathie VENTALON	IBENS, Ecole Normale Supérieure, Paris, France	cathie.ventalon@ens.fr
Jianxin WANG	Durham University, Durham, UK	593191286@qq.com
Irène WANG	LIPhy, Université J. Fourier, Grenoble, France	irene.wang@ujf-grenoble.fr
Benoit WATTELLIER	PHASICS, Saint-Aubin, France	BW@PHASICS.FR
Stephen WEBB	Science and Technology Facilities Council, Oxford, UK	stephen.webb@stfc.ac.uk
Peng XIAO	Institut Langevin, Paris, France	xiaopengaddis@gmail.com
Mantas ZURAUSKAS	University of Oxford, Oxford, UK	mantas.zurauskas@cncb.ox.ac.uk